Template Synthesis of Structure-Controlled Porphyrin Tubes and Those Inclusion and Optical Properties

Yusuke Chiba

2018

Abbreviations

Ac	acetyl
APCI	atmospheric pressure chemical ionization
Ar	aryl
CCD	charge coupled device
CD	cyclodextrin
COSY	correlation spectroscopy
DABCO	1,4diazabicyclo[2,2,2]octane
DCTB	*trans*-2-[3-(4-*tert*-butylphenyl)-2-methyl-2-propenylidenelmalono-nitrile]
DFT	density functional theory
DMF	*N,N*-dimethylformamide
Dppf	1,1'-bis(diphenylphos-phino)ferrocene
EI	electron ionization
ESI	electrospray ionization
Et	ethyl
eq	equation
equiv	equivalent(s)
GPC	gel permeation chromatography
h	hour(s)
HOMO	highest occupied molecular orbital
HR	high resolution
L	ligand
OLED	organic light emitting diode
LHCs	light-harvesting complex system
LUMO	lowest unoccupied molecular orbital
MALDI	matrix assisted laser desorption/ionization
MS	mass spectrometer
min	minute(s)
NMR	nuclear magnetic resonance
NOESY	nuclear Overhauser effect spectroscopy
PET	photoinduced electron transfer
Ph	phenyl
py	pyridine
RI	refractive index
r. t.	room temperature
TAS	transient absorption spectroscopy
TBAF	tetrabutylammonium fluoride
TBAI	tetrabutylammonium iodide
TBS	*tert*-butyldimethylsilyl
^{t}Bu	*tert*-butyl
TFA	trifluoacetic acid
TIPS	triisopropyrsilyl
THF	tetrahydrofuran
TMEDA	*N,N,N',N'*-tetramethylethylenediamine
TOF	time of flight
TPP	tetraphenylporphyrin
TXPTS	tris(2,4-dimethyl-5-sulfanato-phenyl)phosphine trisodium salt
UV	ultraviolet
vis	visible

Contents

General Introduction

Host Molecules

Natural host molecules, including enzymes and ion channels, are known to encapsulate molecules and ions to achieve effective chemical conversion or transportation[1] since the discovery of their structures.[2] Chemists often mimic natural phenomena to solve scientific problems in various fields such as chemical sensors, purification, biomimetic catalysts, and drug delivery systems (Figure 1).[3]

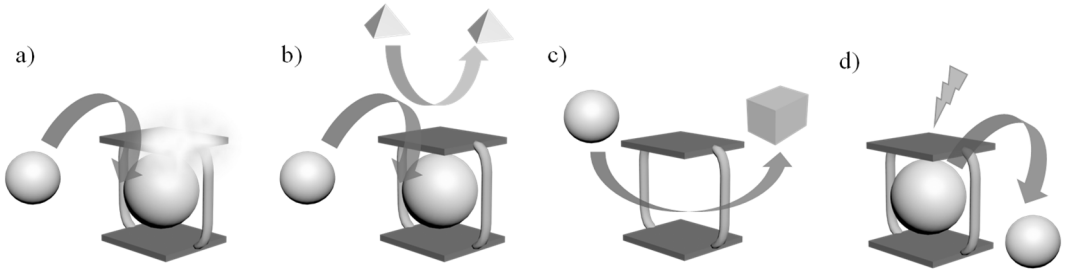

Figure 1. Applications of host–guest chemistry: a) Chemical sensor, b) separation and purification, c) biomimetic catalyst, and d) drug delivery system

This mimic of nature is based on host–guest chemistry. Pedersen reported the first example of host–guest complexes between crown ethers and appropriate sized alkali cations (Figure 2).[4] This finding has opened a new field, that is, host–guest chemistry. Later, Cram *et al.* investigated artificial enzyme models and chiral recognition with chiral crown ethers.[5] Lehn *et al.* successfully synthesized a series of cryptands having three-dimensional cavity.[6] These host molecules have greater affinity for encapsulating alkali cations than the crown ethers.[6] Until then, mainstream research in organic chemistry had focused on molecules consisting of primarily covalent bonds. Host–guest chemistry broke this trend, leading to new chemistry in which non-covalent bonding was used to construct complex structures. In 1987, the Nobel Prize in Chemistry was awarded jointly to Pedersen, Cram, and Lehn for their development of molecular recognition chemistry. To date, various host molecules, including

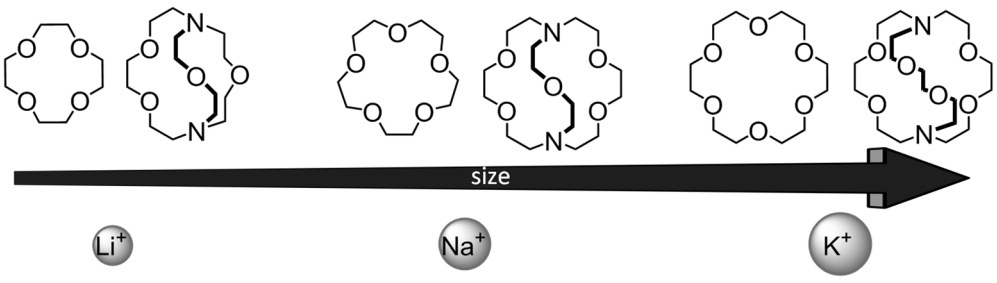

Figure 2. Crown ethers as hosts and appropriately sized alkali cations as guests

cyclodextrins,[7,3a] pillar arenes,[8] calix arenes,[9] cucurbiturils,[10] and cycloparaphenylenes[11] were synthesized to form host–guest complexes with ions and small molecules. Cyclic, cage-shaped, and ball-shaped metallo-supramolecular complexes[12] are newly developed types of host structures; one of the hosts has nanometer-sized cavity as large as proteins and nanoparticles.[13] Host–guest chemistry has been applied to chemical sensors, molecular containers, and unique nanoscale reactors on the basis of previous knowledge on selective molecular recognition.[3]

Recently, chemists have tried to combine the optical properties and defined structural control of host–guest complexes to achieve new functionalities such as rotaxanes. Rotaxanes are mechanically interlocked molecular architectures that consist of a linear dumbbell-shaped component encircled by one or more macrocycles. Stoppers are attached to the ends of the dumbbell which are large enough to mechanically trap the macrocycle(s) and prevent them from de-threading. Rotaxanes can also have different stimuli-responsive stations for fixing macrocycle(s), as their positions can be freely controlled. Stoddart *et al.* first developed a synthetic method for the production of stimuli responsive rotaxanes (Scheme 1a).[14] Other examples of host–guest complexes are the catenanes, which are mechanically interlocked molecular architectures composed of two or more macrocycles. Because macrocycles of catenanes can rotate and move within each other, stimuli-responsive parts can control their

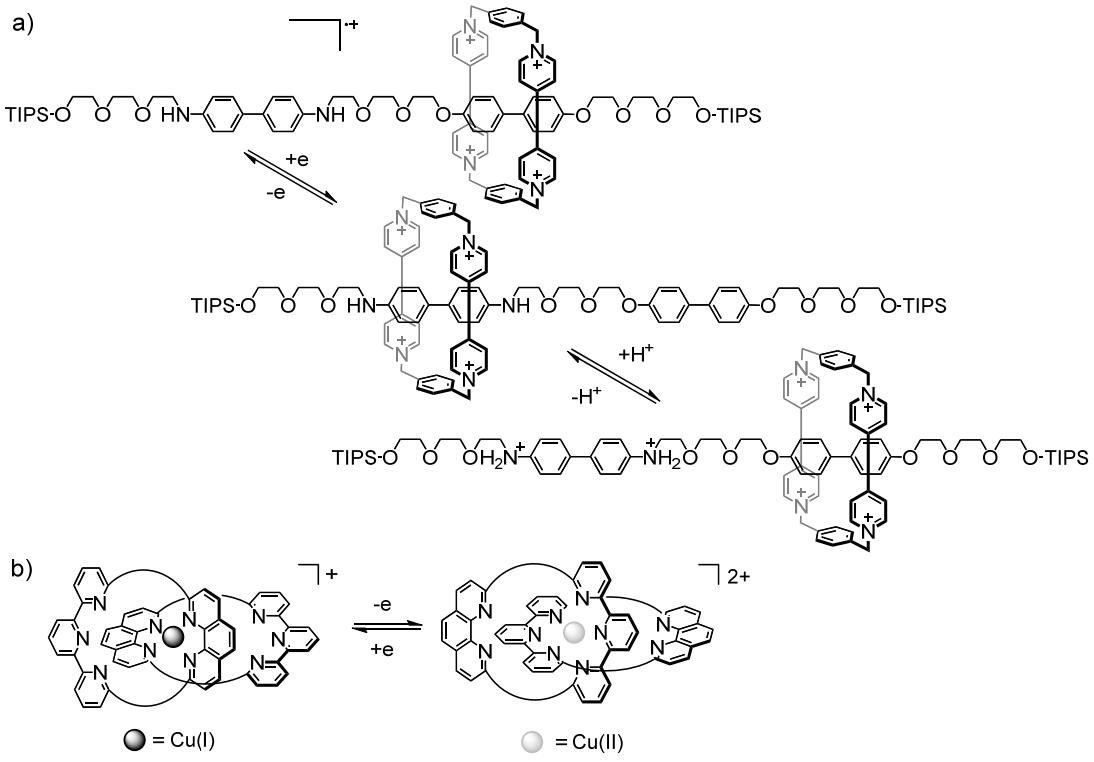

Scheme 1. Stimuli responsive molecular machines: a) a redox and pH active rotaxane, b) a redox active catenane

dynamics: switching rotation or maintaining unidirectional rotation. Sauvage *et al.* developed rotational switches of catenanes that were responsive to electro stimuli (Scheme 1b).[15] Leigh *et al.* reported automatic and unidirectional rotation of catenanes powered by chemical fuels.[16] Their findings regarding switching molecules developed the concept of supramolecular chemistry. In 2016, the Nobel Prize in Chemistry was given to three chemists, including Stoddart and Sauvage, for their development of the chemistry on molecular machines.

Synthesis of Host Molecules

Size recognition and interactions between the hosts and guests are important factors governing the function of host–guest complexes.[17] Crown ethers are known to selectively form host–guest complexes with appropriately sized alkali cations through electrostatic interactions: 12-crown-4 with Li^+, 15-crown-5 with Na^+, and 18-crown-6 with K^+.[4] The resulting molecular structures are related to the interactions between the hosts and guests. Cyclodextrins encapsulate molecules primarily through van der Waals and CH–π interactions.[3c] For pillar arenes, π–π interactions induce the formation of host–guest complexes.[8] Host molecules with two interaction modes can realize the selective recognition of molecules depending on their chemical nature.

Interaction points such as hydrogen bonding sites and π-units can easily be introduced to precursors of host molecules. However, it is challenging to construct two or three-dimensional structures from the precursors to provide size recognition abilities. Generally, cyclization reactions of linear molecules, S_N2 reactions, cross coupling reactions, and metathesis reactions can afford cyclic molecules with different cavity sizes as well as polymers (Figure 3).[18] Entropy disfavors cyclic conformations of molecules, which is the reason why intermolecular reactions proceed during cyclization reactions even when the solution is highly diluted. It is necessary to develop efficient synthetic methods for the generation of host molecules except for cyclodextrins that can be produced by enzyme reactions.[19] Three major methods have been developed to solve the problem.

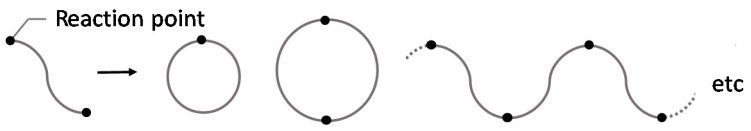

Figure 3. Various byproducts of a typical cyclization reaction

The first is a template method. Templates can fix the precursors to specific cyclic conformations to yield effective cyclization due to the enthalpic effect based on multiple interactions. For example, crown ethers were selectively synthesized via cyclization reactions with appropriately sized alkali cations (Scheme 2).[20]

Scheme 2. Template synthesis of crown ethers

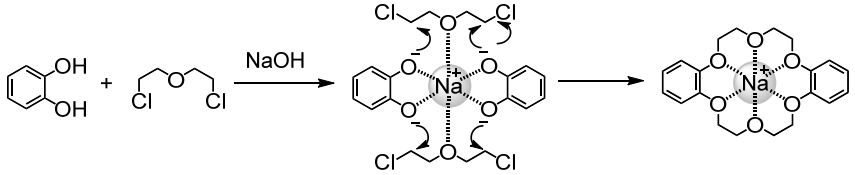

The second method is the dynamic covalent chemistry approach. Dynamic covalent bonds can participate in reversible cleavage–rebondage reactions. For example, imines, disulfides, esters, and alkenes are typical examples. This method can easily produce thermodynamically stable and extremely large structures with molecular weight distributions due to the reversibility of the reactions.[21] Grubbs *et al.* reported the quantitative synthesis of crown ether analogs by combining dynamic covalent chemistry and the template method to accelerate intramolecular cyclization (Figure 4a).[22] Stoddart *et al.* successfully synthesized cage-shaped molecules comprised of two carcerands without a template (Figure 4b).[23] The thermodynamic effect based on multiple bonds led to the selective synthesis.

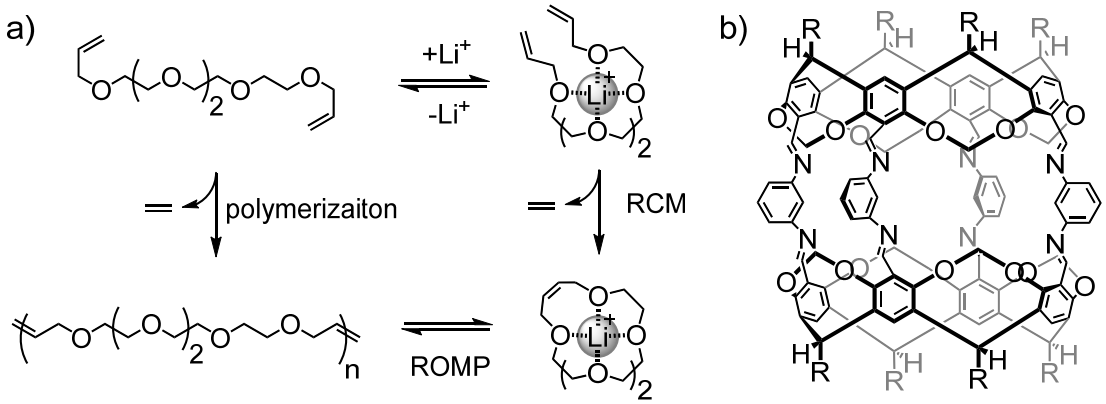

Figure 4. Dynamic covalent chemistry approach for host molecules: a) combination of the template method and dynamic covalent chemistry and b) multiple dynamic covalent bonds.

The third method is the self-assembly method that leverages the coordination between metals (M) and multidentate ligands (L). The shape and size of the host complexes are controlled by three main factors: the M : L ratio, geometry of metals, as well as denticity and shape of the ligands. Fujita *et al.* reported the quantitative synthesis of cyclic complexes, which consisted of four palladium precursors and 4,4'-bipyridines (Figure 5a).[12a] It is also possible to design geometries and symmetries of host complexes, including tetrahedral,[24] cubic (Figure 5b),[25] octahedra,[26] cuboctahedra,[27] and dodecahedra.[28] Recently, the self-assembly strategy produced novel Goldberg polyhedral, which has great impacts in the fields of both chemistry and mathematics.[29]

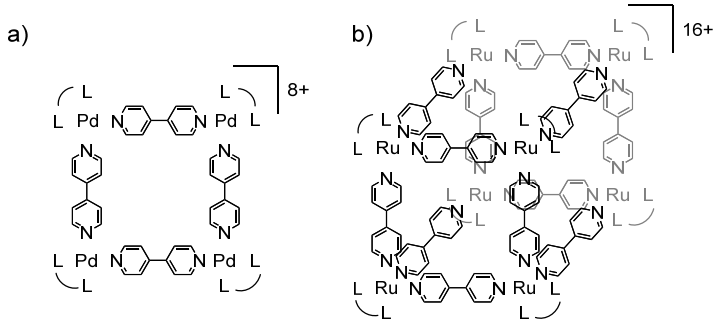

Figure 5. Self-assembly approaches for host complexes, a) Cyclic host and b) cubic host

Molecular Tubes

Molecular tubes are host molecules with a one-dimensional cavity, and are promising for use as transporters (Figure 6a) and in molecular arrangements (Figure 6b).[30] The structures can be constructed with two binding modes: non-covalent and covalent bonds. Molecular tubes constructed by non-covalent bonds can form infinite structures in the solid state and exhibit environmental responsiveness based on weak interactions,[31] whereas covalent molecular tubes have defined robust structures. Moreover, it is easy to tune the optical

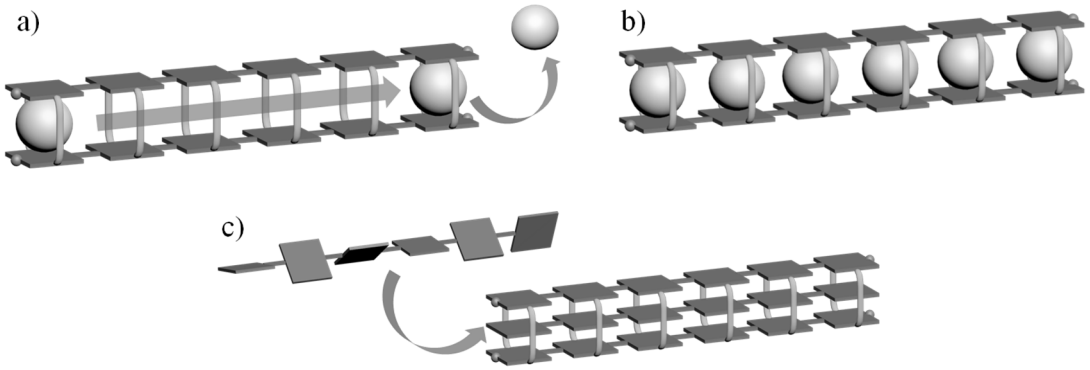

Figure 6. Characteristics of molecular tubes: a) Transporter, b) molecular arrangement, and c) control of molecular dynamics

properties of covalent molecular tubes by modifying their π-systems. Cyclodextrin tubes are known to be able to arrange triiodide[32] and transport ions.[33] Ito *et al.* and Yui *et al.* demonstrated that cyclodextrin tubes could recognize poly(ethylene glycol) as well as small molecules and ions because of its one-dimensional cavity.[34] The complex showed a high association constant because of multiple interactions. In this case, the molecular dynamics of poly(ethylene glycol), including bond rotation, was thought to be restricted in the cavity. Flexible organic molecules often show averaged optical properties such as π-conjugation length and lifetime of excitons, due to the dynamics such as rotation along the axis of covalent bonds.[35] Molecular tubes can fix flexible molecules in the cavity to adopt more defined structures (Figure 6c); this is promising in the construction of efficient optical materials.

Synthesis of Molecular Tubes

To synthesize covalent molecular tubes with attractive properties, multiple reaction points need to be controlled because further reactions producing branched polymers need to be prevented. Carbon nanotubes (CNTs) are regarded as useful carbon materials because of their stability and high electro-thermal conductivity,[36a] and have been widely used since their discovery.[36b] However, it is difficult to produce structure-defined pure CNTs due to the extreme synthetic conditions required. The properties of CNTs depend on the parameters of the adopted structure, including helicity, cavity size, edge structures, and length.[37] Although attempts have been made to develop sequential synthesis methods for the production of CNTs from cycloparaphenylene, a bottom-up method has not yet been realized. However, synthetic methods for cycloparaphenylene with different structures, such as edge structures, have been developed.[11] As described above, it is difficult to develop synthetic methods for covalent molecular tubes. To date, two strategies have been developed for the synthesis of molecular tubes: the self-assembly approach and the template method.

Self-Assembly Strategy

The self-assembly approach consists of two steps: integration of cyclic molecules as the one-dimensional tube through weak interactions and the tubulation reactions (Figure 7). Ghadiri *et al.* demonstrated that cyclic peptides formed non-covalent molecular tubes in organic solvents due to multiple hydrogen bonds among the amide groups.[38] Intermolecular metathesis reactions of the nanotube with alkenes successfully afforded the covalent

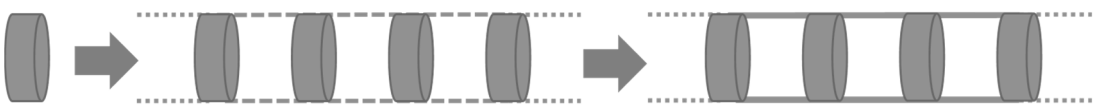

Figure 7. A concept of tubulation through non-covalent molecular tubes

molecular tubes (Figure 8a).[39] The tubulation reaction did not proceed in polar solvents, which suggested that the proximity effect accelerated the tubulation reaction.

The self-assembly method in solution is not effective in the preparation of longer molecular tubes because of the entropy effect. To overcome this challenge, the tubulation method in the crystalline state for the production of long molecular tubes was developed. Generally, the formation of bonds in the crystalline state induces changes in the crystal systems, which suppress further reactions.[40] Some reactions in the crystalline state are topochemical reactions, which are defined as the reactions "wherein the structure of the products is dictated by the geometry and proximity of the reactive sites of the precursors in the lattice".[41] This characteristic enables the production of crystal-sized nanotubes. Topochemical reactions of diynes affords enyne structures, which is effective for producing large π-systems.[42] Shimizu *et al.*,[43] Lauher *et al.*,[44] and Morrin *et al.*[45] reported the syntheses of π-conjugated molecular tubes through topochemical reactions under irradiation or heating following the integration of cyclic molecules with two diynes (Figure 8b). Molecular tubes prepared by topochemical reaction in the crystalline state have very low solubility in organic solvents, which hampers the material applications. The introduction of alkyl units to the cyclic molecules of the molecular tubes solved the solubility issue, with the topochemical reaction proceeding in the gel state.[46]

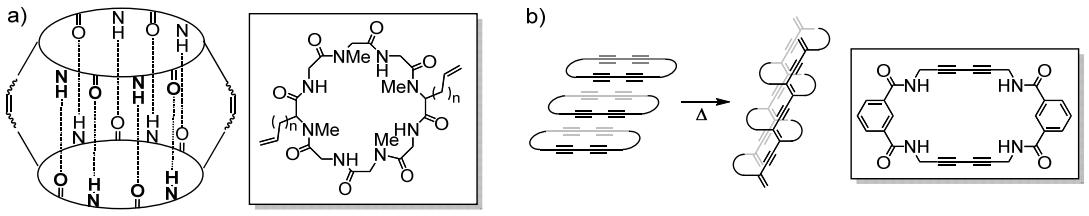

Figures 8. Tubulation through non-covalent molecular tubes: a) Intermolecular metathesis reactions of cyclic peptides and b) Topochemical reactions of cyclic molecule with two diynes

Helical polymers have structural regularity, which can be used as precursors for the production of molecular tubes for fixing the structure (Figure 9). In contrast to the integration of cyclic molecules via weak intermolecular interactions, it is easier to bring reaction points on helical polymers into close proximity by intramolecular conformational changes and control of length of the molecular tubes. Hecht *et al.* reported a first approach to molecular

Figure 9. A concept of tubulation through formation of helical polymers

tube synthesis from a helical polymer.[47a] The *m*-phenylenediethynylene polymer could adopt a helical conformation, in which reactive alkenes were oriented within close proximity for subsequent covalent stabilization of the tubular nanoobject by [2+2] cyclization (Figure 10a).[47] The degree of cross-linking could be roughly estimated to be approximately 20–30%. Itami *et al.* developed a novel synthetic method using efficient cross-linking of 1,3-butadiyne in the main chain of helical poly(*m*-phenylenediethynylene) by light induced chain reactions (Figure 10b).[48]

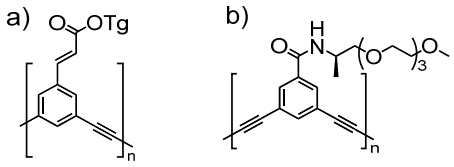

Figure 10. Structures of helical polymers with different reaction point: a) Alkenes and b) diynes

When synthesizing cyclic molecules and polymers as shown in Figure 8 and Figure 10, the low yields were caused by multi-step reactions and purification due to the inefficiency of cyclization and the requirement of narrow molecular weight distributions. It is considered desirable to synthesize molecular tubes from small units (Figure 11). Aida *et al.* demonstrated that an amphiphilic hexaperi-hexabenzocoronene self-assembles to form a discrete nanotubular object in an organic solvent (Figure 12).[49] Supramolecular helical polymers can be effectively converted to molecular tubes by cross linking reactions, such as metathesis reaction,[50] light-induced cyclization,[51] and formation of disulfides.[52]

Figure 11. Tubulation through the formation of a helical polymer from amphiphilic molecules

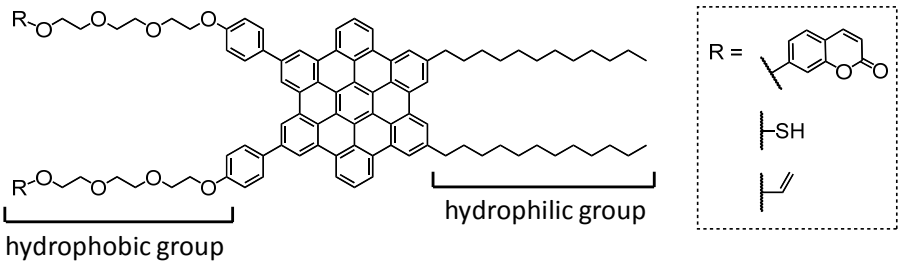

Figure 12. Amphiphilic hexaperi-hexabenzocoronene with cross linking points as a unit of molecular tubes

Template Strategy

The template method is another strategy to prepare molecular tubes. The template molecule can control the length and cavity size of the resultant molecular tubes (Figure 13). Harada *et al.* reported the first template synthesis of long cyclodextrin tubes, in which cyclodextrins formed rotaxanes[53] via non-covalent interactions with poly(ethylene glycol) before the tubulation (Figure 13a, 14a).[32] Zimmerman *et al.* successfully synthesized molecular tubes fixing basic units on template molecules through covalent bonds before the tubulation (Figure 13a, 14b).[54] Chujo *et al.* and Hupp *et al.* synthesized molecular tubes from a porphyrin dimer through a metathesis reaction with a template (Figure 13b, 15a).[55] Anderson *et al.* developed synthetic methods for the production of porphyrin rings with π-

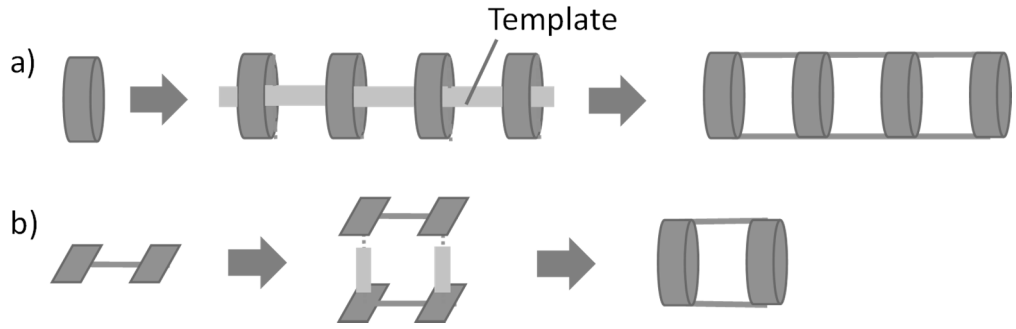

Figure 13. Template-assisted tubulation using cyclic molecules: a) Cyclic or disk structured molecules as basic units and b) linear dimers as basic units

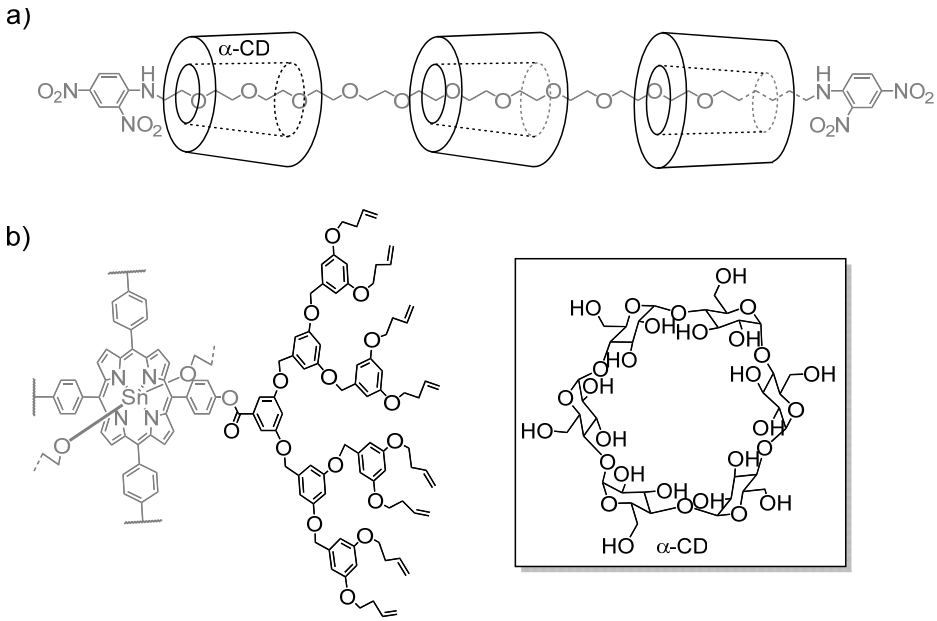

Figure 14. Two methods to bring reaction points around the basic units into close proximity via the template strategy: a) Non-covalent interactions between cyclodextrins and poly(ethylene glycol). b) Covalent bonding between basic units of alkenes and their templates

conjugation along the ring. His group applied the porphyrin rings to the preparation of a three-dimensional π-conjugated porphyrin tube (Figure 13b, 15b).[56]

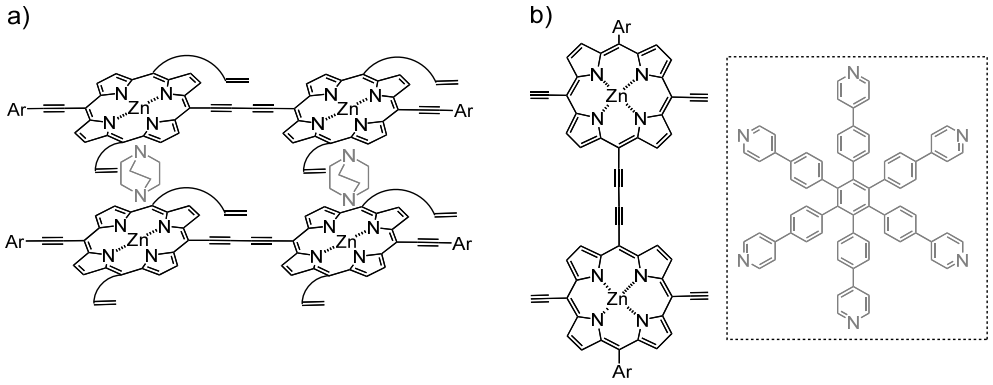

Figure 15. Structures of porphyrin oligomers and template molecules

Functional Molecular Tubes

As described above, two efficient methods (self-assembly and template strategy) have been developed to synthesize molecular tubes. Although π-conjugated molecular tubes have attractive optical properties, it is difficult to control both cavity size and length. In the case of self-assembly, length of molecular tubes depends on the infinite structures.[48] On the other hand, length of molecular tube prepared by the template method is limited to two units of porphyrins. It is a challenging task to control the structures of π-molecular tubes: length and cavity size. Synthetic method for structure-controlled molecular tubes will help to define the properties of the fabricated tubes.

The host–guest ability of molecular tubes, other than those based on cyclodextrin, was ambiguous. The host–guest complexation of molecular tubes has the potential to produce novel materials. Here, the author focuses his attention on π-conjugated porphyrin tubes as functional molecular tubes. Porphyrins are promising units for photovoltaics,[57] artificial photosynthesis,[58] two photon absorption,[59] and conductive materials.[60] The introduction of metals and substituents to the porphyrin units can easily modify the optical properties of the resulting material. In addition to the optical properties, metalloporphyrins can recognize molecules through coordination bonding and π–π interactions,[61] enabling porphyrin tubes to encapsulate molecules based on multiple interactions. In previous methods, porphyrin oligomers with defined length were required to be prepared in advance,[55] and porphyrin tubes longer than two units of porphyrins has never been synthesized. The author's interest focuses on developing a template synthesis technique for both length and cavity size-controlled porphyrin tubes. In this Dissertation, a novel synthetic method for structure-controlled porphyrin tubes (Chapters 1, 3, and 5) and the inclusion ability of cyclic molecules as the basic unit in the porphyrin tube (Chapters 1, 2, and 4) are described.

Thesis Overview

Herein, the focus will be on molecular tubes using optically active porphyrins; the goal is to functionalize the tube through host–guest complexation. It is necessary to develop more efficient and controllable synthetic methods for structure-controlled porphyrin tubes. The following aspects were investigated to realize molecular tubes with defined function and their inclusion abilities: (1) template synthesis of cavity-size controlled porphyrin rings and inclusion abilities through various interactions (Chapter 1). (2) Construction of an artificial photosynthetic system comprised of a porphyrin ring stabilized by a guest complex (Chapter 2). (3) Template synthesis of length controlled porphyrin tubes (Chapter 3, 5). (4) Control of molecular dynamics in the cavity of a porphyrin tube (Chapter 4).

In Chapter 1, the template-assisted synthesis of cavity size controlled porphyrin rings as basic units of porphyrin tubes and their inclusion abilities are described (Figure 16).[62] The cyclic molecules encapsulate different molecules via various interactions. When converting the esters in the side chain to carboxylates, the cyclic molecules formed host–guest complexes even in aqueous solvent.

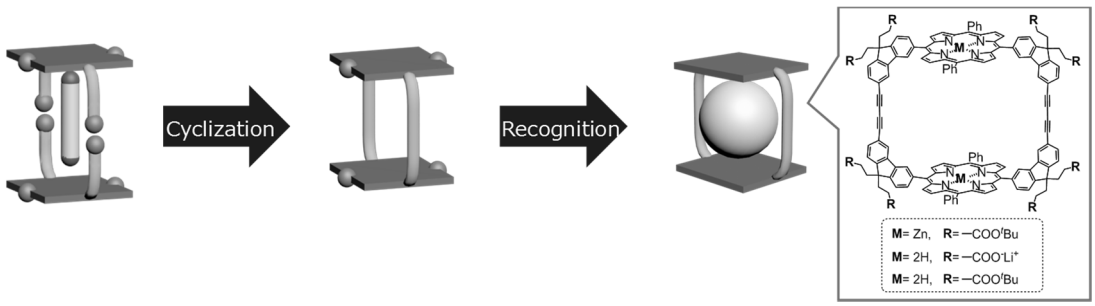

Figure 16. Template-assisted synthesis of cavity size controlled porphyrin rings and their inclusion ability

In Chapter 2, the formation of hetero face-to-face porphyrins composed of a cyclic zinc porphyrin ring and a ruthenium porphyrin is described (Figure 17).[63] Effective photo-induced electron transfer from the zinc porphyrin to ruthenium porphyrin in the cavity of a porphyrin ring was observed, which is promising for artificial photosynthesis. It was determined that coordination bonds between ruthenium atoms and DABCO (1,4-diazabi-cyclo[2.2.2]octane) were kinetically stabilized by the cooperativity effect of the host–guest complexation and coordination bonds.

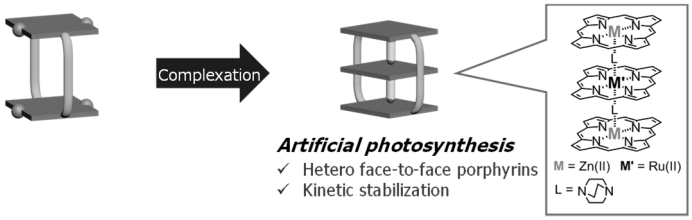

Figure 17. Construction of a hetero face-to-face porphyrin array for artificial photosynthesis

In Chapter 3, a novel template method for synthesis of a length-controlled porphyrin tube via selective dimerization of porphyrin rings is described (Figure 18).[64] Template molecules accelerated the tubulation even when highly diluted. The structures of template molecules were shown to play an important role in the tubulation.

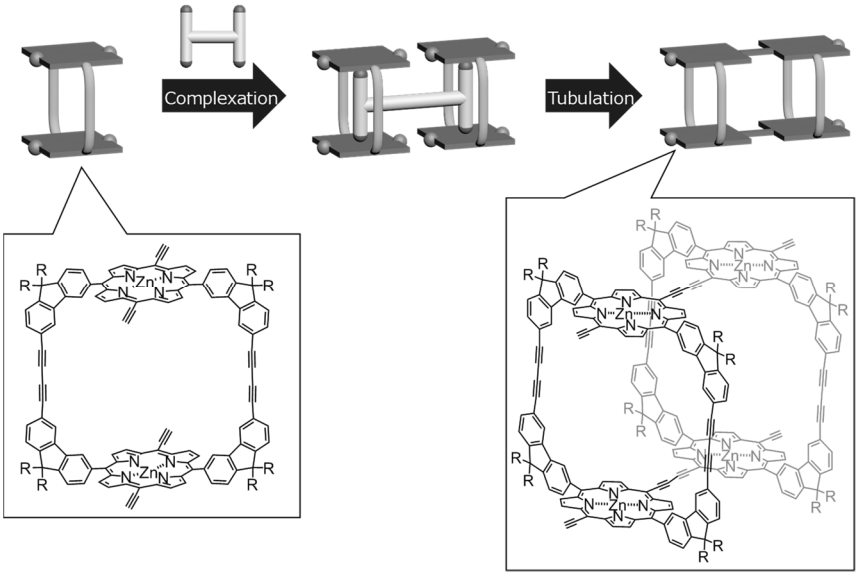

Figure 18. Template-assisted synthesis of a porphyrin tube via selective dimerization of porphyrin rings

In Chapter 4, the inclusion ability of the porphyrin tube was studied. Encapsulating a porphyrin dimer (Figure 19),[65] the porphyrin tube formed a triple-stranded dimer. The host–

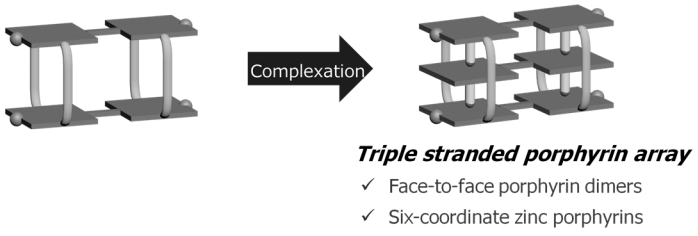

Figure 19. Planarization of a porphyrin dimer in the cavity of the porphyrin tube

guest complexation stabilized a six-coordinated zinc porphyrin, which generally forms a 1 : 1 complex with the amines in solution, due to fixation of the amines in the tube cavity. The NMR studies suggested that the porphyrin dimer was fixed in a planar structure in the cavity.

In Chapter 5, the template-assisted tubulation via selective trimerization of porphyrin rings was performed (Figure 20). In contrast to Chapter 3, trimerization of porphyrin rings proceeded through the efficient complexation between porphyrin rings and the template.[66] The template method can even be applied to longer porphyrin tubes.

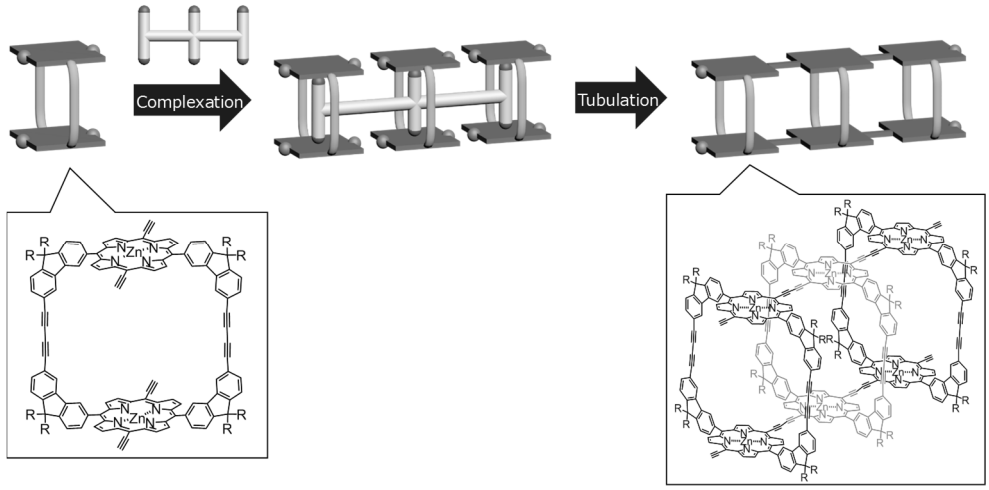

Figure 20. Template-assisted synthesis of a porphyrin tube via selective trimerization

Herein, the two-step template method for the selective synthesis of structure-controlled porphyrin tubes is described. Functionalizing porphyrin tubes based on host–guest complexation is detailed, and the dynamics of guest molecules in the cavity of porphyrin rings as basic units of porphyrin tubes was clarified. The template method and inclusion abilities of the porphyrin tubes are expected to give useful information for the functionalization of the tubes upon host–guest complexation.

References and Notes

1. a) Cooper, G. M. *The Cell, A Molecular Approach*, 2nd ed., Sinauer Associates Inc, Sunderland, UK, **2000**. b) Zheng, J.; Trudeau, M. C. *Handbook of Ion Channels*, CRC Press, New York, USA, **2016**.
2. a) Blake, C. C. F.; Koenig, D. F.; Mair, G. A.; North, A. C. T.; Phillips, D. C.; Sarma, V. R. *Nature* **1965**, *20*, 757. b) Doyle, D. A.; Morais Cabral, J.; Pfuetzner, R. A.; Kuo, A.; Gulbis, J. M.; Cohen, S. L.; Chait, B. T.; MacKinnon, R. *Science* **1998**, *280*, 69.
3. a) Atwood, J. L.; Davies, J. E. D.; Mannicol, D. D.; Vögtle, F. *Comprehensive Supramolecular Chemistry*, Pergamon, Oxford, UK, **1996**. b) Steed, J. W.; Atwood, J. L.

Supramolecular Chemistry, 2nd ed., Wiley, Weinheim, Germany, **2009**. c) Davis, F.; Higson, S. *Macrocycles: Construction, Chemistry and Nanotechnology Applications*, Wiley, Weinheim, Germany, **2011**.

4. a) Pedersen, C. J. *J. Am. Chem. Soc.* **1967**, *89*, 2495. b) Pedersen, C. J. *J. Am. Chem. Soc.* **1967**, *89*, 7017.
5. Kyba, E. P.; Siegel, M. G.; Sousa, L. R.; Sogah, G. D. Y.; Cram, D. J. *J. Am. Chem. Soc.* **1973**, *95*, 2691.
6. Dietrich, B.; Lehn, J.-M.; Sauvage, J.-P. *Tetrahedron Lett.* **1969**, *10*, 2889.
7. a) Villiers, A. *Compt. Rend. Fr. Acad. Sci.* **1891**, *112*, 435. b) Villiers, A. *Compt. Rend. Fr. Acad. Sci.* **1891**, *112*, 536.
8. a) Ogoshi, T.; Kanai, S.; Fujinami, S.; Yamagishi, T.; Nakamoto, Y. *J. Am. Chem. Soc.* **2008**, *130*, 5022. b) Ogoshi, T.; Yamagishi, T.; Nakamoto, Y. *Chem. Rev.* **2016**, *116*. 7937.
9. a) Gutsche, G. D.; Muthukrishnan, R. *J. Org. Chem.* **1978**, *43*, 4905. b) Gutsche, C. D. *Calixarenes: An Introduction,* 2nd ed., Royal Society of Chemistry, Cambridge, UK, **2008**.
10. a) Behrend, R.; Meyer, E.; Rusche, F. *Liebig Ann. Chem.* **1905**, *339*, 1. b) Barrow, S. T.; Kasera, S.; Rowland, M. J.; del Barrio, J.; Scherman, O. A. *Chem. Rev.* **2015**, *115*, 12320.
11. a) Jasti, R.; Bhattacharjee, J.; Neaton, J. B.; Bertozzi, C. R. *J. Am. Chem. Soc.* **2008**, *130*, 17646. b) Lewis. S. L. *Chem. Soc. Rev.* **2015**, *44*, 2221. c) Segawa, Y.; Ito, H.; Itami, K. *Nat. Rev. Mater.* **2016**, *1*, 15002.
12. a) Fujita, M.; Yazaki, J.; Ogura, K. *J. Am. Chem. Soc.* **1990**, *112*, 5645. b) Cook, T. R.; Zheng, Y.-R.; Stang, P. J. *Chem. Rev.* **2013**, *113*, 734.
13. a) Suzuki, K.; Sato, S.; Fujita, M. *Nat. Chem.* **2010**, *2*, 25. b) Fujita, D.; Suzuki, K.; Sato, S.; Yagi-Utsumi, M.; Yamaguchi, Y.; Mizuno, N.; Kumasaka, T.; Takata, M.; Noda, M.; Uchiyama, S.; Kato, K.; Fujita, M. *Nat. Commun.* **2012**, *3*, 1093.
14. Bissell, R. A.; Córdova, E.; Kaifer, A. E.; Stoddart, J. F. *Nature* **1994**, *369*, 133.
15. a) Livoreil, A.; Dietrich-Buchecker, C. O.; Sauvage, J.-P. *J. Am. Chem. Soc.* **1994**, *116*, 9399. b) Cárdenas, D. J.; Livoreil, A.; Sauvage, J.-P. *J. Am. Chem. Soc.* **1996**, *118*, 11980.
16. Wilson, M. R.; Solà, J.; Carlone, A.; Goldup, S. M.; Lebrasseur, N.; Leigh, D. A. *Nature* **2016**, *534*, 235.
17. a) CIBA Foundation Symposium, *Host–Guest Molecular Interactions: From Chemistry to Biology*, Wiley, Weinheim, Germany, **1991**. b) Lodish, H.; Berk, A.; Kaiser, C. A.; Krieger, M.; Scott, M. P.; Bretscher, A.; Ploegh, H.; Matsudaira, P. *Molecular Cell Biology*, W. H. Freeman & Co Ltd, New York, USA, **2007**.
18. Martí-Centelles, V.; Pandeay, M. D.; Burguete, M. I.; Luis, S. V. *Chem. Rev.* **2015**, *115*, 8736.

19. a) Yamamoto, M.; Tanaka, Y.; Horikoshi, K. *Agric. Biol. Chem.* **1972**, *36*, 1819. b) Bender, H. *Arch. Microbiol.* **1977**, *111*, 271. c) Kato, T.; Horikosi, K. *Agric. Biol. Chem.* **1986**, *50*, 2161.
20. a) Pedersen, C. J. *Org. Synth.* **1972**, *52*, 66. b) Greene, R. N. *Tetrahedron Lett.* **1972**, 1793.
21. Furlan, R. L. E.; Otto, S.; Sanders, J. K. M. *Proc. Natl. Acad. Sci. USA* **2002**, *99*, 4801.
22. Maynard, H. D.; Grubbs, R. H. *Macromolecules* **1999**, *32*, 6917.
23. Ro, S.; Rowan, S. J.; Pease, A. R.; Cram, D. J.; Stoddart, J. F. *Org.Lett.* **2000**, *2*, 2411.
24. a) Saalfrank, R. W.; Stark, A.; Peters, K.; von Schnering, H. G. *Angew. Chem., Int. Ed. Engl.* **1988**, *27*, 851. b) Beissel, T.; Powers, R. E.; Raymond, K. N. *Angew. Chem., Int. Ed. Engl.* **1996**, *35*, 1084. c) Ward, M. D. *Chem. Commun.* **2009**, 4487.
25. a) Roche, S.; Haslam, C.; Heath, S. L.; Thomas, J. A. *Chem. Commun.* **1998**, 1681. b) Suzuki, K.; Tominaga, M.; Kawano, M.; Fujita, M. *Chem. Commun.* **2009**, 1638.
26. Hiraoka, S.; Harano, K.; Shiro, M.; Ozawa, Y.; Yasuda, N.; Toriumi, K.; Shionoya, M. *Angew. Chem., Int. Ed.* **2006**, *45*, 6488.
27. a) Olenyuk, B.; Whiteford, J. A.; Fechtenkotter, A.; Stang, P. J. *Nature* **1999**, *398*, 796. b) Argent, S. P.; Adams, H.; Riis-Johannessen, T.; Jeffery, J. C.; Harding, L. P.; Ward, M. D. *J. Am. Chem. Soc.* **2005**, *128*, 72.
28. Olenyuk, B.; Levin, M.D.; Whiteford, J. A.; Shield, J. E.; Stang, P. J. *J. Am. Chem. Soc.* **1999**, *121*, 10434.
29. Fujita, D.; Ueda, Y.; Sato, S.; Mizuno, N.; Kumasaka, T.; Fujita, M. *Nature* **2016**, *540*, 563.
30. a) Bakbo Block, M. A.; Kaiser, C.; Khan, A.; Hecht, S. *Top Curr. Chem.* **2005**, *245*, 89. b) Shimizu, T. *J. Polym. Sci., Part A: Polym. Chem.* **2006**, *44*, 5137. c) Shimizu, T. *Bull. Chem. Soc. Jpn.* **2008**, *81*, 1554. d) Kameta, N.; Minamikawa, H.; Masuda, M. *Soft Matter.* **2011**, *7*, 4539.
31. Bong, D. T.; Clark, T. D.; Granja, J. R.; Ghadiri, M. R. *Angew. Chem., Int. Ed.* **2001**, *40*, 988.
32. Harada, A.; Li, J.; Kamachi, M. *Nature* **1993**, *364*, 516.
33. Mamad-Hemouch, H.; Ramoul, H.; Taha, M. A.; Bacri, L.; Huin, C.; Przybylski, C.; Oukhaled, A.; Thiébot, C.; Patriarche, G.; Jarroux, N.; Pelta, J. *Nano Lett.* **2015**, *15*, 7748.
34. a) Harada, A.; Li, J.; Kamachi, M. *Macromolecules* **1993**, 26, 5698. b) Shimomura T.; Funaki, T.; Ito, K.; Choi, B.-K.; Hashizume, T. *J. Incl. Phenom. Macr. Chem.* **2002**, *44*, 275. c) Ikeda, T.; Lee, W. K.; Ooya, T.; Yui, N. *J. Phys. Chem. B* **2003**, *107,* 14. d) Samitsu, S.; Araki, J.; Shimomura, T.; Ito, K. *Macromolecules* **2008**, *41*, 5385.

35. a) Grozema, F. C.; van Duijnen, P. T.; Berlin, Y. A.; Ratner, M. A.; Siebbeles, L. D. A. *J. Phys. Chem. B* **2002**, *106*, 7791. b) Grimsdale, A. C.; Chan, K. L.; Martin, R. E.; Jokisz, P. G.; Holmes, A. B. *Chem. Rev.* **2009**, *109*, 897. c) Samiullah, M.; Moghe, D.; Scherf, U.; Guha, S. *Phys. Rev. B: Condens. Matter* **2010**, *82*, 205211.
36. a) Iijima, S. *Nature* **1991**, *354*, 56. b) Saito, R.; Dresselhaus, G.; Dresselhaus, M. S. *Physical Properties of Carbon Nanotubes*, Imperial College Press, London, UK, **1998**.
37. a) Wildoer, J. W. G.; Venema, L. C.; Rinzler, A. G.; Smalley, R. E.; Dekker, C. *Nature* **1998**, *391*, 59. b) Dresselhaus, M. S.; Dresselhaus, G.; Avouris, P. *Carbon Nanotubes Synthesis, Structure, Properties, and Applications,* Springer, New York, USA, **2001**.
38. Ghadiri, M. R.; Granja, J. R.; Milligan, R. A.; McRee, D. E.; Khazanovich, N. *Nature* **1993**, *366*, 324.
39. Clark, T. D.; Ghadiri, M. R. *J. Am. Chem. Soc.* **1995**, *117*, 12364.
40. Schmidt, G. M. J. *Pure Appl. Chem.* **1971**, *27*, 647.
41. Wegner, G. *Pure Appl. Chem.* **1977**, *49*, 443.
42. Wegner, G. *Z. Naturforsch. B* **1969**, *24*, 824.
43. Xu, Y.; Smith, M. D.; Geer, M. F.; Pellechia, P. J.; Brown, J. C.; Wibowo, A. C.; Shimizu, L. S. *J. Am. Chem. Soc.* **2010**, *132*, 5334.
44. Hsu, T.-J.; Fowler, F. W.; Lauher, J. W. *J. Am. Chem. Soc.* **2012**, *134*, 142.
45. Rondeau-Gagne, S.; Neabo, J. R.; Desroches, M.; Larouche, J.; Brisson, J.; Morin, J.-F. *J. Am. Chem. Soc.* **2013**, *135*, 110.
46. Rondeau-Gagne, S.; Neabo, J. R.; Desroches, M.; Levesque, I.; Daigle, M.; Cantin, K.; Morin, J.-F. *Chem. Commun.* **2013**, *4*, 9546.
47. a) Hecht, S.; Khan, A. *Angew. Chem., Int. Ed.* **2003**, *42*, 6021. b) Nelson, J. C.; Saven, J. G.; Moore, J. S.; Wolynes, P. G. *Science* **1997**, *277*, 1793.
48. Maeda, K.; Hong, L.; Nishihara, T.; Nakanishi, Y.; Miyauchi, Y.; Kitaura, R.; Ousaka, N.; Yashima, E.; Ito, H.; Itami, K. *J. Am. Chem. Soc.* **2016**, *138*, 11001.
49. Hill, J. P.; Jin, W.; Kosaka, A.; Fukushima, T.; Ichihara, H.; Shimomura, T.; Ito, K.; Hashizume, T.; Ishii, N.; Aida, T. *Science* **2004**, *304*, 1481.
50. a) Jin, W.; Fukushima, T.; Kosaka, A.; Niki, M.; Ishii, N.; Aida, T. *J. Am. Chem. Soc.* **2005**, *127*, 8284. b) Yamamoto, T.; Fukushima, T.; Yamamoto, Y.; Kosaka, A.; Jin, W.; Ishii, N.; Aida, T. *J. Am. Chem. Soc.* **2006**, *128*, 14337.
51. Motoyanagi, J.; Fukushima, T.; Kosaka, A.; Ishii, N.; Aida, T. *J. Polym. Sci., Part A: Polym. Chem.* **2006**, *44*, 5120.
52. Motoyanagi, J.; Fukushima, T.; Ishii, N.; Aida, T. *J. Am. Chem. Soc.* **2006**, *128*, 4220.
53. Harada, A.; Li, J.; Kamachi, M. *Nature* **1992**, *356*, 325.
54. Kim, Y.; Mayer, M. F.; Zimmerman, S. C. *Angew. Chem., Int. Ed.* **2003**, *42*, 1121.

55. a) Ishida, T.; Morisaki, Y.; Chujo, Y. *Tetrahedron Lett.* **2006**, *47*, 5265. b) Youm, K.-T.; Nguyen, S. T.; Hupp, J. T. *Chem. Commun.* **2008**, 3375.
56. Neuhaus, P.; Cnossen, A.; Gong, J. Q.; Herz, L. M.; Anderson, H. L. *Angew. Chem., Int. Ed.* **2015**, *54*, 7344.
57. a) Guldi, D. M. *Chem. Soc. Rev.* **2002**, *31*, 22. b) Li, L.-L.; Diau, E. W.-G. *Chem. Soc. Rev.* **2013**, *42*, 291.
58. a) Fukuzumi, S.; Kojima, T. *J. Mater. Chem.* **2008**, *18*, 1427. b) Drain, C. M.; Varotto, A.; Radivojevic, I. *Chem. Rev.* **2009**, *109*, 1630. c) Medforth, C. J.; Wang, Z.; Martin, K. E.; Song, Y.; Jacobsen, J. L.; Shelnutt, J. A. *Chem. Commun.* **2009**, 7261.
59. Pawlicki, M.; Collins, H. A.; Denning, R. G.; Anderson, H. L. *Angew. Chem., Int. Ed.* **2009**, *48*, 3244.
60. a) Grozema, F. C.; Houarner-Rassin, C.; Prins, P.; Siebbeles, L. D. A.; Anderson, H. L. *J. Am. Chem. Soc.* **2007**, *129*, 13370. b) Sedghi, G.; García-Suárez, V. M.; Esdaile, L. J.; Anderson, H. L.; Lambert, C. J.; Martín, S.; Bethell, D.; Higgins, S. J.; Elliott, M.; Bennett, N.; Macdonald, J. E.; Nichols, R. J. *Nat. Nanotech.* **2011**, *6*, 517.
61. Kadish, K. M.; Smith, K. M.; Guilard, R. *The Porphyrin Handbook* Vol. 6, Academic Press, Sandiego, USA, **2000**.
62. Terao, J.; Chiba, Y.; Fujihara, T.; Tsuji, Y. *Chem. Lett.* **2014**, *43*, 1374.
63. Chiba, Y.; Liu, M.; Tachibana, Y.; Fujihara, T.; Tsuji, Y.; Terao, J. *Chem. Asian. J.* **2017**, *12*, 1900.
64. Chiba, Y.; Tachibana, Y.; Fujihara, T.; Tsuji, Y.; Terao, J. *manuscript in preparation.*
65. Chiba, Y.; Fujihara, T.; Tsuji, Y.; Terao, J. *manuscript in preparation.*
66. Chiba, Y.; Oka, Y.; Fujihara, T.; Tsuji, Y.; Terao, J. *manuscript in preparation.*

Chapter 1

Template Synthesis of Cavity Size-Controlled Porphyrin Rings and the Inclusion Abilities

As a unit of a porphyrin tube, synthetic methods and the inclusion properties of cavity size-controlled porphyrin rings are reported. The cyclic molecules were selectively synthesized via template synthesis inhibiting excess polymerization. The cyclic molecules have two molecular recognition points; metals in porphyrins and π–conjugated planes of porphyrins. In organic solvent, the porphyrin rings encapsulated a pyridine derivative and fullerene through coordination bonds, π–π interactions, and charge transfer interactiona respectively. Upon conversion of esters on the cyclic molecule to carboxylates, the cyclic molecules recognized permethylated α-cyclodextrin via weak hydrophilic hydrophobic interactions in water. The porphyrin tube constructed by the porphyrin rings can recognize molecules through the multiple interactions.

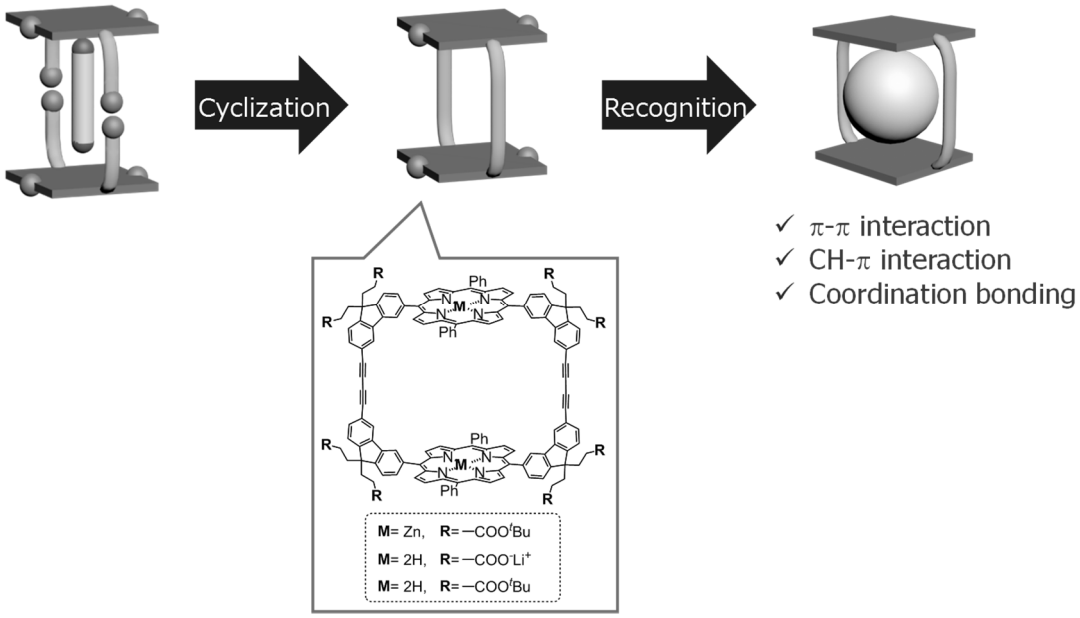

1-1. Introduction

Functionalization of molecular tubes constructed by covalent bonds via host–guest complexations will lead to novel materials that is capable of transporting and arranging molecules. Few examples[1] showed the host–guest complexes and the properties except for cyclodextrin tubes,[2] although synthetic methods for molecular tubes have been reported.[3] It is essential to investigate the inclusion ability of molecular tubes toward applications. Considering cyclic molecules as basic units of molecular tubes, the inclusion ability of the cyclic molecules can be regarded as equivalents of one of the molecular tubes. If the cyclic molecules can form host–guest complexes with different guest molecules, the molecular tubes comprising of the cyclic molecules can realize various functionalization combining their functions.

Host–guest complexations proceed based on size complementarity and intermolecular interactions between host and guest molecules. Macrocyclic molecules[4] such as crown ethers,[5] cyclodextrins,[6] calix arenes,[7] pillar arenes,[8] and cucurbiturils[9] have been widely studied as host molecules to encapsulate different molecules or ions. These hosts can recognize appropriate size of guests. As a result, guest molecules can fit into their molecular cavities to form host–guest complexes. Not only size recognition but also interactions that are stronger than solvation of the host or guest are important in constructing the complexes; these include non-covalent bonds such as electrostatic and hydrophobic interactions, hydrogen bonds, van der Waals interactions, and charge-transfer interactions.[10]

Porphyrin rings were reported as functional host molecules capable of encapsulating fullerenes.[11] The complexes are promising for solar cells because of donor–accepter interactions between porphyrins[12] and fullerenes.[13] In terms of synthesizing cyclic molecules, however, cyclization reactions are difficult due to competitive polymerizations. Sanders *et al.* developed a synthetic method for porphyrin rings using amine template.[14] In this method, cyclization reactions with the template molecules under highly diluted conditions effectively afforded the cyclic molecules with controlling dimerization and trimerization.

In organic solvents, porphyrin rings can recognize π conjugate molecules and amines through π–π interactions, charge transfer interactions, and coordination bonds.[11] If a porphyrin ring as a basic unit of the porphyrin tube recognizes different molecules in not only organic solvents but also water, the porphyrin tube is expected to be functionalized based on various host–guest complexation including weak CH–π interactions. In this chapter, template assisted synthesis of the cavity size-controlled porphyrin rings with hydrophobicity or hydrophilicity and the inclusion abilities will be reported.

1-2. Results and Discussions

1-2-1. Design of Porphyrin Rings

A porphyrin ring **A** consists of a rigid cyclic π-conjugated system with zinc porphyrins and fluorenes (Figure 1-1). The two opposite porphyrins are connected by butadiyne moieties. **A** can undergo different interactions with guests, such as the formation of coordination bonds between zinc atoms of the porphyrins and nitrogen atoms of a guest molecule, or π–π interactions arising from the π-conjugated planes of the porphyrins. Transforming the ester groups on the external surface of **B** to carboxylate groups gives rise to **C** which would be soluble in water. **C** can encapsulate lipophilic molecules through hydrophobic interactions in water.

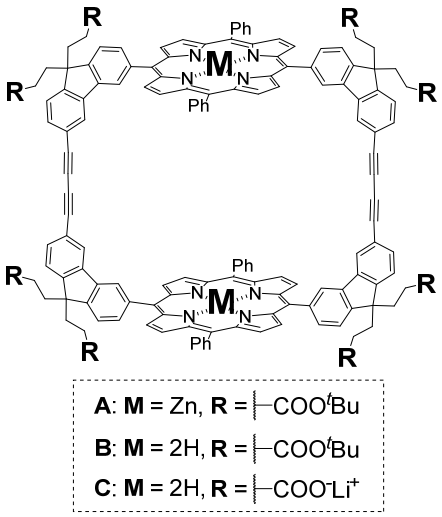

Figure 1-1. Porphyrin rings.

1-2-2. Template Synthesis of Porphyrin Rings

The key starting material **4** was prepared in four steps from the previously reported 3,6-dibromofluorene **1**,[15] which was esterified and subjected to Sonogashira coupling followed by Miyaura borylation reactions to introduce the alkyne and boron functional groups, respectively (Scheme 1-1). The synthesis of **B** is summarized in Scheme 1-2. The Suzuki–Miyaura cross-coupling reaction of **4** with dibromo zinc porphyrin **5**, followed by deprotection of the *tert*-butyldimethylsilyl (TBS) groups afforded **6**. The Sanders group reported an amine-template synthesis based on the coordination between the metal centers (zinc atoms) of metalloporphyrins and pyridine derivatives for the selective synthesis of porphyrin rings.[14]

Scheme 1-1. Synthesis of the fluorene unit

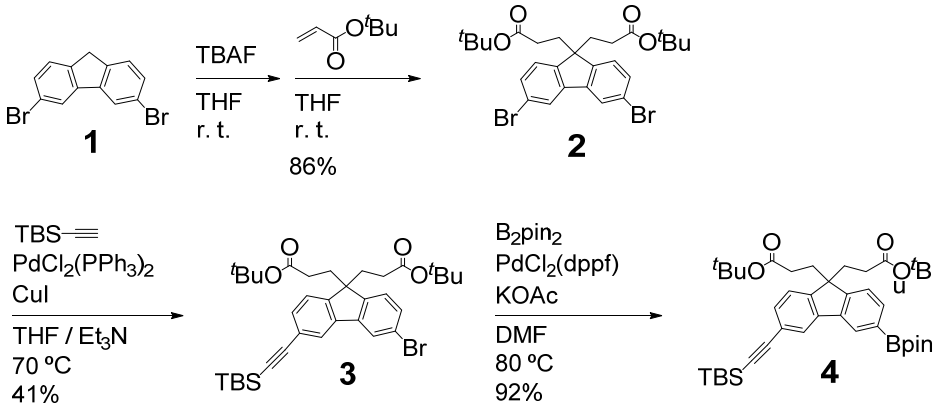

In this method, the precursors of the porphyrin rings approach each other because of coordination bonds between the zinc ions in the porphyrin and the nitrogen atoms in the bipyridine, which leads to the formation of the porphyrin rings in high yield. Based on this method, the cyclodimerization of **6** under high-dilution conditions using 1,4-di(pyridin-4-yl)benzene **7** as the template, followed by the removal of zincs and the template with acid, afforded free base porphyrin ring **B** in 62% yield (the templating effects of **7** can be clearly seen in Figure 1-7 in the Experimental Section). The hydrolysis of **B** with trifluoroacetic acid (TFA) followed by transformation of the carboxylic acid groups to the corresponding lithium salts by Li_2CO_3 afforded water-soluble porphyrin ring **C**. The metalation of **B** with zinc acetate yielded zinc porphyrin ring **A**. Although the *tert*-butyl groups of the ester moieties were disordered, the preliminary cavity size of the porphyrin ring was estimated by single-crystal X-ray structure analysis for **A**⊃**7** (Figure 1-2). In the cavity, the van der Waals height and width are 14.2 and 16.0 Å (Figure 1-8 in the Experimental Section), respectively. During our investigation of the inclusion abilities of the porphyrin rings, this preliminary cavity size was used as a reference for selecting guest molecules for the formation of host–guest complexes.

Scheme 1-2. Synthesis of porphyrin rings **A**, **B**, and **C**.

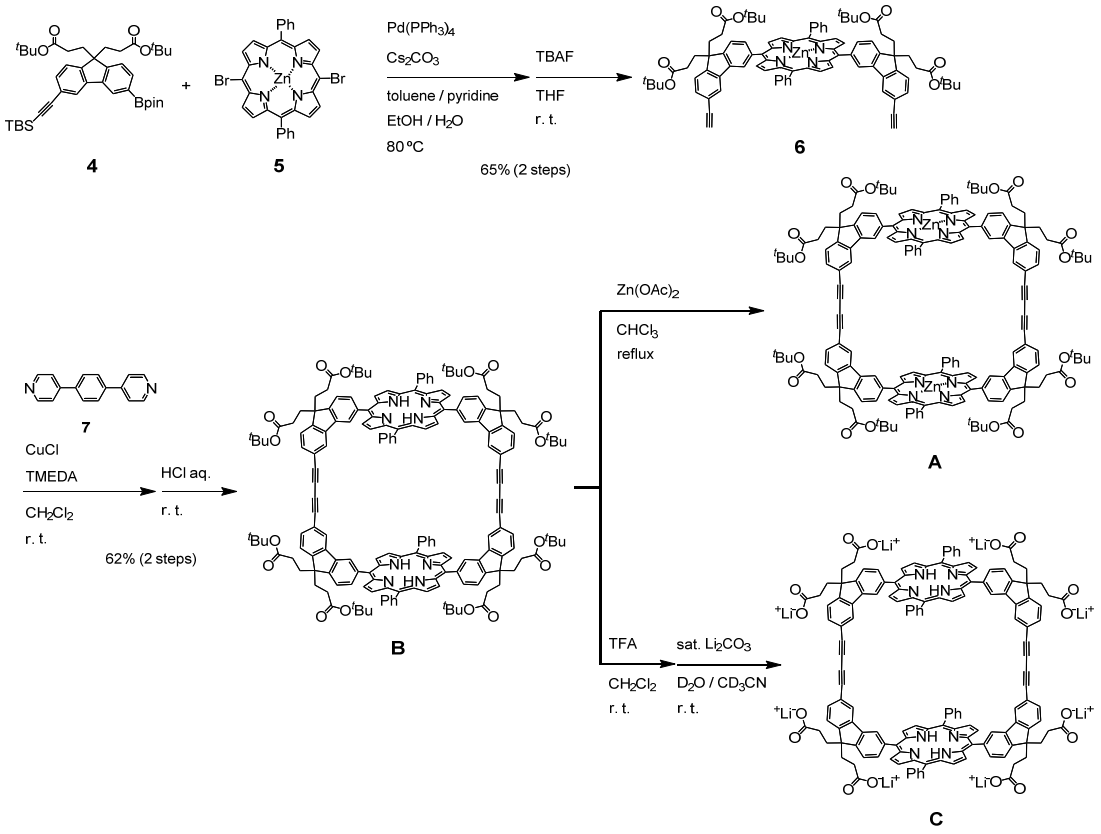

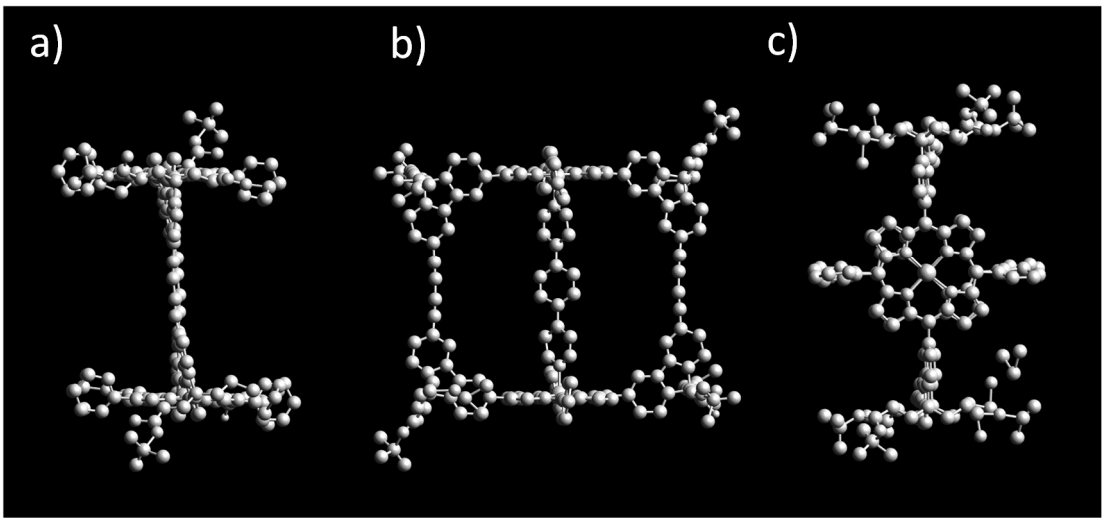

Figure 1-2. Single crystal X-ray structure of **A⊃7:** a) Side view, b) Front view, and c) Top view. A template molecule **7** was removed from (a) and (c) for the clarity.

1-2-3. The Inclusion Ability of Porphyrin Rings

The inclusion abilities of the porphyrin rings **A**, **B**, and **C** were then investigated. First, zinc porphyrin ring **A** and **7** were selected to form a host–guest complex through coordination bonds between the zinc atoms of **A** and the nitrogen atoms of **7**. When **7** (0.8–3.2 mM) was added to a 1.6 mM solution of **A** in $CDCl_3$ as shown in Scheme 1-3, new signals appeared in the high-field region of the ^1H NMR spectrum of the resulting complex **A⊃7** (Figure 1-3). These peaks can be attributed to **7** after coordination with the zinc porphyrin, resulting in the upfield shift of the signals owing to the ring current effect of the porphyrin. When **A** was titrated with 0–1 equiv of **7**, the ratio of **A⊃7** to total **7** increased with the increasing amount

Scheme 1-3. Synthesis of **A⊃7** through the coordination bonds

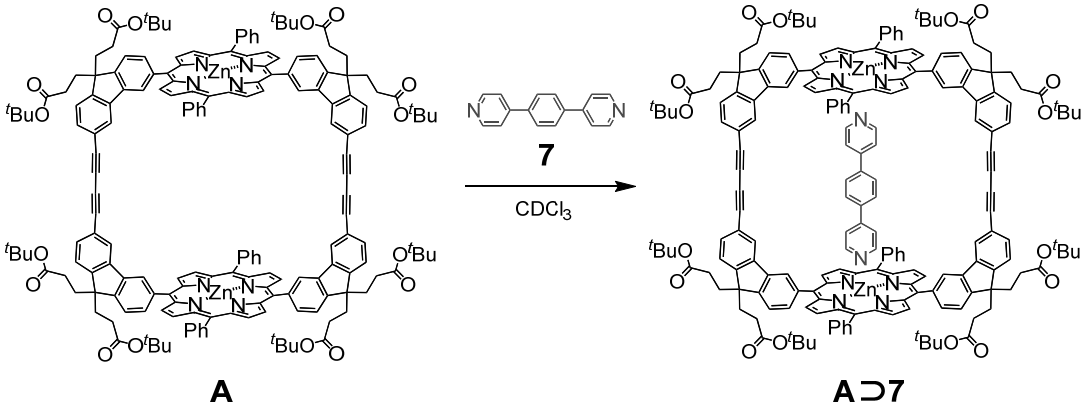

of guest (Figure 1-4). In the case of **7** > 1.0 equiv, the ratio of **A**⊃**7** did not change (Figure 1-4). This result indicates that the pair formed not a 1 : 2 coordination complex but a 1 : 1 host–guest complex, **A**⊃**7**, owing to two possible coordination bonds between the zinc centers in the opposing porphyrin rings and the nitrogen atoms of **7**.

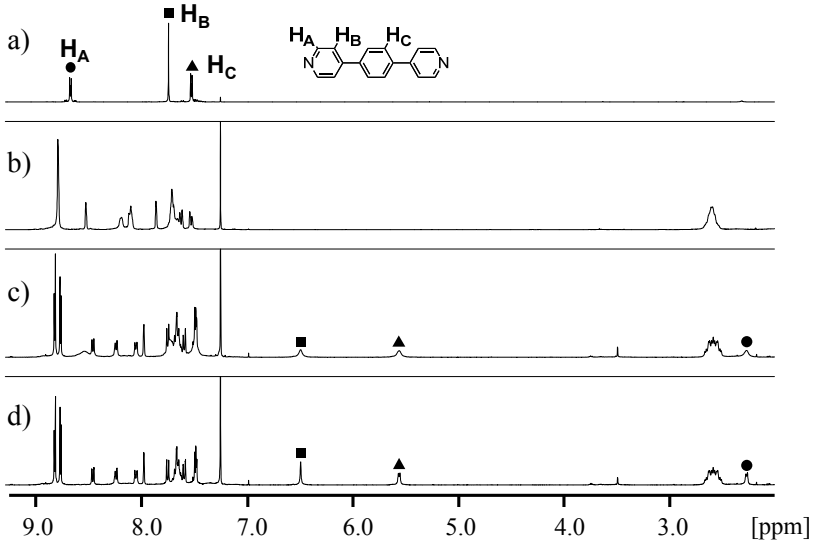

Figure 1-3. ^{1}H NMR spectra ($CDCl_3$, 298 K, 500 MHz) of **A** at a concentration of 1.6 mM with different equivalents of **7**: (a) **7**, (b) **A**, (c) 2.0 equiv of **7**, (d) 1.0 equiv of **7**. A circle, triangle, square indicate protons of H_A, H_B, and H_C assigned to **7**, respectively.

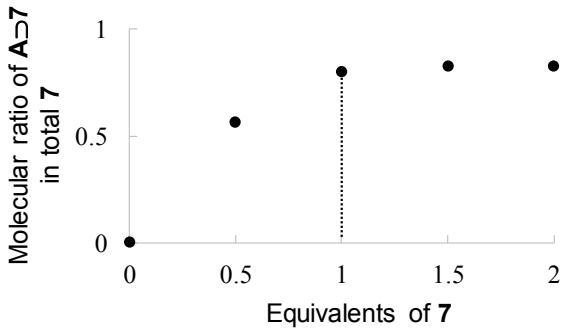

Figure 1-4. Molecular ratios of **A**⊃**7** to total **7** in the ^{1}H NMR spectra upon the addition of **7** to **A**.

Next, free base porphyrin ring **B** and **C60** were chosen as the host and guest molecules, respectively, to form a complex based on π–π interactions and charge transfer interation between the porphyrin and C_{60} (Scheme 1-4).[11] The matrix-assisted laser desorption/ionization time of flight (MALDI-TOF) MS spectrum of a 1 : 1 mixture of **B** and **C60** showed a peak at *m/z* 3418.262 ([**B** + **C60** + H^+]) (Figure 1-9 in the Experimental Section). Moreover, when 1.0 equiv of **C60** was added to a 1.1 mM solution of **B** in toluene-d_8, the C_{60} peak shifted from 142.14 to 141.59 pm in the ^{13}C NMR spectrum (Figure 1-10 in the Experimental Section). These results indicate the formation of the 1 : 1 inclusion complex **B** ⊃ **C60**.

Scheme 1-4. Synthesis of **B**⊃**C60** through the π–π interaction

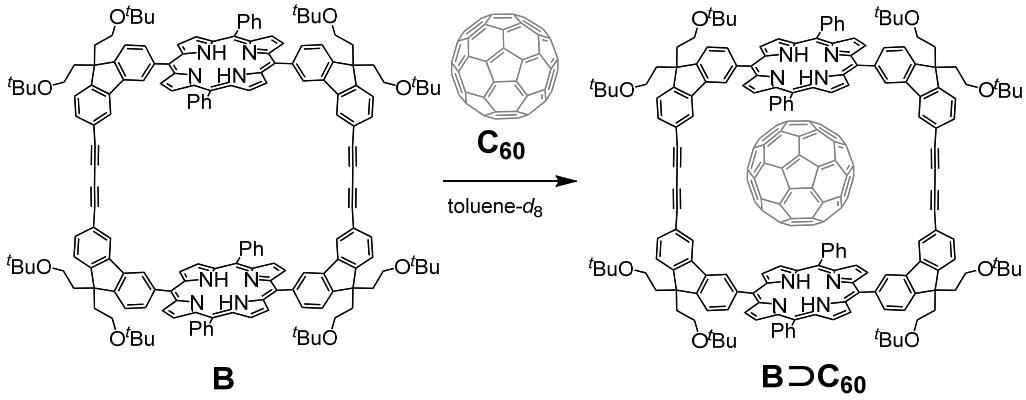

The water-soluble porphyrin ring **C** was expected to encapsulate a hydrophobic molecule with the proper size for the porphyrin ring cavity in water. The potential guest, permethylated α-cyclodextrin (PM α-CD), is a circular truncated cone whose maximum and minimum diameters are 18.5 and 11.0 Å (smaller than the cavity size of **C**), respectively.[16] A PM α-CD derivative having [1]-rotaxane structure **8**[17] was selected as a guest molecule to form **C**⊃**8** through hydrophilic–hydrophobic interactions (Scheme 1-5). When **8** was added to a 1.8 mM solution of porphyrin ring **C** in a saturated solution of Li_2CO_3 in D_2O / CD_3CN (1 /

Scheme 1-5. Synthesis of **B**⊃**8** through the hydrophobic interaction

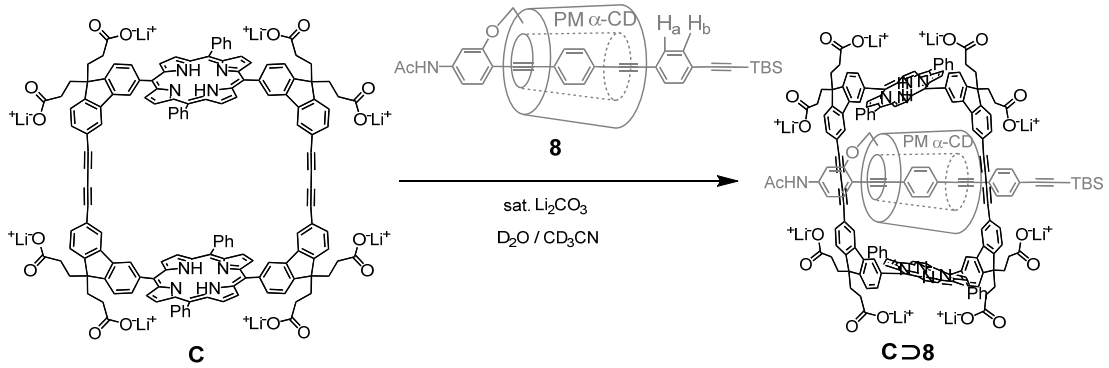

1, v / v), the peaks due to the PM α-CD (bracket around 3 ppm) and its molecular axis (circles) in the ^{1}H NMR spectrum shifted to the higher field because of the ring-current effects of the porphyrins (Figures 1-5). Although the peaks of H_a and H_b for the uncomplexed tri(phenyleneethynylene) axis of **8** appear as a singlet (a black circle in Figure 1-5a), those of **C**⊃**8** are split into two peaks owing to different ring-current effects from the porphyrins (Figures 1-5 c–e). That is, their distances from the porphyrin rings are different after the formation of **C**⊃**8** (Scheme 1-5). When the equivalents of [1]-rotaxane **8** were increased from 0.23 to 2.3 equiv by NMR titration, the chemical shift change of the peak assigned to the molecular axis ranged from 0.14 to 0.07 ppm (Figures 1-5). As guest exchange was fast on

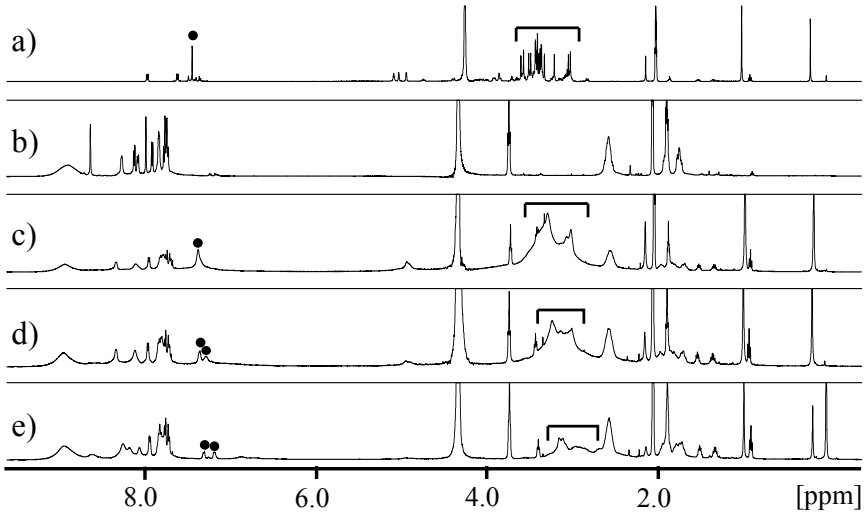

Figure 1-5. ^{1}H NMR spectra (D_2O / CD_3CN (1 / 1), 298 K, 500 MHz) of **C** at a concentration of 1.8 × 10 mM with different equivalents of **8**: (a) **8**, (b) **C**, (c) 2.3 equiv of **8**, (d) 1.2 equiv of **8**, and (e) 0.47 equiv of **8**. Circles indicate the protons H_a and H_b in Scheme 1-5. The bracket shows the protons assigned to the permethylated α-cyclodextrin moiety.

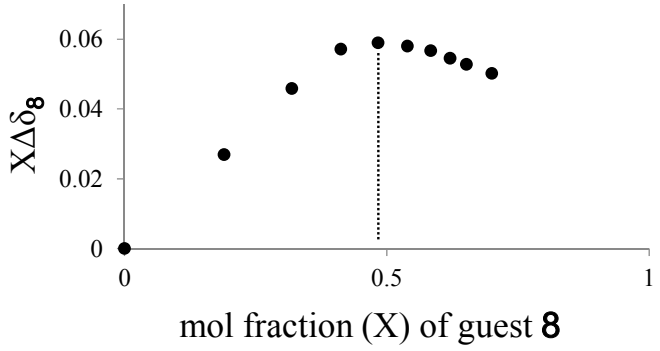

Figure 1-6. Job plots of various mixtures of **C** and **8** for H_a (Scheme 1-5) in a solution of saturated Li_2CO_3 in D_2O / CD_3CN (1 / 1, v / v). X indicates the mole fraction of guest molecule **8**, and $\Delta\delta_5$ is the change in the chemical shift of H_a for complexed versus free guest molecule **8**.

the NMR time scale, it was possible to observe a single peak corresponding to the average peak between **8** and **C** ⊃ **8**. Moreover, the amount of the free **8** increased when its concentration was increased to 2.3 equivalents. The Job plots for H_a upon the mixing of **C** with **8** showed a typical signature pattern for the formation of the 1 : 1 host–guest complex, **C**⊃**8** (Figure 1-6). This structure is the so-called host-in-host complex, which has rarely been reported.[18]

1-3. Conclusion

In conclusion, template-assisted cyclic dimerization of porphyrins with two alkynes successfully afforded cavity size-controlled porphyrin rings as units of porphyrin tubes The porphyrin rings could encapsulate different guests, exploiting various intermolecular interactions such as the formation of coordination bonds, as well as π–π , charge transfer, and CH-π interactions. The inclusion ability of porphyrin rings is expected to be equivalent of one of the porphyrin tube. The molecular recognition will lead to a novel functionalization of the porphyrin tube based on host–guest complexation.

1-4. Experimental Section

1-4-1. General Remarks

Materials: Reagents were purchased from commercial sources and used without further purification. Solvents were purified as follows: Reaction solvents were degassed through freeze-pump-thaw (three times), before use. Dry toluene and THF was purchased from Kanto Chemical and further purified by passage through activated alumina under positive argon pressure as described by Grubbs *et al.*[19] 3,6-dibromofluorene **1**,[15] 5,15-dibromo-10,20-diphenylporphinato]zinc(II) **5**,[20] and PM α-CD derivative **8**,[21] and 1-(4-iodophenyl)-2-(*tert*-butyldimethylsilyl)acetylene **10**[22] were prepared according to the reported procedures.

NMR Spectroscopy: ^{1}H NMR spectra were measured on a JEOL ECX-400 spectrometer and a Bruker AVANCE-500 spectrometer. The ^{1}H NMR chemical shifts are reported relative to tetramethylsilane (TMS, 0.00 ppm) or residual protonated solvents (7.26 ppm) in $CDCl_3$, or (5.32 ppm) in CD_2Cl_2. The ^{13}C NMR chemical shifts are reported relative to tetramethylsilane (TMS, 0.00 ppm) or solvent (77.16 ppm) in $CDCl_3$, (53.84 ppm) in CD_2Cl_2, or (136.44 ppm) in toluene-d_8.

Preparative recycling gel permeation chromatography (GPC): Preparative recycling GPC was performed with a JAI LC9104 System equipped with JAIGEL-1H and 2H columns, a JAI UV DETECTOR 310, and a JAI RI DETRCTOR RI-5, a JAI LC9130NEXT System equipped with

JAIGEL-2H and 2.5H columns, a JAI UV DETECTOR 370NEXT, and a JAI RI DETRCTOR RI 700NEXT, a JAI LC9140 System equipped with JAIGEL-2.5H and -3H columns, a JAI UV DETECTOR 310, and a JAI RI DETRCTOR RI-5.

Mass spectroscopy (MS): Matrix assisted laser desorption/ionization time-of-flight (MALDI-TOF) mass spectra were obtained with α-cyano-4-hydroxycinnamic acid (CHCA) as a matrix and NaTFA as a cationization reagent on Thermo Fisher Scientific LTQ orbitrapXL. ESI and atmospheric pressure chemical ionization (APCI) mass spectra were obtained on Thermo Fisher Scientific EXACTIVE.

1-4-2. Synthetic Procedures

Synthesis of 2

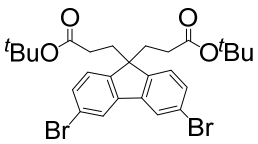

1 (8.00 g, 24.7 mmol) was dissolved in THF under Ar before adding tetrabutyl ammonium fluoride (61.8 mL, 1 M in THF, 61.8 mmol). The solution was stirred at r. t. for 30 min, after which *tert*-butyl acrylate (12.0 mL, 86.5 mmol) was added. The solution was stirred at r. t. for 80 min followed by the addition of water. The organic layer was extracted with CH_2Cl_2, and evaporated. The residue was purified by silica gel column chromatography (EtOAc / hexane = 1 / 16) to yield **2** (12.3 g, 86%) as a pale orange solid.

HR-MS (APCI-MS): (m/z) 601.0554 ([**1**+Na^+], $C_{27}H_{32}Br_2O_4Na$, calcd. 601.0565)
^{1}H NMR (500 MHz, CD_2Cl_2, r. t.): δ 7.83 (s, 2H, Ar-*H*), 7.49 (d, 2H, *J* = 8.1 Hz, Ar-*H*), 7.28 (d, 2H, *J* = 8.0 Hz, Ar-*H*), 2.31 (t, 4H, *J* = 8.2 Hz, -CH_2CH_2COO^{t}Bu), 1.42 (t, 4H, *J* = 8.2 Hz, -CH_2CH_2COO^{t}Bu), 1.28 (s, 18H, -COOC(CH_3)$_3$).
^{13}C NMR (126 MHz, CD_2Cl_2, r. t.): δ 172.43, 147.77, 142.40, 131.46, 125.31, 123.88, 121.93, 80.34, 53.95, 34.56, 30.26, 28.08.

Synthesis of 3

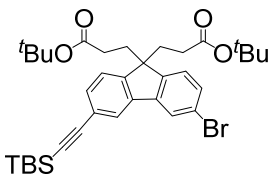

2 (4.00 g, 6.89 mmol), $PdCl_2(PPh_3)_2$ (244 mg, 0.348 mmol) and CuI (32.2 mg, 0.169 mmol) were dissolved in degassed THF : Et_3N (9 : 2, 330 mL) under Ar. (*tert*-Butyldimethylsilyl)acetylene (2.60 mL, 14.0 mmol) was added. The solution was stirred at 70 ºC for 14 h, and passed through the Celite pad followed by the addition of water. The organic layer was extracted with CH_2Cl_2, after which the residue was purified by silica gel column chromatography (EtOAc / hexane = 1 / 8) and GPC with $CHCl_3$ as an eluent to yield **3** (1.70 g, 41%) as a yellowish brown solid.

HR-MS (APCI-MS): (m/z) 661.2310 ([**3**+Na^+], $C_{35}H_{47}BrO_4SiNa$, calcd. 661.2319)

^{1}H NMR (500 MHz, CD_2Cl_2, r. t.): δ 7.87 (s, 1H, Ar-*H*), 7.80 (s, 1H, Ar-*H*), 7.48 (d, 2H, *J* = 8.0 Hz, Ar-*H*), 7.36 (d, 1H, *J* = 8.0 Hz, Ar-*H*), 7.29 (d, 1H, *J* = 8.0 Hz, Ar-*H*), 2.34 (t, 4H, *J* = 8.2 Hz, -CH_2CH_2COO^{t}Bu), 1.43 (m, a peak of H_2O was overlapped, CH_2CH_2COO^{t}Bu), 1.29 (s, 18H, -COOC(CH_3)$_3$), 1.03 (s, 9H, -$SiMe_2C(CH_3)_3$). 0.22 (s, 6H, -Si(CH_3)$_2$^{t}Bu).

^{13}C NMR (126 MHz, CD_2Cl_2, r. t.): δ 172.47, 149.41, 147.64, 142.97, 140.50, 132.46, 131.24, 125.30, 124.08, 123.87, 123.68, 123.19, 122.01, 106.02, 93.11, 80.29, 54.27, 34.71, 30.32, 28.18, 26.43, 17.08, –4.35.

Synthesis of 4

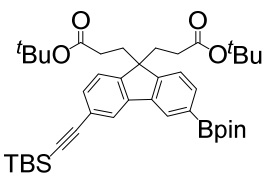

3 (1.42 g, 2.07 mmol), bis(pinacolato)diboron (1.66 g, 6.54 mmol), $PdCl_2$(dppf) (107 mg, 0.131mmol), and KOAc (904 mg, 9.17 mmol) were dissolved in dehydrated DMF (28.0 mL) under Ar. The solution was stirred at 80 ºC for 24 h and passed through the Celite pad followed by the addition of water. The organic layer was extracted with CH_2Cl_2, after which the residue was purified by silica gel column chromatography (EtOAc / hexane = 1 / 4) and GPC with $CHCl_3$ as an eluent to yield **4** (1.30 g, 92%) as a pale yellow solid.

HR-MS (APCI-MS): (m/z) 709.4055 ([**4**+Na^+], $C_{41}H_{59}BO_6SiNa$, calcd. 709.4066)

^{1}H NMR (500 MHz, CD_2Cl_2, r. t.): δ 8.14 (s, 1H, Ar-*H*), 7.88 (s, 1H, Ar-*H*), 7.78 (d, 1H, 7.50 Hz, Ar-*H*), 7.44 (d, 1H, *J* = 7.70 Hz, Ar-*H*), 7.41 (d, 1H, *J* = 7.50 Hz, Ar-*H*), 7.35 (s, 1H, Ar-*H*), 2.32 (t, 4H, *J* = 7.50 Hz, -CH_2CH_2COO^{t}Bu), 1.36-1.40 (m, several peaks overlapped, 4H and 12H, -CH_2CH_2COO^{t}Bu and B(pin)-*H*), 1.27 (s, 18H, -COOC(CH_3)$_3$), 1.03 (s, 9H, -$SiMe_2C(CH_3)_3$), 0.21 (s, 6H, -Si(CH_3)$_2$^{t}Bu).

^{13}C NMR (126 MHz, CD_2Cl_2, r. t.): δ 172.63, 152.03, 149.00, 141.74, 140.26, 134.99, 131.59, 126.76, 124.00, 123.48, 122.97, 122.91, 106.30, 92.62, 84.34, 80.19, 54.38, 34.84, 30.35, 28.11, 26.37, 25.14, 17.03, –4.41.

Synthesis of 6

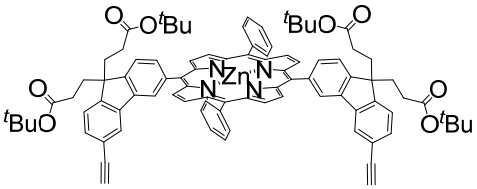

4 (1.22 g, 1.78 mmol), **5** (404 mg, 0.591 mmol), $Pd(PPh_3)_4$ (313 mg, 0.269 mmol), and Cs_2CO_3 (2.44 g, 7.42 mmol) were dissolved in degassed toluene / EtOH / H_2O (8 / 5 / 5, 14.4 mL) and dehydrated pyridine (0.50 mL) under Ar. The solution was stirred at 80 ºC for 12 h and passed through the Celite pad followed by the addition of water. The organic layer was extracted with CH_2Cl_2, after which the residue was purified by GPC with $CHCl_3$ as an eluent. The product was dissolved in degassed THF (160 mL) before tetrabutyl ammonium fluoride (1.18 mL, 1 M in

THF, 1.18 mmol) was added. The solution was stirred at r. t. for 40 min. The organic layer was extracted with CH_2Cl_2 and purified by GPC with $CHCl_3$ to yield **6** (544 mg, 65%) as a purple solid.

HR-MS (ESI-MS): (m/z) 1413.564([**6**+H^+], $C_{90}H_{86}N_4O_8Zn$, calcd. 1413.565)
^{1}H NMR (400 MHz, $CDCl_3$, r. t.): δ 9.02 (s, 8H, Ar-*H*), 8.58 (s, 2H, Ar-*H*), 8.28 (m, 6H, Ar-*H*), 7.89 (s, 2H, Ar-*H*), 7.77 (m, 8H, Ar-*H*), 7.53 (m, 4H, Ar-*H*), 3.03 (s, 2H, -C≡C-*H*), 2.58 (m, 8H, -CH_2CH_2COO^{t}Bu), 1.83 (m, 8H, -CH_2CH_2COO^{t}Bu), 1.43 (s, 36H, -COOC(CH_3)$_3$).
^{13}C NMR (126 MHz, $CDCl_3$, r. t.): δ 172.87, 172.84, 150.48, 150.37, 149.80, 147.49, 142.93, 142.65, 141.44, 138.77, 134.76-134.65 (several peaks overlapped), 132.33, 132.09, 131.99, 127.66, 126.71, 126.50, 124.14, 123.45, 121.72, 121.49, 121.29, 120.95, 83.80, 80.55, 54.09, 34.92, 30.52, 28.23.

Synthesis of B

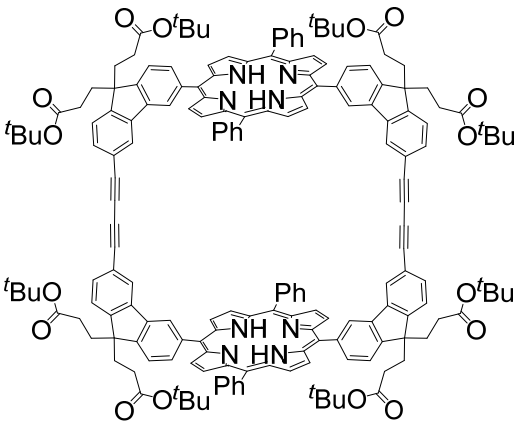

6 (504 mg, 0.354 mmol) and **7** (467 mg, 2.12 mmol) were dissolved in dehydrated CH_2Cl_2 (450 mL) and dried TMEDA (1.6 mL) under Ar before CuCl (2.46 g, 24.8 mmol) was added slowly. Ar was substituted to dry air, after which the solution was stirred at r. t. for 18 h. The solution was passed through the Celite pad before extracted with CH_2Cl_2. The solution was acidified by conc. HCl aq. The organic layer was extracted with CH_2Cl_2 and purified by GPC with $CHCl_3$ as an eluent to yield **B** (299 mg, 62%) as a purple solid.

HR-MS (MALDI TOF-MS): 2698.270 ([**B**+H^+], $C_{180}H_{169}N_8O_{16}$, calcd. 2698.265)
^{1}H NMR (500 MHz, $CDCl_3$, r. t.): δ 8.82 (s, 16H, Ar-*H*), 8.56 (s, 4H, Ar-*H*), 8.23 (br, 4H, Ar-*H*), 8.14-8.12 (m, 8H, Ar-*H*), 7.89 (s, 4H, Ar-*H*), 7.74-7.55 (m, 24H, Ar-*H*), 2.67-2.56 (m, 16H, -CH_2CH_2COO^{t}Bu), 1.92-1.76 (m, 16H, -CH_2CH_2COO^{t}Bu), 1.44 (s, 36H, -COOC(CH_3)$_3$), –2.64 (s, 4H, N*H*).
^{13}C NMR (126 MHz, $CDCl_3$, r. t.): δ 172.82, 150.35, 147.74, 142.16, 142.04, 141.46, 138.72, 135.09, 134.79-134.70 (several peaks overlapped), 132.64, 127.82, 126.79-126.22 (several peaks overlapped), 124.16, 123.66, 121.47, 121.35, 120.47, 119.80, 81.68, 80.60, 74.14, 54.19, 34.94, 30.54, 28.26.

Synthesis of A

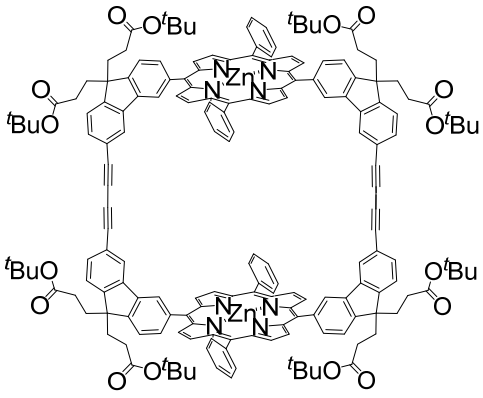

B (39.9 mg, 0.0148 mmol) and $Zn(OAc)_2$ (179 mg, 0.975 mmol) were dissolved in $CHCl_3$. The solution was refluxed overnight followed by the addition of water. The organic layer was extracted with CH_2Cl_2. Evaporation of an organic layer afforded **A** (31.3 mg, 79%). **A** was used for the complexation with **7** without further purification.

HR-MS (MALDI-TOF MS): (m/z) 2821.085 ([**A**]$^+$, $C_{180}H_{164}N_8O_{16}Zn_2$, calcd. 2821.085).

^{1}H NMR (500 MHz, $CDCl_3$, r. t.): δ 8.89 (s, 16H, Ar-*H*), 8.53 (s, 4H, Ar-*H*), 8.20 (d, 4H, *J* = 6.1 Hz, Ar-*H*), 8.11 (s, 8H, Ar-*H*), 7.84 (s, 4H, Ar-*H*), 7.72-7.66 (m, 16H, Ar-*H*), 7.62 (d, 4H, *J* = 8.9 Hz, Ar-*H*), 7.51 (d, 4H, *J* = 7.9 Hz, Ar-*H*), 2.58-2.52 (m, 16H, -C*H*$_2$CH$_2$COO^{t}Bu), 1.86-1.72 (16H, m, -CH$_2$C*H*$_2$COO^{t}Bu), 1.40 (s, 72H, -COOC(C*H*$_3$)$_3$).

^{13}C NMR (126 MHz, $CDCl_3$, r. t.): δ 172.84, 150.42, 150.35, 150.25, 147.46, 142.85, 142.68, 141.57, 138.56, 134.98, 134.66, 134.56, 132.64, 132.23, 131.95, 129.34, 127.58, 126.64, 126.61, 126.07, 124.02, 123.64, 123.55, 121.41, 121.18, 120.74, 93.13, 81.71, 80.58, 74.09, 54.13, 34.92, 30.51, 28.24.

Synthesis of C

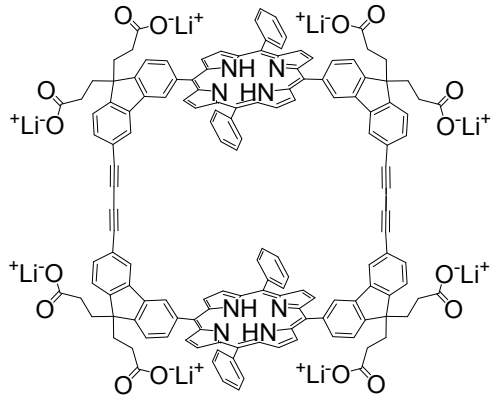

B (40.3 mg, 0.0149 mmol) was dissolved in CH_2Cl_2, followed by addition of TFA (680 μl, 8.86 mmol). The solution was stirred at r. t. overnight. The solid was obtained by filtration after addition of hexane to the solution. The solid was dissolved in sat. Li_2CO_3 solution in D_2O / CD_3CN (1 / 1, v / v) to yield **C**. **C** was used for the complexation with **8** without further purification.

Synthesis of 8

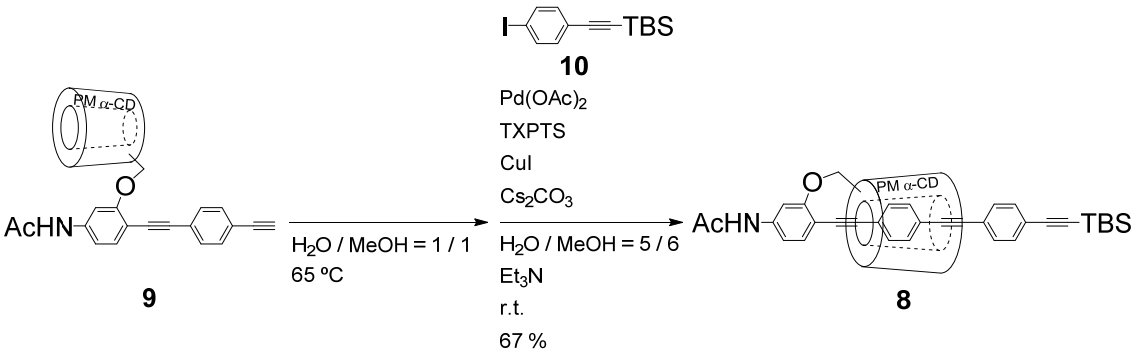

9 (1.05 g, 0.712 mmol) was dissolved in H_2O / MeOH (1 / 1, 30 mL) and then the solution was heated at 65 °C for 1 h under Ar. Cooling to r. t., the solution was added dropwise to a solution, MeOH / Et_3N (3 / 1, 4.0 mL), in which 1-(4-iodophenyl)-2-(*tert*-butyldimethylsilyl)acetylene **10** (368 mg, 1.07 mmol), $Pd(OAc)_2$ (16.2 mg, 0.0722 mmol), tris(2,4-dimethyl-5-sulfanatophenyl)phosphine trisodium salt (TXPTS) (71.7 mg, 0.110 mmol), CuI (0.95 mg, 0.0365 mmol), and Cs_2CO_3 (581 mg, 1.78 mmol) were dissolved, and then the reaction mixture was stirred at r. t. under Ar overnight. After the organic layer extracted with EtOAc, the solution was dried over Na_2SO_4. Purification of the residue by GPC with $CHCl_3$ as an eluent afforded **8** (803 mg, 67%) as a light yellow solid.

HR-MS (ESI-MS): 1699.817 ([**8**+NH_4^+], $C_{85}H_{123}N_2O_{31}Si$, calcd. 1699.819)

^{1}H NMR (500 MHz, CDCl$_3$, r. t.): δ 8.04 (d, 2H, *J* = 7.85 Hz, Ar-*H*), 7.60 (d, 2H, *J* = 7.85 Hz, Ar-*H*), 7.44-7.36 (m, 7H, Ar-*H*), 7.22(s, 1H, N*H*), 5.09-4.82 (m, 6H, CD-H_1), 4.41-2.84 (m, 87H, CD-*H*, OCH_3), 2.21 (s, 3H, -COCH_3), 1.00 (s, 9H, -SiMe$_2$C(CH_3)$_3$), 0.19 (s, 6H, -Si(CH_3)$_2$^{t}Bu)

^{13}C NMR (126 MHz, CDCl$_3$, r. t.): δ 168.33, 162.69, 139.91, 133.87, 132.54, 132.07, 131.53, 131.45, 123.67, 123.55, 122.99, 122.67, 114.29, 112.90, 112.00, 105.27, 100.94, 100.64, 100.33, 100.28, 100.10, 98.24, 95.14, 93.30, 90.95, 90.64, 88.74, 83.98, 82.99, 82.85, 82.71, 82.63, 82.55, 82.51, 82.29-81.18 (several peaks overlapped), 72.34, 72.05, 71.91, 71.74-71.28, 70.86, 70.37, 62.15, 62.04 (several peaks overlapped), 61.92, 61.90, 61.77, 59.24, 59.22, 59.10, 58.89, 58.84, 58.50, 58.17, 57.98, 57.85, 57.81, 57.67, 26.28, 24.97, 16.87, –4.50.

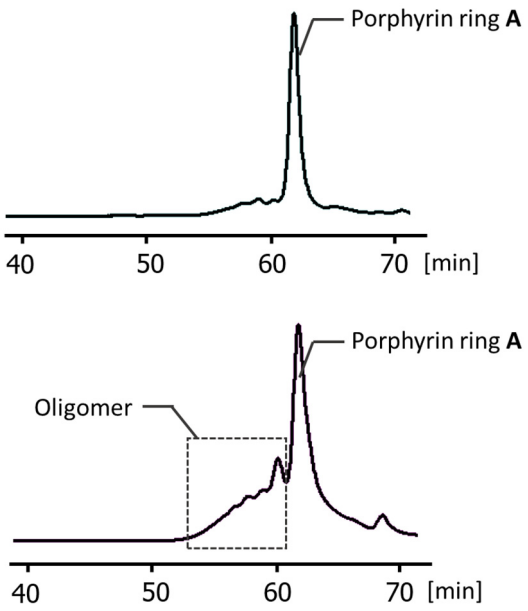

Figure 1-7. Analytical SEC chromatograms for cyclic dimerization of **6** with template molecule **7** (top) and without **7** (bottom) using THF as the eluent (UV). The dimerization conditions were the same for both reactions except for the presence or absence of **7**.

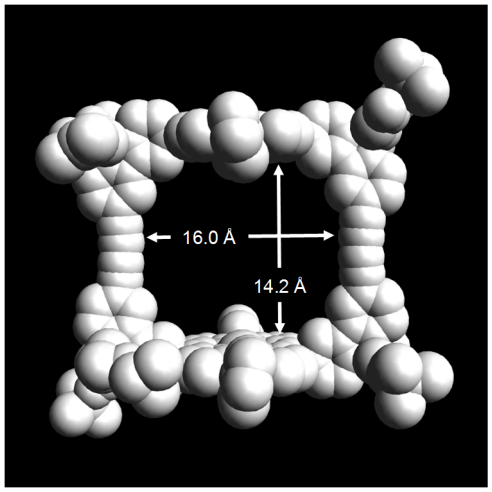

Figure 1-8. Single crystal structre of **A⊃7**, double-headed arrows indicate cavity size of porphyrin ring **A**.

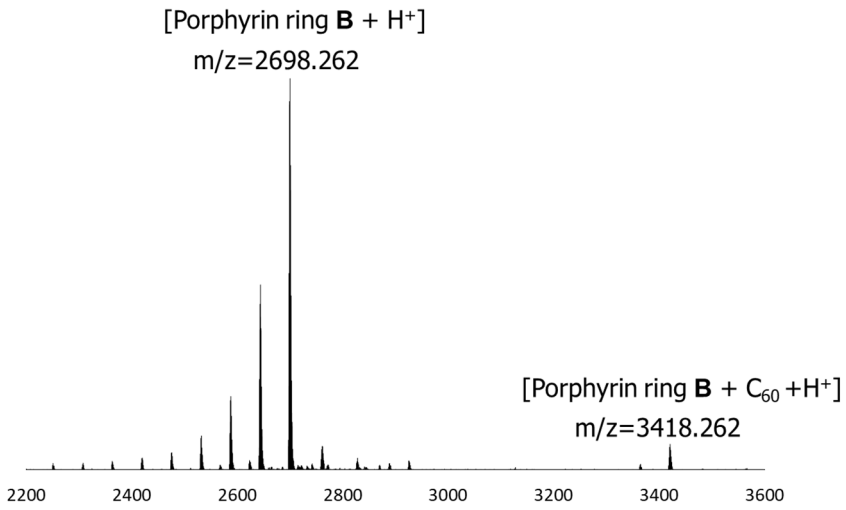

Figure 1-9. MALDI TOF-MS spectrum of a solution of a mixture with porphyrin ring **B** and **C60**.

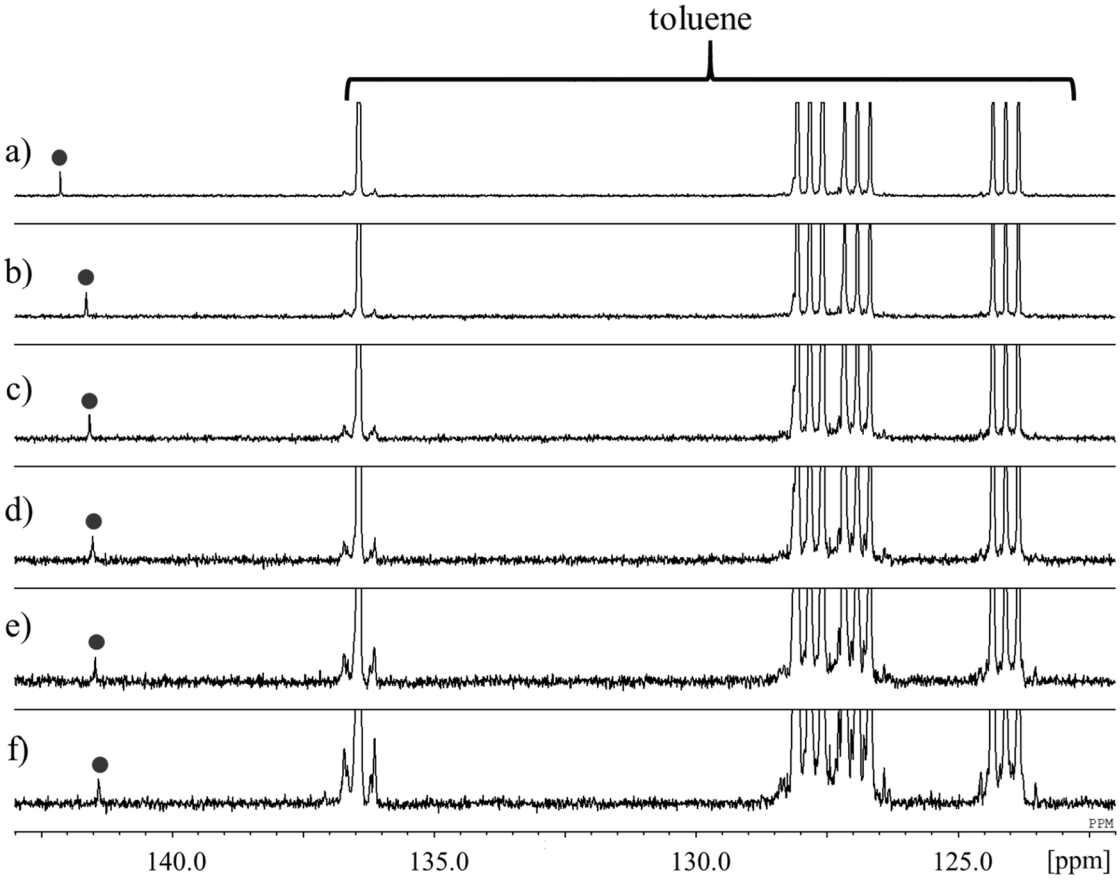

Figure 1-10. ^{13}C NMR spectra (toluene-d_8, 298 K, 400 MHz) of **B** at a concentration of 1.1 mM with different equivalents of **C60** : a) **C60**, b) 1.5 equiv of **C60**, c) 1.0 equiv of **C60**, d) 0.67 equiv of **C60**, e) 0.43 equiv of **C60**, and f) 0.25 equiv of **C60**. Circles indicate the peaks of **C60**.

References and Notes

1. a) Koh, K. N.; Araki, K.; Shinkai, S.; Asfarum, Z.; Vicens, J. *Tetrahedron Lett.* **1995**, *36*, 6095. b) Kim, S. K.; Lee, J. K.; Lee, S. H.; Lim, M. S.; Lee, S. W.; Sim, W.; Kim, J. S. *J. Org. Chem.* **2004**, 69, 2877.
2. a) Kalashnikov, Ph. A.; Kotel'nikov, G. V.; Moiseeva, S. P.; Topchieva, I. N. *Colloid J.* **2004**, *66*, 542. b) Samitsu, S.; Araki, J.; Shimomura, T.; Ito, K. *Macromolecules* **2008**, *41*, 5385. c) Mamad-Hemouch, H.; Ramoul, H.; Taha, M. A.; Bacri, L.; Huin, C.; Przybylski, C.; Oukhaled, A.; Thiébot, B.; Patriarche, G.; Jarroux, N. Pelta, J. *Nano Lett.* **2015**, *15*, 7748. d) Shimomura, T.; Funaki, T.; Ito, K.; Choi, B.; Hashizume, T. *J. Incl. Phenom. Macrocycl. Chem.* **2002**, *44*, 275. e) Liu, Y.; Yang, Z.-X.; Chen, Y.; Song, Y.; Shao, N. *ACS Nano* **2008**, *2*, 554.
3. a) Harada, A.; Li, J.; Kamachi, M. *Nature* **1993**, *364*, 516. b) Clark, T. D.; Ghadiri, M. R. *J. Am. Chem. Soc.* **1995**, *117*, 12364. c) Hecht, S.; Khan, A. *Angew. Chem., Int. Ed.* **2003**, *42*, 6021. d) Jin, W.; Fukushima, T.; Kosaka, A.; Niki, M.; Ishii, N.; Aida, T. *J. Am. Chem. Soc.* **2005**, *127*, 8284. e) Ishida, T.; Morisaki, Y.; Chujo, Y. *Tetrahedron Lett.* **2006**, *47*, 5265. f) Xu, Y.; Smith, M. D.; Geer, M. F.; Pellechia, P. J.; Brown, J. C.; Wibowo, A. C.; Shimizu, L. S. *J. Am. Chem. Soc.* **2010**, *132*, 5334.
4. a) Atwood, J. L.; Davies, J. E. D.; Mannicol, D. D.; Vögtle, F. *Comprehensive Supramolecular Chemistry*, Pergamon, Oxford, UK, **1996**. b) Steed, J. W.; Atwood, J. L. *Supramolecular Chemistry*, 2nd ed., Wiley, Weinheim, Germany, **2009**. c) Davis, F.; Higson, S. *Macrocycles: Construction, Chemistry and Nanotechnology Applications*, Wiley, Weinheim, Germany, **2011**.
5. a) Pedersen, C. J. *J. Am. Chem. Soc.* **1967**, *89*, 7017. b) Vögtle, F.; Weber, E. *Host-Guest Complex Chemistry: Macrocycles*, Spinger Verlag, Heidelberg, Germany,**1985**.
6. a) Villiers, A. *Compt. Rend. Fr. Acad. Sci.* **1891**, *112*, 435. b) Villiers, A. *Compt. Rend. Fr. Acad. Sci.* **1891**, *112*, 536. c) Atwood, J. L.; Davies, J. E. D.; MacNicol, D. D.; Vögtle, F. *Comprehensive Supramolecular Chemistry, Vol. 3. Cyclodextrins,* Pergamon, Oxford, UK, **1996**.
7. a) Gutsche, G. D.; Muthukrishnan, R. *J. Org. Chem.* **1978**, *43*, 4905. b) Gutsche, C. D. *Calixarenes: An Introduction,* 2nd ed., Royal Society of Chemistry, Cambridge, UK, **2008**.
8. a) Ogoshi, T.; Kanai, S.; Fujinami, S.; Yamagishi, T.; Nakamoto, Y. *J. Am. Chem. Soc.* **2008**, *130*, 5022. b) Ogoshi, T.; Yamagishi, T.; Nakamoto, Y. *Chem. Rev.* **2016**, *116*. 7937.
9. a) Behrend, R.; Meyer, E.; Rusche, F. *Liebig Ann. Chem.* **1905**, *339*, 1. b) Barrow, S. T.; Kasera, S.; Rowland, M. J.; del Barrio, J.; Scherman, O. A. *Chem. Rev.* **2015**, *115*, 12320.
10. a) CIBA Foundation Symposium, *Host-Guest Molecular Interactions: From Chemistry to Biology*, Wiley, Weinheim, **1991**. b) Lodish, H.; Berk, A.; Kaiser, C. A.; Krieger, M.;

Scott, M. P.; Bretscher, A.; Ploegh, H.; Matsudaira, P. *Molecular Cell Biology*, W. H. Freeman & Co Ltd., New York, **2007**.

11. a) Tashiro, K.; Aida, T.; Zheng, J.-Y.; Kinbara, K.; Saigo, K.; Sakamoto, S.; Yamaguchi, K. *J. Am. Chem. Soc.* **1999**, *121*, 9477. b) Sakaguchi, K.; Kamimura, T.; Uno, H.; Mori, S.; Ozako, S.; Nobukuni, H.; Ishida, M.; Tani, F. *J. Org. Chem.* **2014**, *79*, 2980. c) Zhu, B.; Chen, H.; Lin, W.; Ye, Y.; Wu, J.; Li, S. *J. Am. Chem. Soc.* **2014**, *136*, 15126. d) Kang, B.; Totten, R. K.; Weston, M. H.; Hupp, J. T.; Nguyen, S. T. *Dalton Trans.* **2012**, *41*, 12156. e) Yu, C.; Long, H.; Jin, Y.; Zhang, Y. *Org. Lett.* **2016**, *18*, 2946. f) Yu, C.; Jin, Y.; Zhang, W. *Chem. Rec.* **2015**, *15*, 97. g) Hernandez-Eguía, L. P.; Escudero-Adan, E. C.; Pinzon, J. R.; Echegoyen, L.; Ballester, P. *J. Org. Chem.* **2011**, *76*, 3258. h) Kang, B.; Totten, R. K.; Weston, M. H.; Hupp, J. T.; Nguyen, S. T. *Dalton Trans.* **2012**, *41,* 12156. i) Ding, H.; Meng, X.; Cui, X.; Yang, Y.; Zhou, T.; Wang, C.; Zeller, M.; Wang, C. *Chem. Comm.* **2014**, *50*, 11162. j) Durot, S.; Taesch, J.; Heitz, V. *Chem. Rev.* **2014**, *114*, 8542.
12. Fukuzumi, S. *Phys. Chem. Chem. Phys.* **2008**, *10*, 2283.
13. Sariciftci, N. S.; Smilowitz, L.; Heeger, A. J.; Wudl, F. *Science* **1992**, *258*, 1474.
14. Anderson, H. L.; Sanders, J. K. M. *Angew. Chem., Int. Ed. Engl.* **1990**, *29*, 1400.
15. Kobin, B.; Grubert, L.; Blumstengel, S.; Henneberger, F.; Hecht, S. *J. Mater. Chem.*, **2012**, *22*, 4383.
16. Masai, H.; Terao, J.; Seki, S.; Nakashima, S.; Kiguchi, M.; Okoshi, K.; Fujihara, T.; Tsuji, Y. *J. Am. Chem. Soc.* **2014**, *136*, 1742.
17. a) Terao, J.; Tsuda, S.; Tanaka, Y.; Okoshi, K.; Fujihara, T.; Tsuji, Y.; Kambe, N. *J. Am. Chem. Soc.* **2009**, *131*, 16004. b) Terao, J.; Tanaka, Y.; Tsuda, S.; Kambe, N.; Taniguchi, M.; Kawai, T.; Saeki, A.; Seki, S. *J. Am. Chem. Soc.* **2009**, *131*, 18046.
18. a) Sawada, T.; Hisada, H.; Fujita, M. *J. Am. Chem. Soc.* **2014**, 136, 4449. b) Kawase, T.; Tanaka, K.; Shiono, N.; Seirai, Y.; Oda, M. *Angew. Chem., Int. Ed.* **2004**, *43*, 1722. c) Day, A. I.; Blanch, R. J.; Arnold, A. P.; Lorenzo, S.; Lewis, G. R.; Dance, I. *Angew. Chem., Int. Ed.* **2002**, *41*, 275.
19. Pangborn, A. B.; Giardello, M. A.; Grubbs, R. H.; Rosen, R. K.; Timmers, F. J. *Organometallics* **1996**, *15*, 1518.
20. DiMagno, S. G.; Lin, V. S. Y.; Therien, M. J. *J. Org. Chem.* **1993**, *58*, 5983.
21. Tsuda, S.; Terao, J.; Kambe, N. *Chem. Lett.* **2009**, *38*, 76.
22. Terao, J.; Homma, K.; Konoshima, Y.; Imoto, R.; Masai, H.; Matsuda, W.; Seki, S.; Fujihara, T.; Tsuji, Y. *Chem. Commun.* **2014**, *50*, 658.

Chapter 2

Kinetically Stabilized Hetero Face-to-Face Porphyrin Array Using the Porphyrin Ring and Its Optical Property

To develop an artificial photosynthesis system, a hetero face-to-face porphyrin array composed of zink porphyrin ring (**ZnCP**) and **RuTPP(DABCO)$_2$** (**TPP**: 5,10,15,20-tetraphenylporphyrin, **DABCO**: 1,4-diazabicyclo[2.2.2]octane) in 1 : 1 molar ratio was prepared. The ruthenium atom–DABCO bonds in **RuTPP(DABCO)$_2$** was stabilized by the host–guest complexation, although a porphyrin array comprised of **ZnTPP** and **RuTPP(DABCO)$_2$** in 2 : 1 molar ratio dissociated at r. t.. Kinetic analysis of the ligand substitution reaction of **RuTPP(DABCO)$_2$** and that in **ZnCP** revealed the stabilization mechanism of the ruthenium atom–DABCO bonds. Photoinduced electron transfer (PET) from the zinc porphyrin to the ruthenium porphyrin was observed in the porphyrin array. The host–guest stabilization of unstable complex for construction of a donor–accepter–donor structure is expected to be a new method for an artificial photosynthesis.

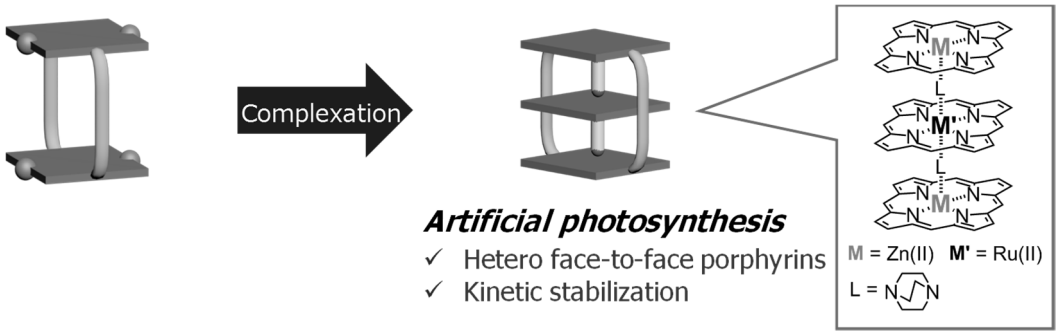

2-1. Introduction

The mimic of photosynthesis, which efficiently converts sunlight into chemical energy, can provide important solutions to the energy crisis.[1] The detailed structures of photosynthetic systems in nature revealed that their efficient use of light energy is related to the sequential energy transfer among the light-harvesting complex systems (LHCs).[2] First, the LHC2 complex, which consists of a 3D array of multi-porphyrins, absorbs sunlight.[3] The energy is quickly transferred to the LHC1 complex and then to the reaction center. This directional energy flow is based on the precise positional relationship among the LHCs and the reaction center, which have different UV-vis absorption properties.

One of the motifs in artificial photosynthesis is orientation-controlled hetero porphyrin arrays composed of different metalloporphyrins. Due to its directional coordination bonding is an easy and useful tool to position molecules regularly. Using this tool, scientists have prepared hetero face-to-face porphyrin arrays with three porphyrins and two bidentate ligands (Figure 2-1a).[4] The porphyrins in these arrays are parallel, as observed in natural photosynthetic systems.[2] In this case, the ligands should have two abilities: (1) form stable complexes and (2) recognize different metals (M and M' in Figure 2-1). A stable hetero face-to-face porphyrin array was also constructed using unsymmetrical bidentate ligands, in order to create different binding enthalpies with different metals.[4] However, the pyridyl group in Ru- or Rh-based porphyrins has low nucleophilicity, leading to weak metal–ligand interaction. Zinc porphyrin, being a promising unit for artificial photosynthesis,[5] has been used for the hetero porphyrin array in only one case.[4b] However, the complex's dissociation equilibrium was observed at r. t., causing ambiguous structure determination. Therefore, it is important to develop a synthetic strategy for preparing stable porphyrin arrays with versatile metals.

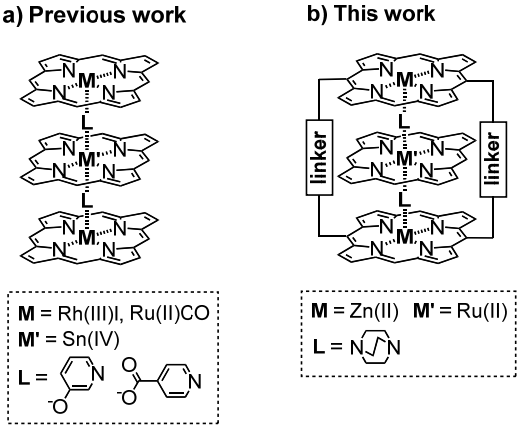

Figure 2-1. Structures of hetero face-to-face porphyrin arrays.

2-2. Results and Discussions

2-2-1. Synthesis of Hetero Face-to-Face Porphyrin Arrays

Two hetero face-to-face porphyrin arrays were prepared from different synthetic methods. The complex of ruthenium porphyrin-bis-1,4-diazabicyclo[2.2.2]octane (DABCO) was used as a unit in the two arrays. **RuTPP(DABCO)$_2$** (TPP: 5,10,15,20-tetraphenylporphyrin) was synthesized for the first time, and used for its ability to form six-coordinated complex with DABCO, which has a higher affinity for zinc porphyrins than pyridine (Scheme2-1).[6] The two hetero face-to-face porphyrin arrays were prepared from zinc and ruthenium porphyrins, with or without applied host–guest chemistry (Figure 2-1b). A comparison of the two porphyrin arrays revealed the stabilization of the weak ruthenium atom–DABCO bonds in **RuTPP(DABCO)$_2$** by host–guest complexation.

RuTPP(DABCO)$_2$ was synthesized as follows. **RuTPP(CO)(py)** was prepared by a method modified from the previous literature,[7] and stirred with excess DABCO in toluene under irradiation with a high-pressure Hg lamp at r. t. for 130 min (Scheme 2-1). Evacuating the solvent and excess DABCO in vacuum afforded **RuTPP(DABCO)$_2$**. The complex formation was supported by electrospray ionization mass spectrometry (ESI-MS) and ^{1}H NMR spectrum. Two sets of NMR triplets are located at around 0.85 and -2.52 ppm which are –2.0 and –5.4 ppm upfield from the methylene peak of free DABCO, because of different ring-current effects of the porphyrin.

Scheme 2-1. Synthesis of **RuTPP(DABCO)$_2$**

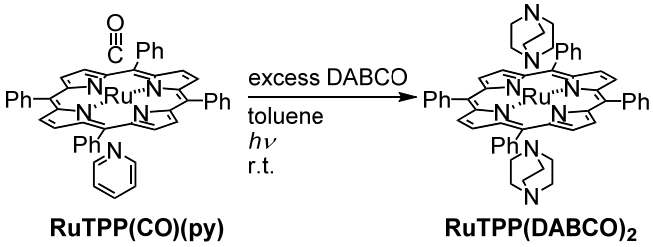

RuTPP(CO)(py) **RuTPP(DABCO)$_2$**

The prepared **RuTPP(DABCO)$_2$** and **ZnTPP** were mixed in 1 : 2 molar ratio (Scheme 2-2). The formation of a hetero face-to-face porphyrin array was indicated by the ^{1}H NMR spectrum (Figure 2-2a). The two protons of DABCO in **RuTPP(DABCO)$_2$** were shifted to a high field (from 0.85 and –2.52 ppm to –4.4 ppm). In the ^{1}H NMR spectrum, the protons of DABCO located between two porphyrins are observed around –5 ppm.[8] The broad singlet peak observed at around –4.4 ppm corresponded to the chemical shift of methylene protons of DABCO placed between two porphyrins. However, this porphyrin array decomposed at r. t. since the NMR peaks gradually shifted to lower field due to the smaller ring-current effect. The decomposition is attributed to the instability of **RuTPP(DABCO)$_2$**, whose ^{1}H NMR spectra over time are shown in Figure 2-9 in the Experimental Section. The integral of free

DABCO gradually increased at r. t. while that of **RuTPP(DABCO)$_2$** decreased. A comparison between the conversion rate of **RuTPP(DABCO)$_2$** and the generation rate of free DABCO based on the initial **RuTPP(DABCO)$_2$** concentration revealed that only one DABCO dissociated from **RuTPP(DABCO)$_2$** with time (Scheme 2-5 and Figure 2-10 in the Experimental Section). Because new peaks did not be observed in ^{1}H NMR spectrum after the dissociation reaction, fast ligand exchanges between **RuTPP(DABCO)** and DABCO were thought to proceed. Therefore, the ruthenium atom–DABCO bond is thermodynamically unstable, thereby degrading the face-to-face porphyrin array.

Scheme 2-2. Synthesis of the hetero porphyrin array comprised of **ZnTPP** and **RuTPP(DABCO)$_2$**

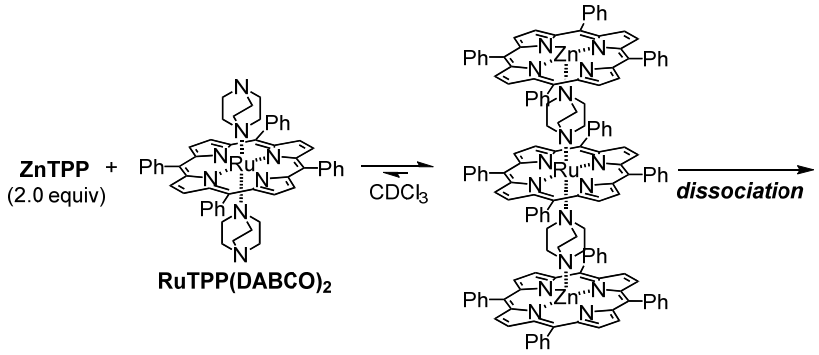

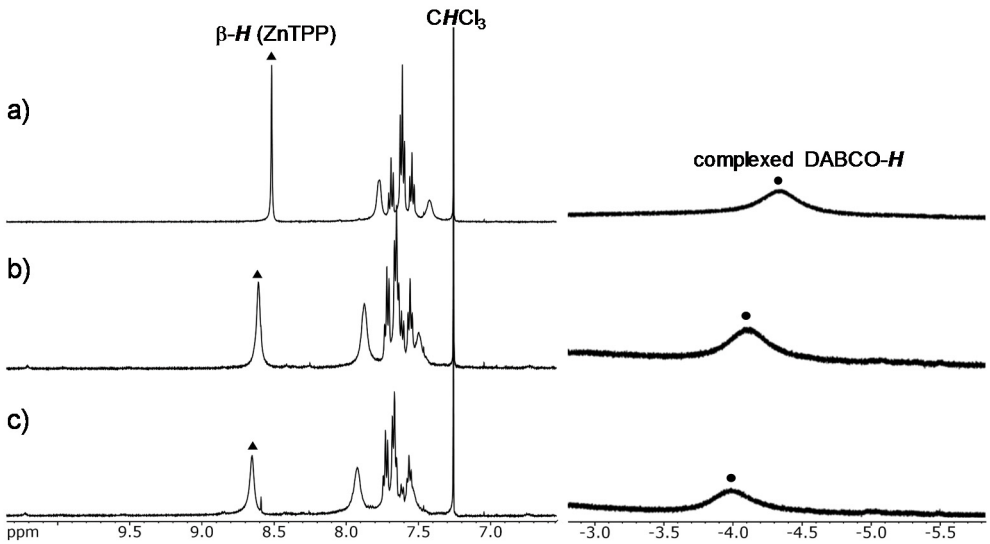

Figure 2-2. ^{1}H NMR (500 MHz) spectra of **ZnTPP** and **RuTPP(DABCO)$_2$** mixed in 2 : 1 molar ratio after a) 20 min, b) 24 h, and c) 40 h in $CDCl_3$ at 298 K.

In order to suppress the dissociation of DABCO from **RuTPP(DABCO)$_2$**, another face-to-face porphyrin was prepared through host–guest complexation. Porphyrin rings and cages are well-known motifs in studying the mechanism of aritificial photosynthetic devices because the host molecules encapsulate different fullerenes as promising accepter molecules.[9]

Scheme 2-3. Construction of a face-to-face porphyrin array from **ZnCP** and **RuTPP(DABCO)$_2$**.

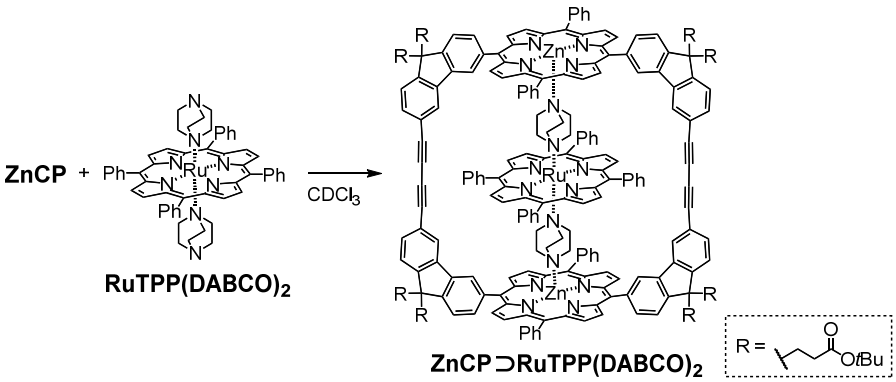

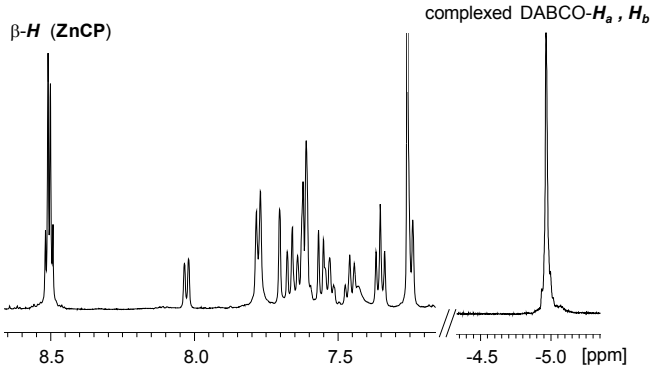

Figure 2-4. ^{1}H NMR spectrum (500 MHz) of **ZnCP⊃RuTPP(DABCO)$_2$** in $CDCl_3$ at 298 K.

Previously, porphyrin rings that could encapsulate molecules by various interactions, such as coordination bonds, π–π interaction, and hydrophilic–hydrophobic interaction were reported.[10] However, there has been no report of porphyrin rings which were used for a porphyrin array. In this study, zinc porphyrin ring (**ZnCP**) was synthesized by a previously reported method[10] as the host molecule containing zinc porphyrin, which can form a complex with amines (Scheme 2-3). The target complex, **ZnCP ⊃ RuTPP(DABCO)$_2$**, was selectively prepared by mixing **ZnCP** and **RuTPP(DABCO)$_2$** in $CHCl_3$ at r. t., followed by purification by a preparative gel permeation chromatography (GPC). In the ^{1}H NMR spectrum of the product, the singlet peak at around −4.9 ppm again corresponded to the chemical shift of methylene protons of DABCO placed between two porphyrins (Figure 2-4).[8]

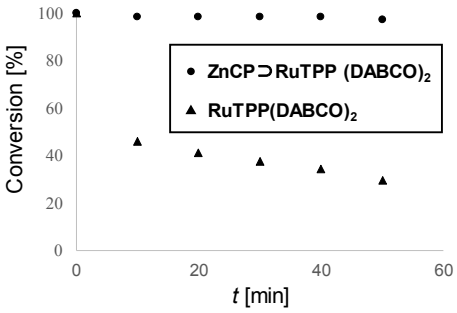

Figure 2-5. Conversion rates of **ZnCP⊃RuTPP(DABCO)$_2$** and **RuTPP(DABCO)$_2$** at 90 °C in toluene-d_8 based on ^{1}H NMR (500 MHz) spectra.

Two kinds of protons (H_a, H_b) of DABCO in **ZnCP⊃RuTPP(DABCO)$_2$** suffered the ring current effect to the same extent from zinc and ruthenium porphyrins, which was the reason why only the singlet peak of the methlene protons was observed. The ^{1}H NMR and matrix-assisted laser desorption/ionization time of flight (MALDI-TOF) MS spectra also indicated that the ratio of **ZnCP** : **RuTPP(DABCO)$_2$** was 1 : 1, suggesting the formation of **ZnCP⊃RuTPP(DABCO)$_2$**. When their ^{1}H NMR spectra in toluene-d_8 at 90 °C were compared (Figure 2-5), **ZnCP ⊃ RuTPP(DABCO)$_2$** was stable while **RuTPP(DABCO)$_2$** quickly decomposed. Therefore, **RuTPP(DABCO)$_2$** was stabilized by host–guest complexation with **ZnCP**.

2-2-2. Kinetic Analysis of the Stabilization of ZnCP⊃RuTPP(DABCO)$_2$

Next, the stabilization mechanism of **RuTPP(DABCO)$_2$** in **ZnCP ⊃ RuTPP(DABCO)$_2$** based on ligand substitution reaction kinetics was evaluated. Ligand substitution reaction of **RuTPP(DABCO)$_2$** is shown in Scheme 2-4. **L** is a ligand, whereas k_1 and k_2 mean reaction rate constants, respectively. Reaction rates of the first and second steps can be described as follow: $v_1 = k_1$[**RuTPP(DABCO)$_2$**][**L**] and $v_2 = k_1$[**RuTPP(DABCO)L**][**L**]. In the case of [**RuTPP(DABCO)$_2$**] << [**L**], the first step can be regarded as a pseudo-first-order reaction because [**L**] is assumed to be constant, which is why v_1 can be drawn as $v_1 = k_1'$[**RuTPP(DABCO)$_2$**] ($k_1' = k_1$[**L**]). In the ligand substitution reaction, conversion ratio of **RuTPP(DABCO)$_2$** is analysed to determine k_1'. Then arrhenius plots of k_1' with different temperature afford activation energy (E_a) and frequency factor (A). *tert*-Butyl isocyanide (^{t}BuNC) was used as the substituting ligand because isocyanide has a low nucleophilicity and high ability to form complex with transition metals. Hence, the DABCO in **RuTPP(DABCO)$_2$** can be replaced with isocyanide to maintain zinc–DABCO bonds of **ZnCP⊃RuTPP(DABCO)$_2$**. After heating at 35 °C with 14 equiv. of ^{t}BuNC, **RuTPP(DABCO)$_2$** (0.3 μM) was gradually converted to **RuTPP(^{t}BuNC)$_2$** according to the ^{1}H NMR spectra over time (Scheme 2-5 and Figure 2-11 in Experimental Section). The mono-substituted complex was not observed in this case, due to the strong trans effect of isocyanide that promotes the dissociation of DABCO.[11] The substitution reaction was expected to occur through the seven-coordinated ruthenium,[12] because the conversion rate of **RuTPP(DABCO)$_2$** depended on the equivalent of ^{t}BuNC (Figure 2-12 in Experimental Section). In the case of **ZnCP⊃RuTPP(DABCO)$_2$** (0.3 μM), both **RuTPP(^{t}BuNC)$_2$** and DABCO were produced at higher temperatures (Figure 2-14

Scheme 2-4. Ligand substitution reactions of **RuTPP(DABCO)$_2$**

Table 2-1. Comparison of activation energy (E_a) and frequency factor (A) of substitution reactions by isocyanide for **RuTPP(DABCO)$_2$** and **ZnCP⊃RuTPP(DABCO)$_2$**

Unit	E_a [kJ mol^{-1}]	$A\times10^{16}$ [M^{-1} h^{-1}]
RuTPP(DABCO)$_2$	1.5	5.6×10^{4}
ZnCP⊃RuTPP (DABCO)$_2$	1.3	4.1

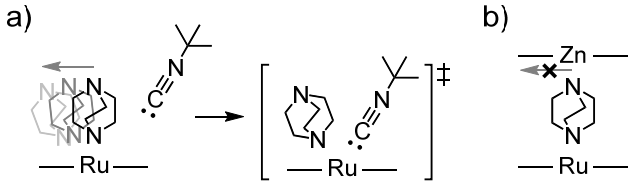

Figure 2-6. Sliding modes of DABCO on the ruthenium porphyrin to reach the transition state (‡) of the ligand substitution reaction: a) Without and b) With **ZnCP**. The arrows mean the sliding movements of DABCO coordinated to porphyrin.

in Experimental Section). The measured rate constants at different temperatures lead to the activation energy (E_a) and frequency factor (A), whose values are shown in Table 2-1. A comparison between **RuTPP(DABCO)$_2$** and **ZnCP ⊃ RuTPP(DABCO)$_2$** revealed that the dramatic reduction in A is key to the stabilization of ruthenium atom–DABCO bonds in the latter, which can be rationalized as follows. The sliding mode of DABCO in **RuTPP(DABCO)$_2$** (Figure 2-6a, horizontal gray arrow) is the key step for the isocyanide to associate with Ru in the substitution reaction. In the case of **ZnCP⊃RuTPP(DABCO)$_2$**, however, the porphyrin ring inhibits the formation of the transition state, by reducing the degrees of freedom of DABCO (Figure 2-6b, horizontal gray arrow). Hence, the ruthenium atom–DABCO bonds in **ZnCP⊃RuTPP(DABCO)$_2$** is stabilized by the kinetic effect even at high temperature (Figure 2-5).

2-2-3. Investigation of the Optical Property of ZnCP⊃RuTPP(DABCO)$_2$

The optical property of **ZnCP⊃RuTPP(DABCO)$_2$** was also investigated. According to the UV-vis spectra (Figure 2-7a), in **RuTPP(DABCO)$_2$** the zinc and ruthenium porphyrins did not interact with each other in the ground and exciting states, because the spectrum was a superposition of those of **ZnCP**–DABCO mixture and **RuTPP(DABCO)$_2$**. **ZnCP** emits light at 610 nm based on a π–π* transition (λ_{ex} = 430 nm, Figure 2-7b). On the other hand, **RuTPP(DABCO)$_2$** did not emit light, probably due to non-radiative deactivation on the Ru metal (λ_{ex} = 408 nm). When excited at 430 nm (mainly exciting Zn porphyrin), the intense fluorescence from **ZnCP⊃RuTPP(DABCO)$_2$** at its maximum emission wavelength was 85% lower than that from the **ZnCP**–DABCO mixture It was expected that the quenched emission

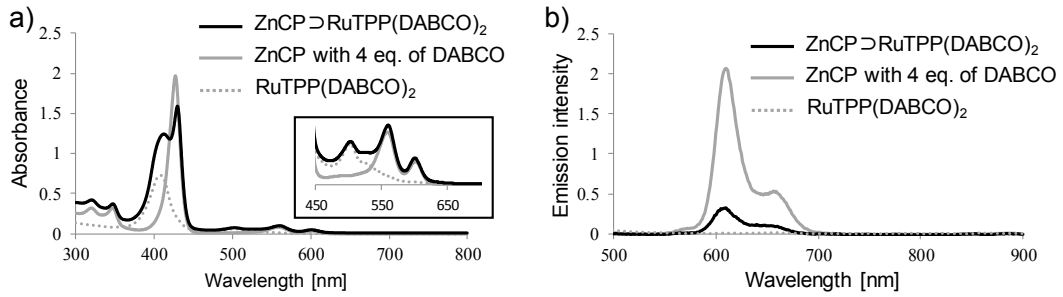

Figure 2-7. (a) Absorption and (b) emission spectra of **ZnCP⊃RuTPP(DABCO)$_2$** (black lines), **ZnCP** mixed with 4 equivalents of DABCO (gray lines, excited at 430 nm), and **RuTPP(DABCO)$_2$** (gray dotted lines, excited at 408 nm), at 4.0×10^{-3} mM in $CHCl_3$.

for **ZnCP**–DABCO mixture was caused by energy or electron transfer from the zinc porphyrins to ruthenium porphyrin.

Finally, the detailed photoreaction dynamics of **ZnCP⊃RuTPP(DABCO)$_2$** was examined. The transient absorption spectrum of **ZnCP** at 1 ns after the excitation showed a negative value at 660 nm (Figure 2-8a), originated from the tail of the **ZnCP** singlet excited state decay (in agreement with the emission shown in Figure 2-7b),[13] while both spectra observed at 1 and 5 ns after the excitation indicated two absorptions at 760 and 850 nm, corresponding to the triplet excited state of zinc porphyrin (λ_{ex} = 540 nm, Figure 2-8a).[14] In the case of **ZnCP⊃RuTPP(DABCO)$_2$**, a single broad peak was observed at 720–850 nm from 1 ns (λ_{ex} = 550 nm to excite mainly the zinc porphyrin, Figure 2-8b). Photo electrochemical measurement[15] proved that the zinc porphyrin formed a one-electron oxidation state at +1.37 V (Figures 2-17–2-20 in Experimental Section). Accordingly, the broad peak (600–850 nm) in the transient absorption spectrum of **ZnCP⊃RuTPP(DABCO)$_2$** (Figure 2-21 in Experimental Section) is attributed to the one-electron oxidation state of **ZnCP**. Therefore, a radical cation of zinc porphyrin is formed after the photoexcitation of zinc porphyrin in **ZnCP⊃RuTPP(DABCO)$_2$**.

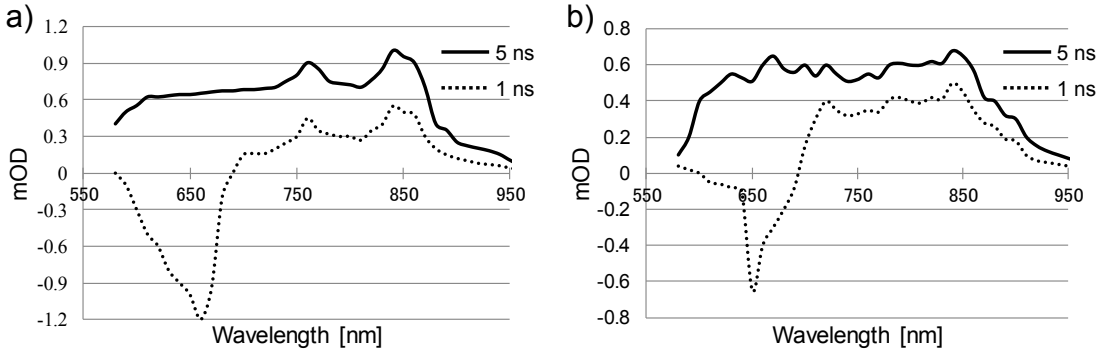

Figure 2-8. Transient absorption spectra of a) **ZnCP** (excited at 540 nm) and b) **ZnCP⊃RuTPP(DABCO)$_2$** (excited at 550 nm) with time delays of 1 and 5 ns in $CHCl_3$.

The reason for the zinc porphyrin quenching in **ZnCP⊃RuTPP(DABCO)$_2$** can be explained as follows. At first, after being excited at 550 nm, the electron is transferred from zinc porphyrin to ruthenium porphyrin within 1 ns, followed by non-radiative deactivation. The electron transfer reaction is not intermolecular but intramolecular, because the measurement was conducted at sufficiently diluted concentration (~40 μM), so that intermolecular reaction was negligible. The one-electron reduction of ruthenium porphyrin was thought to have short lifetime within nanoseconds because the peaks corresponding to it were not observed by nanosecond visible transient absorption spectroscopy. **ZnCP⊃RuTPP(DABCO)$_2$** has a D–A–D structure constructed through coordination bonds, in which zinc porphyrin is the donor molecule (D) while ruthenium porphyrin is the accepter molecule (A).

2-3. Conclusion

In conclusion, two face-to-face type porphyrin arrays with zinc porphyrin, one of the promising units for artificial photosynthesis, and **RuTPP(DABCO)$_2$** were prepared. The unstable ruthenium atom–DABCO bonds in **RuTPP(DABCO)$_2$** were stabilized by a zinc porphyrin ring through host–guest complexation. The prepared porphyrin array was a motif for artificial photosynthesis, since photoinduced electron transfer (PET) from the zinc porphyrin to ruthenium porphyrin occurred. The stabilization of an unstable complex through host–guest complexation shown here is expected to be a new method for constructing donor–accepter structures.

2-4. Experimental Section

2-4-1. General Remarks

Materials: Reagents were purchased from commercial sources and used without further purification. Solvents were purified as follows: reaction solvents were degassed through freeze-pump-thaw (three times), before use. Dry toluene was purchased from Kanto Chemical and further purified by passage through activated alumina under positive argon pressure as described by Grubbs *et al.*[16] **RuTPP(CO)(py)**[7] and **ZnTPP**[17] were prepared according to the reported procedures.

NMR Spectroscopy: ^{1}H NMR spectra were measured on a Bruker AVANCE-500 spectrometer. The ^{1}H NMR chemical shifts are reported relative to tetramethylsilane (TMS, 0.00 ppm) or residual protonated solvent (7.26 ppm) in $CDCl_3$. The ^{13}C NMR chemical shifts are reported relative to tetramethylsilane (TMS, 0.00 ppm) or solvent (77.16 ppm) in $CDCl_3$ or (136.44 ppm) in toluene-d_8.

Preparative recycling gel permeation chromatography (GPC): Preparative recycling GPC was performed with a JAI LC9104 System equipped with JAIGEL-1H and 2H columns, a JAI UV DETECTOR 310, and a JAI RI DETRCTOR RI-5, a JAI LC9130NEXT System equipped with JAIGEL-2H and 2.5H columns, a JAI UV DETECTOR 370NEXT, and a JAI RI DETRCTOR RI 700NEXT, a JAI LC9140 System equipped with JAIGEL-2.5H and -3H columns, a JAI UV DETECTOR 310, and a JAI RI DETRCTOR RI-5.

Mass spectroscopy (MS): Matrix assisted laser desorption/ionization time-of-flight (MALDI-TOF) mass spectra were obtained with α-cyano-4-hydroxycinnamic acid (CHCA) as a matrix and NaTFA as a cationization reagent on Thermo Fisher Scientific LTQ orbitrapXL. ESI mass spectra were obtained on Thermo Fisher Scientific EXACTIVE.

Steady-state photoluminescence spectroscopy: Photoluminescence spectra of a porphyrin solution were obtained in a 1 x 1 cm^2 quartz glass cuvette with 90^o incident excitation using a PTI UV-Vis fluorometer (Photon Technology International, Inc.) with slit widths of 1.0 mm (4.0 nm resolution) at r. t.. The spectra were monitored using a photomultiplier detector in a wavelength range between 400 and 800 nm, and corrected for the spectral response of the grating in the emission monochromator and the detector.

Nanosecond visible transient absorption spectroscopy: A home-built nanosecond visible transient absorption spectroscopy (ns-Vis-TAS) was employed to monitor excited state and charge transfer dynamics. The measurements were performed by monochromatic probe light

from Xe lamp (Photon Technology International) through two monochromators (Acton, Princeton Instruments) with a pump pulse from an N_2 laser (LTB Lasertechnik Berlin GmbH, MNL 202-C) pumped dye laser (LTB Lasertechnik Berlin GmbH, ATM200, 700 ps pulse duration). Transient absorption signals were captured by a photodiode-based detection system (Unisoku Co., Ltd., TSP-2000SN, time resolution: 1.2 ns) with an oscilloscope (Tektronix, TDS 3052C, 500 MHz, 5 GS/s) at 10 Hz excitation repetition rate at 22 °C. The excitation intensity was tuned to 50~80 μJ/cm^2. Transient spectra were corrected for the spectral response of the grating in the monochromator and the detector. No change in the steady-state absorption spectra before and after the transient experiments was observed, suggesting that the samples were stable during the optical experiments.

Spectroelectrochemical measurements: Spectroelectrochemical measurements were performed in a thin layer optical cell with a three-electrode configuration (ALS Co., Ltd.). The spectroelectrochemical cell consisting of a platinum mesh electrode, a platinum wire electrode and a compact Ag / AgCl electrode as a working, counter and reference electrodes, respectively, was placed in an absorption spectrometer (UV-2450, SHIMADZU). Porphyrin absorption spectra were measured by monitoring intensity change of the probe light passing through the Pt mesh electrode in the cell containing 0.1 μM porphyrin and 0.1 M lithium perchlorate (supporting electrolyte) in a mixture of acetonitrile and chloroform (1 : 1 vol%), after the bias application into the mesh electrode for approximately 5 min. The bias was applied from 0 V with +0.1 V steps following the measurement of the reference line after 15 min stabilization at 0 V vs. Ag / AgCl. The absorption difference spectra were obtained by subtracting this reference line from the spectrum observed at the applied bias after 10 min stabilization.

2-4-2. Synthetic Procedures

Synthesis of RuTPP(DABCO)$_2$

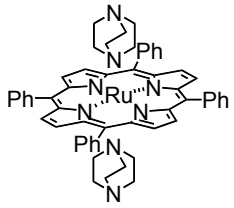

RuTPP(CO)(py) (86.2 mg, 0.105 mmol) and DABCO (561 mg, 5.01 mmol) were dissolved in toluene (400 mL). The solution was stirred at r.t. for 130 min with Ar bubbling under irradiation using high-pressure Hg lamp. The solvent and excess DABCO were removed under evacuation at 55 °C to afford **RuTPP(DABCO)$_2$** (84.3 mg, 86%) as a orange solid. DABCO couldn't be completely removed because **RuTPP(DABCO)$_2$** was slowly decomposed to yield a free DABCO in some solvents such as $CHCl_3$ and toluene even at r. t.. **RuTPP(DABCO)$_2$** was used for a next reaction and analysis without any purification. DABCO of the ruthenium porphyrin slowly dissociates at r. t. even in the solid state. It was the reason why the peak corresponding to free DABCO was observed in ^{1}H and ^{13}C NMR spectra.

HR-MS (ESI-MS) (m/z) 938.3377 ([RuTPP(DABCO)$_2$]$^+$, $C_{56}H_{52}N_8Ru$, calcd. 938.3358).
^{1}H NMR (500 MHz, $CDCl_3$, r. t.): δ 8.01 (12H, br, Ar-H), 7.95 (8H, br, Ar-H), 7.65 (8H, br, Ar-H), 0.85 (12H, br, DABCO-*H*), –2.52 (12H, br, DABCO-*H*).
^{13}C NMR (126 MHz, $CDCl_3$, r. t.): δ 144.98 (two peaks overlapped), 142.63, 133.93, 132.98, 127.14, 126.75, 45.08 (two peaks overlapped).

Synthesis of RuTPP(^{t}BuNC)$_2$

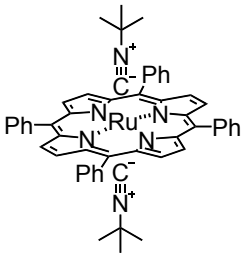

RuTPP(CO)(py) (14.3 mg, 0.0174 mmol) and pyridine (0.204 mL, 1.81 mmol) were dissolved in toluene (69 mL). The solution was stirred at r. t. for 180 min with Ar bubbling under irradiation with a high-pressure Hg lamp. The solvent and excess ^{t}BuNC were removed under evacuation at 35 °C. The crude product was filtered through silica gel with $CHCl_3$ as an eluent, followed by purification by GPC to afford **RuTPP(^{t}BuNC)$_2$** (11.6 mg, 76%) as the orange solid.

HR-MS (ESI-MS) (m/z) 880.2817 ([RuTPP(tBuNC)$_2$]$^+$, $C_{54}H_{46}N_6Ru$, calcd. 880.2827).
^{1}H NMR (500 MHz, $CDCl_3$, r. t.): δ 8.40 (s, 8H, Ar-*H*), 8.14-8.13 (m, 8H, Ar-*H*), 7.67-7.66 (m, 12H, Ar-*H*), –0.45 (s, 18H, -C(C*H*$_3$)$_3$).
^{13}C NMR (126 MHz, $CDCl_3$, r. t.): δ 143.71, 143.60, 134.24, 131.35, 126.86, 126.33, 121.24, 53.50, 29.19.

Synthesis of ZnCP⊃RuTPP(DABCO)$_2$

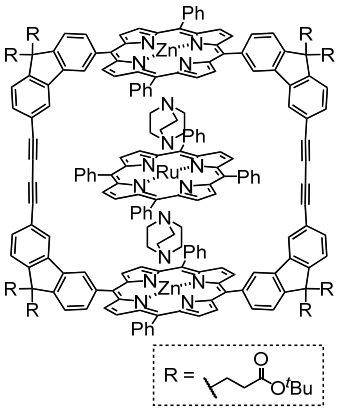

ZnCP (10.1 mg, 3.57 μmol) and **RuTPP(DABCO)$_2$** (4.2 mg, 4.5 μmol) were dissolved in $CHCl_3$. The mixture was purified by GPC. The product and another **RuTPP(DABCO)$_2$** (1.1 mg, 1.2 μmol) was mixed in $CHCl_3$ because the product contained free **ZnCP**. Purification of the mixture by GPC in the same way afforded the purple solid **ZnCP⊃RuTPP(DABCO)$_2$** (12.7 mg, 95%).

HR-MS (MALDI-TOF MS) (m/z) 3540.240 ([**ZnCP ⊃ RuTPP(DABCO)$_2$**+H$^+$-2DABCO], $C_{180}H_{164}N_8O_{16}Zn_2$, calcd. 3540.232);

^{1}H NMR (500 MHz, CDCl$_3$, r. t.): δ 8.51 (d, *J* = 4.3 Hz, 8H, Ar-*H*), 8.50 (d, *J* = 4.6 Hz, 8H, Ar-*H*), 8.03 (d, *J* = 6.9 Hz, 4H, Ar-*H*), 7.78 (several peaks overlapperd, 12H, Ar-*H*), 7.70 (s, 4H, Ar-*H*), 7.66 (t, *J* = 9.2 Hz, 8H, Ar-*H*), 7.62 (several peaks overlapped, 12H, Ar-*H*), 7.56 (d, *J* = 8.4 Hz, 4H, Ar-*H*), 7.53 (t, *J* = 6.9 Hz, 4H, Ar-*H*), 7.46 (t, *J* = 7.8 Hz, 4H, Ar-*H*), 7.43 (br, 8H, Ar-*H*), 7.35 (t, *J* = 7.6 Hz, 8H, Ar-*H*), 7.25 (solvent peak overlapped, 4H, Ar-*H*), 2.59-2.56 (m, 16H, -C*H*$_2$CH$_2$COO*t*Bu), 1.86-1.74 (m, 16H, -CH$_2$C*H*$_2$COO*t*Bu), 1.43 (s, 72H, -COOC(C*H*$_3$)$_3$), –4.97 (s, 24H, DABCO-*H*).

^{13}C NMR (126 MHz, CDCl$_3$, r. t.): δ 172.83, 150.23, 149.75, 149.38, 147.29, 142.83, 142.75, 141.50, 141.28, 138.07, 134.45, 134.42, 133.55, 132.77, 132.67, 131.73, 131.20, 129.19, 128.37, 127.39, 127.30, 126.72, 126.49, 126.13, 125.82, 123.83, 123.69, 122.99, 121.71, 121.11, 120.63, 119.60, 81.59, 80.60, 74.74, 54.14, 41.56, 39.20, 34.91, 30.53, 29.85, 28.27.

^{1}H-^{1}H NOESY spectrum of **ZnCP⊃RuTPP(DABCO)$_2$**

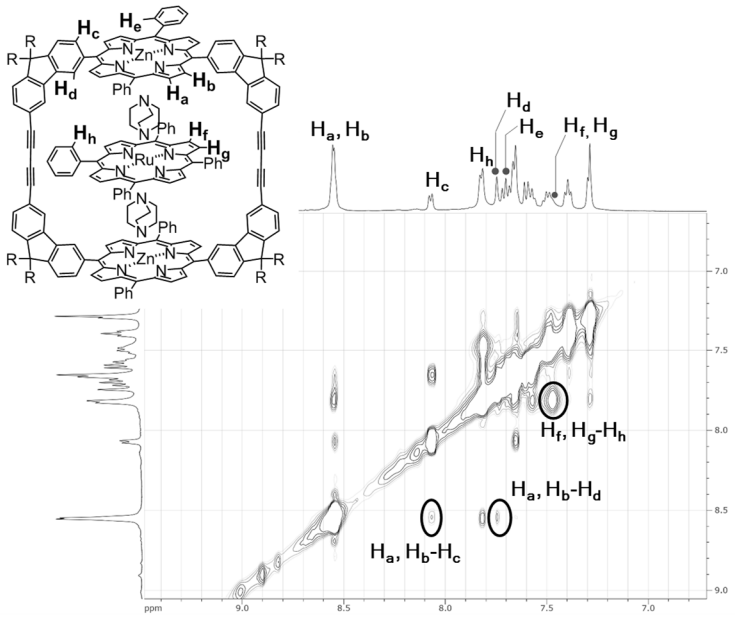

2-4-3. Investigation of the Stability for RuTPP(DABCO)$_2$ and Porphyrin Arrays

2-4-3-1. Dissociation Behavior of DABCO from RuTPP(DABCO)$_2$

Scheme 2-5. Dissociation of DABCO from **RuTPP(DABCO)$_2$**

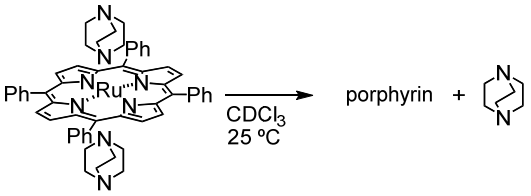

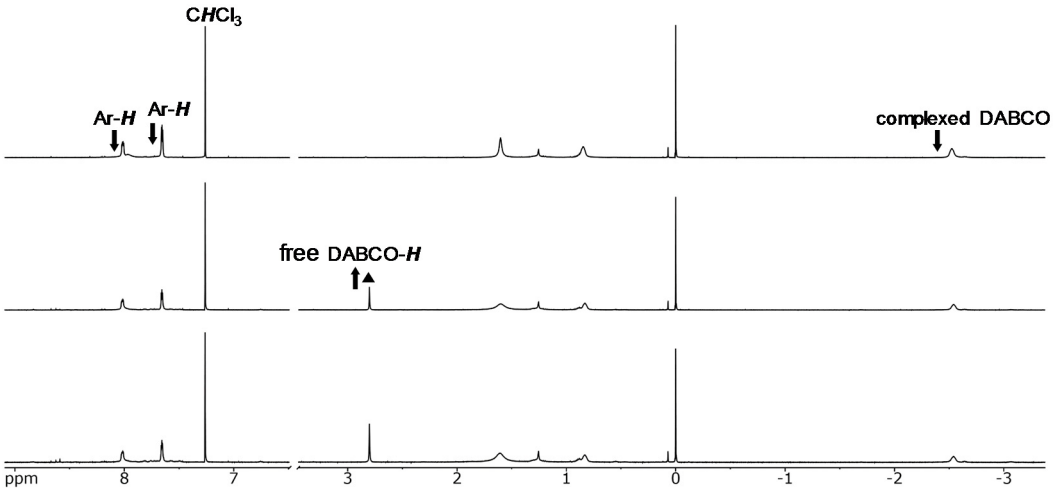

Figure 2-9. ^{1}H NMR spectra (500 MHz) of **RuTPP(DABCO)$_2$** in $CDCl_3$ at 298 K over time. a) 10 min, b) 20 h, and c) 48 h. 1,3,5-Trimethoxybenzene was added as an internal standard. Triangle indicates free DABCO.

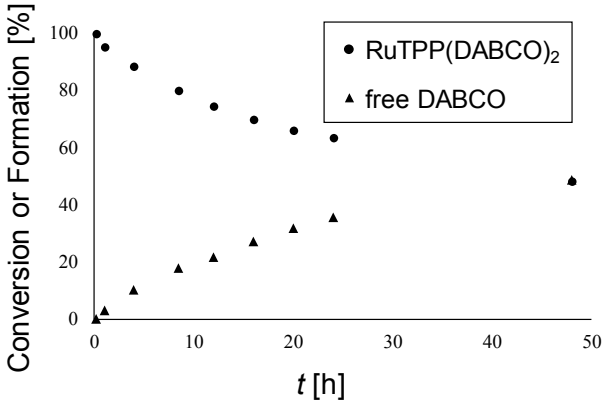

Figure 2-10. Conversion rate of **RuTPP(DABCO)$_2$** (circles) and generation rate of free DABCO (triangles) based on the initial concentration of **RuTPP(DABCO)$_2$** in $CDCl_3$ at r. t. over time (*t*). Conversion rate of **RuTPP(DABCO)$_2$** was mesuared from the peak corresponding to DABCO.

2-4-3-2. Substitution Reaction of DABCO of RuTPP(DABCO)$_2$ by ^{t}BuNC

Scheme 2-6. Substitution reactions of **RuTPP(DABCO)$_2$** by ^{t}BuNC

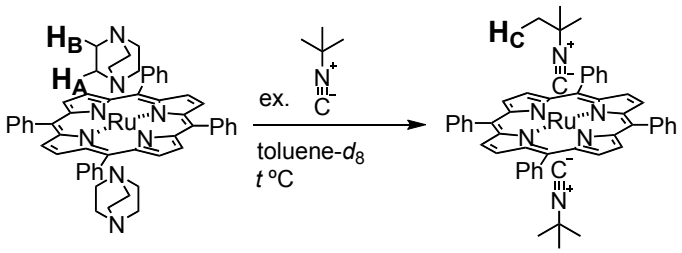

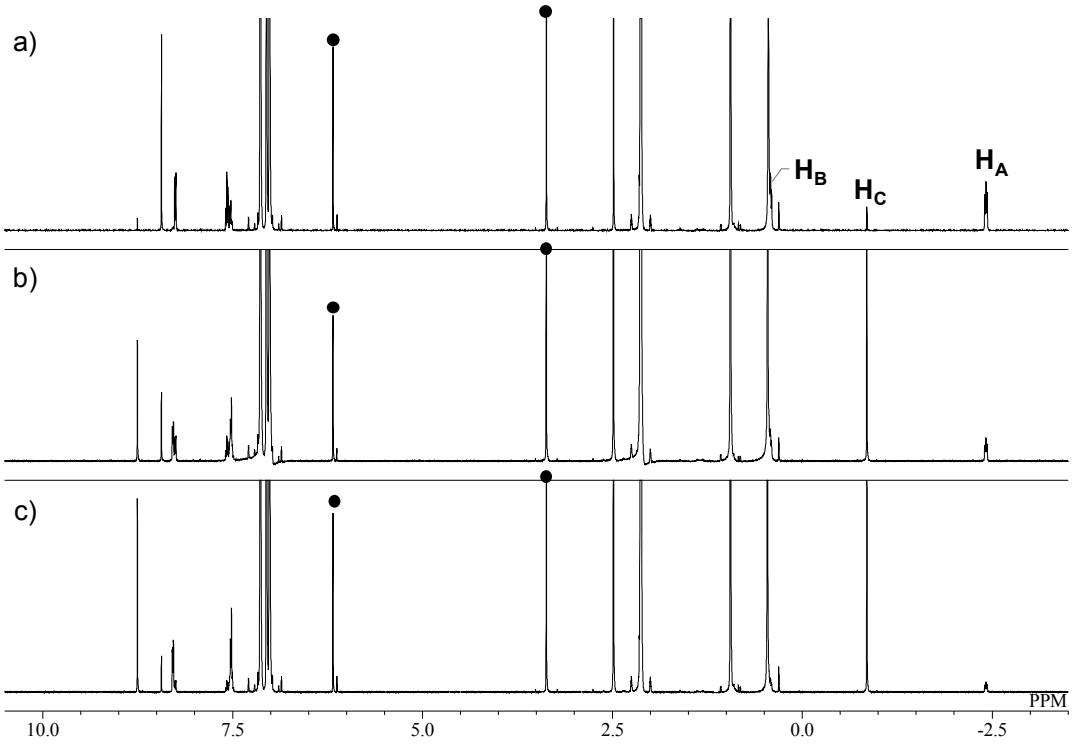

Figure 2-11. ^{1}H NMR spectra (500 MHz, toluene-d_8) of substitution reactions of **RuTPP(DABCO)$_2$** by ^{t}BuNC at 55 °C over time. a) 0 min, b) 30 min, and c) 60 min. 1,3,5-Trimetholybenzen (circles) was added as an internal standard.

Scheme 2-7. Substitution reactions of **RuTPP(DABCO)$_2$** with varying equivalents of ^{t}BuNC

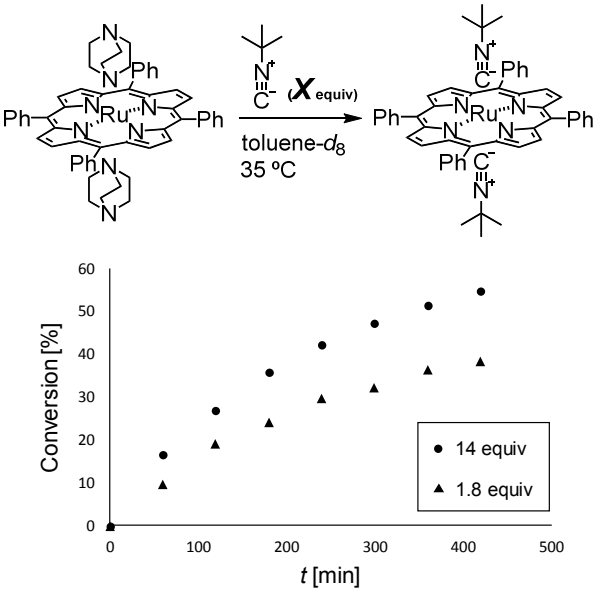

Figure 2-12. Conversion rate of the substitution reactions of **RuTPP(DABCO)$_2$** with 1.8 equiv (triangles) and 14 equiv (circles) of ^{t}BuNC.

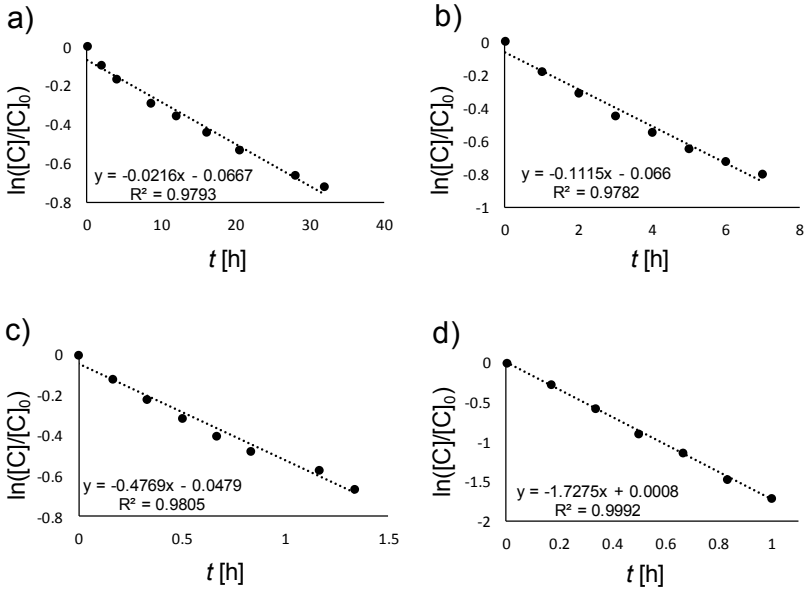

Figure 2-13. Conversion rate of **RuTPP(DABCO)$_2$** to **RuTPP(^{t}BuNC)$_2$** with 14 equiv. of ^{t}BuNC at (a) 25 °C, (b) 35 °C, (c) 45 °C, and (d) 55 °C in toluene-d_8. 1,3,5-Trimethoxybenzene was added as an internal standard. $[C]_0$: initial concentration of **RuTPP(DABCO)$_2$**. The fitted straight line shows that the substitution reactions obey pseudo-first order kinetics.

Scheme 2-7. Substitution reaction of **RuTPP(DABCO)$_2$** of **ZnCP⊃RuTPP(DABCO)$_2$** by ^{t}BuNC

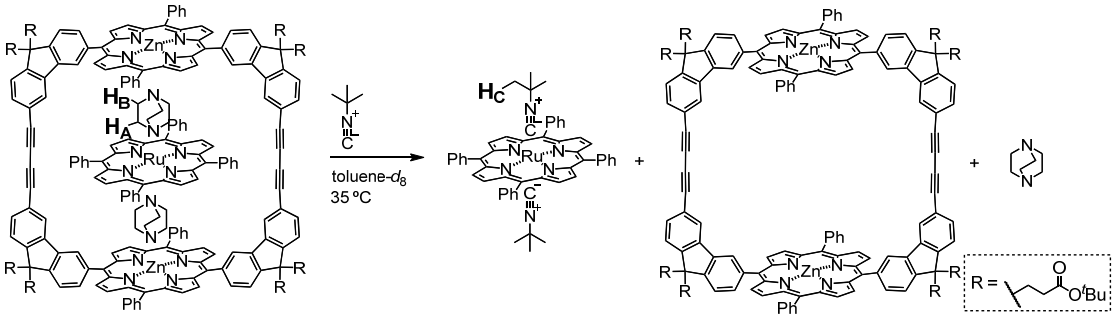

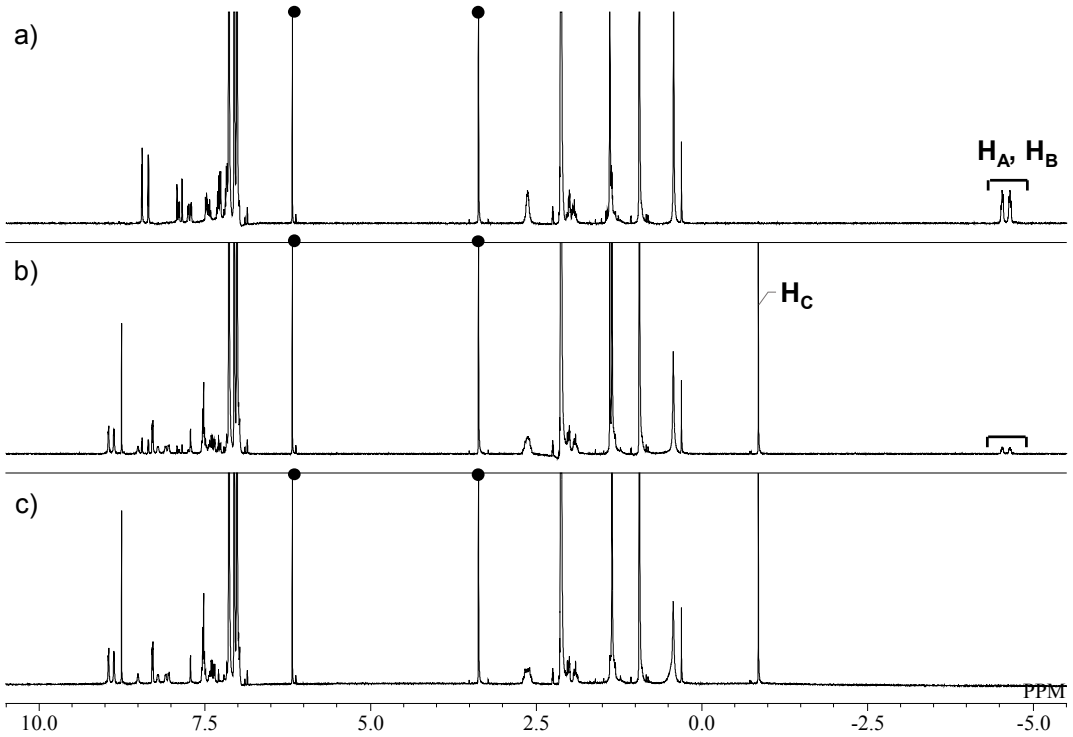

Figure 2-14. ^{1}H NMR spectra (500 MHz, toluene-d_8) of substitution reaction of **RuTPP(DABCO)$_2$** in **ZnCP⊃RuTPP(DABCO)$_2$** by ^{t}BuNC at 105 °C over time. a) 0 min, b) 20 min, and c) 80 min. 1,3,5-Trimetholybenzene (circles) was added as an internal standard.

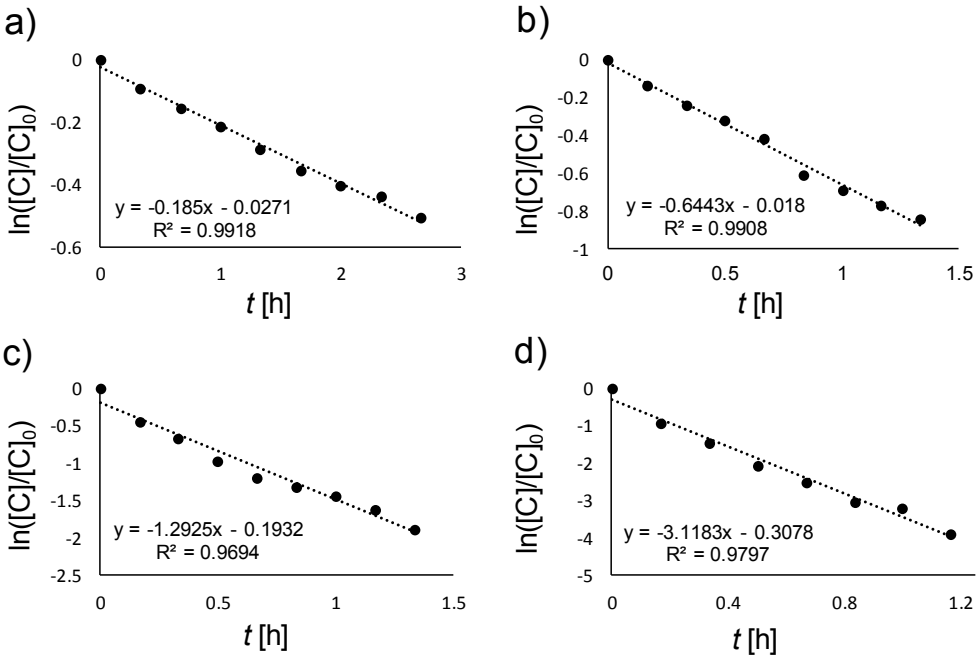

Figure 2-15. Conversion rate of **RuTPP(DABCO)$_2$** in **ZnCP ⊃ RuTPP(DABCO)$_2$** to **RuTPP(^{t}BuNC)$_2$** with excess ^{t}BuNC at (a) 75 ºC, (b) 85 ºC, (c) 95 ºC, and (d) 105 ºC in toluene-d_8. 1,3,5-Trimethoxybenzene was added as an internal standard. $[C]_0$: initial concentration of **RuTPP(DABCO)$_2$**. The fitted straight line shows that the substitution reaction is pseudo-first order.

2-4-4-3. Kinetic Analysis of Substitution Reactions of RuTPP(DABCO)$_2$ and ZnCP⊃ RuTPP(DABCO)$_2$

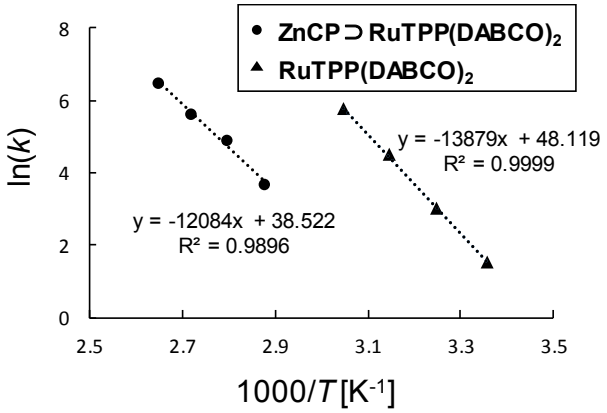

Figure 2-16. Arrhenius plots of ligand substitution reactions of **RuTPP(DABCO)$_2$** (triangles) and **ZnCP⊃RuTPP(DABCO)$_2$** (circles) by ^{t}BuNC in toluene-d_8.

2-4-4-4. Optical Properties of ZnCP, RuTPP(DABCO)$_2$ and Porphyrin Arrays

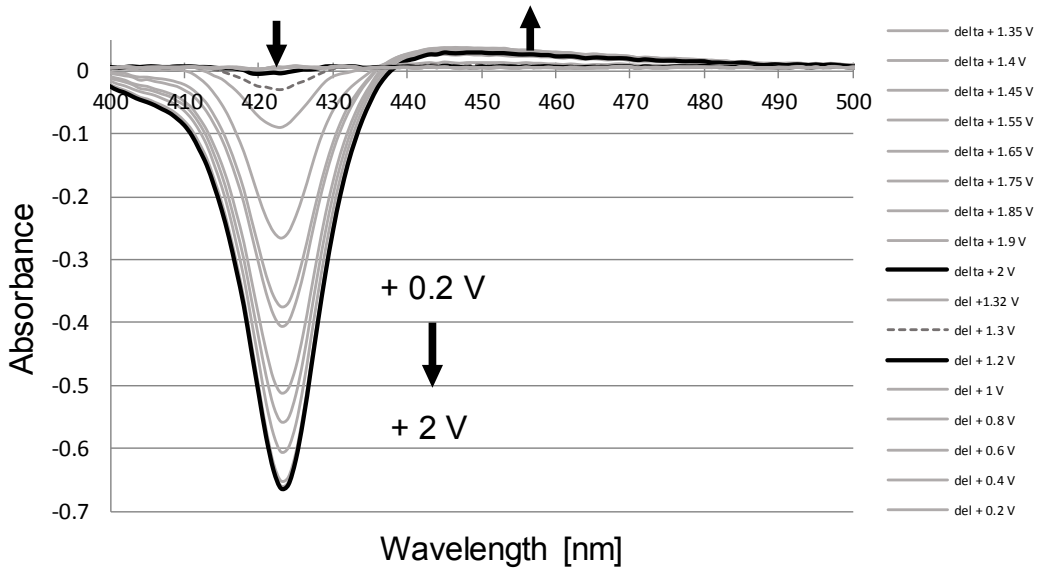

Figure 2-17. Absorption difference spectra of a **ZnCP** solution, obtained by increasing positive applied bias. The number in the figure indicates applied bias (vs. Ag / AgCl).

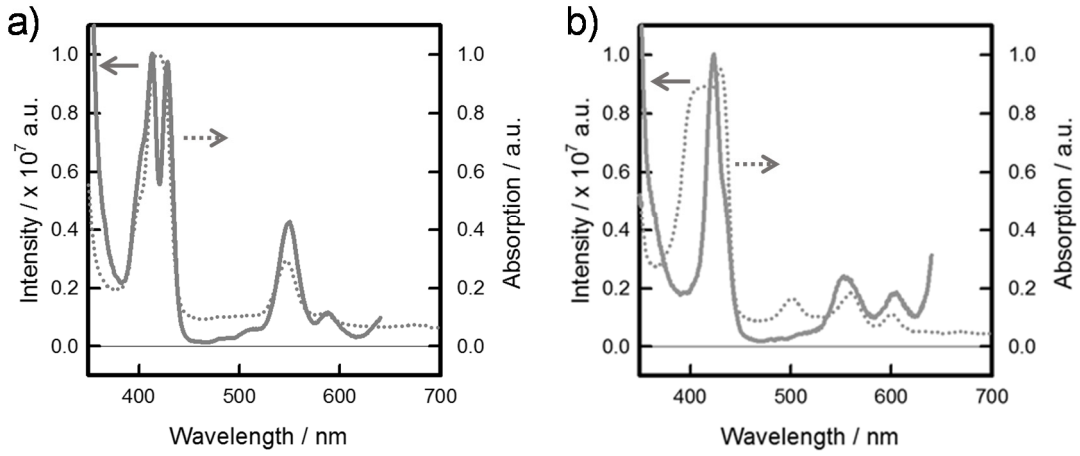

Figure 2-18. Excitation (solid line) and absorption spectra (dotted line) of (a) **ZnCP** and b) **ZnCP ⊃ RuTPP(DABCO)$_2$** in $CHCl_3$. Excitation spectra were monitored at peaks of emission spectra for each sample.

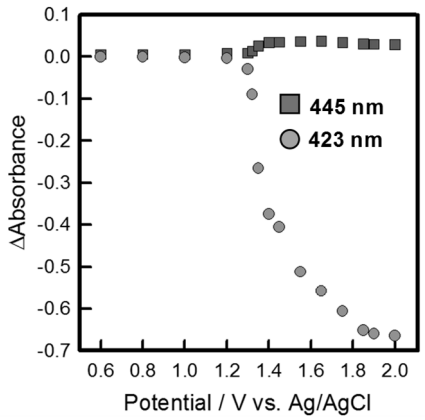

Figure 2-19. Absorbance difference of a **ZnCP** solution at bleach (423 nm, circles) and positive (445 nm, squares) peaks.

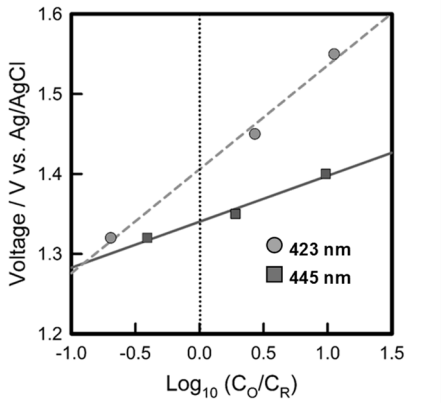

Figure 2-20. $Log_{10}(C_O/C_R)$ calculated from the absorbance difference data, plotted as a function of applied bias. An oxidation potential of Zn porphyrin in **ZnCP** is estimated as 1.37 V.

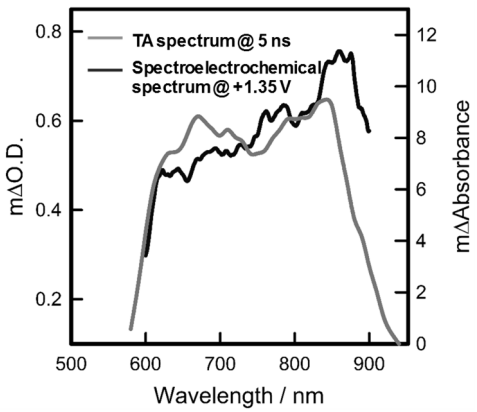

Figure 2-21. Transient absorption spectrum of **ZnCP⊃RuTPP(DABCO)$_2$** (gray line), obtained at 5 ns after 550 nm excitation. The oxidized state spectrum of a **ZnCP** solution, generated by applying bias at +1.35 V vs. Ag/AgCl, is shown as black line for comparison.

References and Notes

1. Tachibana, Y.; Vayssieres, L.; Durrant, J. R. *Nat. Photonics* **2012**, *6*, 511.
2. a) McDermott, G.; Prince, S. M.; Freer, A. A.; Hawthornthwaite-Lawless, A. M.; Papiz, M. Z.; Cogdell, R. J.; Isaacs, N. W. *Nature* **1995**, *374*, 517. b) Freer, A.; Prince, S.; Sauer, K.; Papiz, M.; Hawthornthwaite-Lawless, A.; McDermott, G.; Cogdell, R.; Isaacs, N. W. *Structure* **1996**, *4*, 449. c) Papiz, M. Z.; Prince, S. M.; Hawthornthwaite-Lawless, A. M.; McDermott, G.; Freer, A. A.; Isaacs, N. W.; Cogdell, R. *J. Trends Plant Sci.* **1996**, *1*, 198. d) Scheuring, S.; Lévy, D.; Rigaud, J.-L. *Biochim. Bioys. Acta* **2005**, *1712*, 109. e) Collings, A. F.; Critchley, C. *Artificial Photosynthesis: From Basic Biology to Industrial Application*, Wiley-VCH, Weinheim, Germany, **2005**. f) Razeghifard, R. *Natural and Artificial Photosynthesis: Solar Power as an Energy Source*, Wiley-VCH, Weinheim, Germany, **2013**.
3. a) Sundström, V. *Annu. Rev. Phys. Chem.* **2008**, *59*, 53. b) Sener, M.; Strümpfer, J.; Hsin, J.; Chandler, D.; Scheuring, S.; Hunter, C. N.; Schulten, K. *ChemPhysChem* **2011**, *12*, 518. c) Lüer, L.; Moulisová, V.; Henry, S.; Polli, D.; Brotosudarmo, T. H. P.; Hoseinkhani, S.; Brida, D.; Lanzani, G.; Cerullo, G.; Cogdell, R. J. *Proc. Natl. Acad. Sci. U. S. A.* **2012**, *109*, 1473.
4. a) Maiya, B. G.; Bampos, N.; Kumar, A. A.; Feeder, N.; Sanders, J. K. M. *New J. Chem.* **2001**, *25*, 797. b) Fallon, G. D.; Langford, S. J.; Lee, M. A.–P.; Lygris, E. *Inorg. Chem. Commun.* **2002,** *5*, 715. c) Schetti, V. S.; Pareek, Y.; Ravikanth, M. *Coord. Chem. Rev.* **2012**, *256*, 2816. d) Khodov, I. A.; Alper, G. A.; Mamardashvili, G. M.; Mamardashvili, N. Zh. *J. Mol. Str.* **2015**, *1099*, 174.
5. Fukuzumi, S. *Phys. Chem. Chem. Phys.* **2008**, *10*, 2283.
6. Hunter, C. A.; Meah, M. N.; Sander, J. K. M. *J. Am. Chem. Soc.* **1990**, *112,* 5773.
7. Bonnet, J. J.; Eaton, S. S.; Eaton, G. R.; Holm, R. H.; Ibers, J. A. *J. Am. Chem. Soc.* **1973**, *95*, 2141.
8. Mak, C. C.; Bampos, N.; Sanders, J. K. M. *Chem. Commun.* **1999**, 1085.
9. a) Tashiro, T.; Aida, T.; Zheng, J.-Y.; Kinbara, K.; Saigo, K.; Sakamoto, S.; Yamaguchi, K. *J. Am. Chem. Soc.* **1999**, *121*, 9477. b) Zheng, J.-Y.; Tashiro, K.; Hirabayashi, Y.; Kinbara, K.; Saigo, K.; Aida, T.; Sakamoto, S.; Yamaguchi, K. *Angew. Chem., Int. Ed.* **2001***, 40,* 1857. c) Yamaguchi, T.; Ishii, N.; Tashiro, K.; Aida, T. *J. Am. Chem. Soc.* **2003**, *125*, 13934. d) Ouchi, A.; Tashiro, K.; Yamaguchi, K.; Tsuchiya, T.; Akasaka, T.; Aida, T. *Angew. Chem., Int. Ed.* **2006***, 45,* 3542. e) Shoji, Y.; Tashiro, K.; Aida, T. *J. Am. Chem. Soc.* **2006**, *128*, 10690. f) Yanagisawa, M.; Tashiro, K.; Yamasaki, M.; Aida, T. *J. Am. Chem. Soc.* **2007**, *129*, 11912. g) Canevet, D.; Pérez, E. M.; Martín, N. *Angew. Chem., Int. Ed.* **2011***, 50,* 9248. h) Hernandez-Eguía, L. P.; Escudero-Adan, E.

C.; Pinzon, J. R.; Echegoyen, L.; Ballester, P. *J. Org. Chem.* **2011**, *76*, 3258. i) Kang, B.; Totten, R. K.; Weston, M. H.; Hupp, J. T.; Nguyen, S. T. *Dalton Trans.* **2012**, *41,* 12156. j) Kang, B.; Totten, R. K.; Weston, M. H.; Hupp, J. T.; Nguyen, S. T. *Dalton Trans.* **2012**, *41*, 12156. k) Sakaguchi, K.; Kamimura, T.; Uno, H.; Mori, S.; Ozako, S.; Nobukuni, H.; Ishida, M.; Tani, F. *J. Org. Chem.* **2014**, *79*, 2980. l) Zhu, B.; Chen, H.; Lin, W.; Ye, Y.; Wu, J.; Li, S. *J. Am. Chem. Soc.* **2014**, *136*, 15126. m) Ding, H.; Meng, X.; Cui, X.; Yang, Y.; Zhou, T.; Wang, C.; Zeller, M.; Wang, C. *Chem.Commun.* **2014**, *50*, 11162. n) Yu, C.; Long, H.; Jin, Y.; Zhang, Y. *Org. Lett.* **2016**, *18*, 2946. o) Durot, S.; Taesch, J.; Heitz, V. *Chem. Rev.* **2014**, *114*, 8542. p) Yu, C.; Jin, Y.; Zhang, W. *Chem. Rec.* **2015**, *15*, 97.

10. Terao, J.; Chiba, Y.; Fujihara, T.; Tsuji, Y. *Chem. Lett.* **2014**, *43*, 1374.
11. a) Dulaimi, J. P.; Clark, R. J. H.; Humphrey, D. G. *J. Chem. Soc., Dalton Trans.* **2000**, 933. b) Wong, C.-Y.; Lai, L.-M.; Leung, H.-F.; Wong, S.-H. *Organometallics* **2009**, *28*, 3537.
12. Domazetis, G.; James, B. R.; Dolphin, D. *Inorg. Chim. Acta* **1981**, *54*, L47.
13. Tachibana, Y.; Haque, S. A.; Mercer, I. P.; Durrant, J. R.; Klug, D. R. *J. Phys. Chem. B* **2000**, *104*, 1198.
14. a) Otake, M.; Itou, M.; Araki, Y.; Ito, O.; Kido, H. *Inorg. Chem.* **2005**, *44*, 8581. b) Imahori, H.; Tamaki, K.; Araki, Y.; Sekiguchi, Y.; Ito, O.; Sakata, Y.; Fukuzumi, S. *J. Am. Chem. Soc.* **2002**, *124*, 5165.
15. Matta, S. K.; Kakiage, K.; Makuta, S.; Veamatahau, A.; Aoyama, Y.; Yano, T.; Hanaya, M.; Tachibana, Y. *J. Phys. Chem. C* **2014**, *118*, 28425.
16. Pangborn, A. B.; Giardello, M. A.; Grubbs, R. H.; Rosen, R. K.; Timmers, F. J. *Organometallics* **1996**, *15*, 1518.
17. Vail, S. A.; Schuster, D. I.; Guldi, D. M.; Isosomppi, M.; Tkachenko, N.; Lemmetyinen, H.; Palkar, A.; Echegoyen, L.; Chen, X.; Zhang, J. Z. H. *J. Phys.Chem. B* **2006**, *110*, 14155.

Chapter 3

Template Synthesis of a Length-Controlled Porphyrin Tube via Selective Dimerization of Porphyrin Rings and Its Mechanism

A molecular length and cavity size-controlled porphyrin tube was successfully synthesized using a two-step amine template method, cyclization and tubulation. The template assisted tubulation under a highly diluted condition accelerated a dimerization of the porphyrin rings, whereas the reaction hardly proceeded in the absence of the template molecule. It was revealed that length of alkyl linkers in the template molecules reflected the rate of the tubulation. The template molecule with 1,4-di(pyridin-4-yl)benzene had a high affinity for the porphyrin ring based on the chelate effect, which made porphyrin rings close to each other. The porphyrin tube had an extended conjugation length and sharp Q band due to diminution of a rotational isomerization between two porphyrins based on the rigid structure.

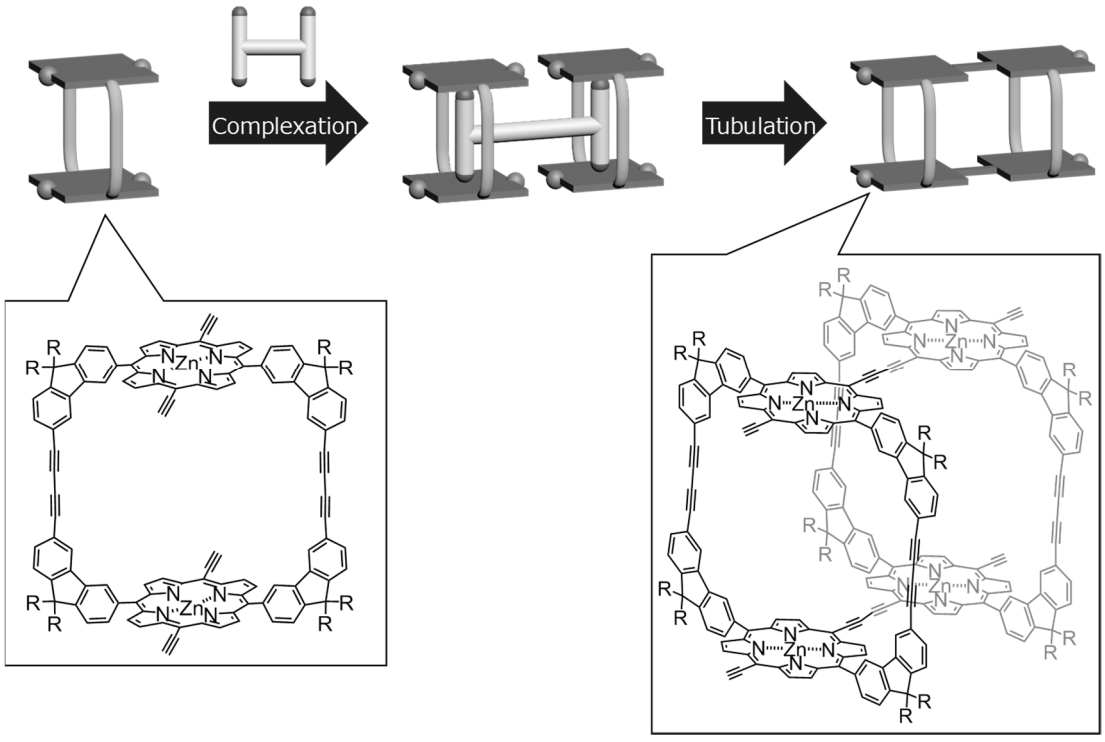

3-1. Introduction

Molecular tubes with regular and one-dimensional cavities attract an attention in terms of transporting and arranging small guest ions and molecules.[1] The combined functions of molecular tubes and guest molecules will provide novel functions. For example, optically characteristic porphyrin tubes encapsulated fullerenes to form peapod structures which were regarded as solar cell motifs[2] because of the electron donor property of porphyrins[3] and the electron accepter one of fullerenes.[4] The functionality depends on the structural characteristics of the molecular tubes such as molecular length and cavity size. Therefore, it is important to develop a synthetic method for structure-controlled porphyrin tubes.

Until now porphyrin tubes have been synthesized by two binding modes. One is a non-covalent method, in which porphyrin rings are linked to each other via coordination, hydrogen bonds, and π–π interactions. Aida *et al.* reported synthesis of a porphyrin tube using multi coordination of zinc porphyrin oligomer.[5] Porphyrin rings are known to have a high ability to encapsulate fullerene[6] and stabilize a charge separate state.[2a] Aida *et al.*[2d] and Tani *et al.*[2e] revealed host–guest complexation between porphyrin tubes and fullerenes to form peapod structures in solid state. In the above examples, the structures receive environmental influence because of the structures constructed by weak interactions. It is hard to control molecular length of the molecular tube due to the reversible bond formation and cleavage, although a self-organization is easy and useful method to construct large structures. Porphyrin tubes constructed by covalent bonds have a merit in terms of the structural stability to the environment compared to non-covalent porphyrin tubes. However, it is difficult to synthesize molecular tubes because many reaction points must be appropriately controlled. Therefore, selective synthesis of molecular tubes is a challenging task. Amine template method is an elegant synthetic strategy to construct complicated porphyrin structures; cyclic and cage-shape structures.[7] Chujo *et al.,*[8a] Hupp *et al.,*[8b] and Anderson *et al.*[8c] reported synthesis of more challenging porphyrin tubes by amine template methods

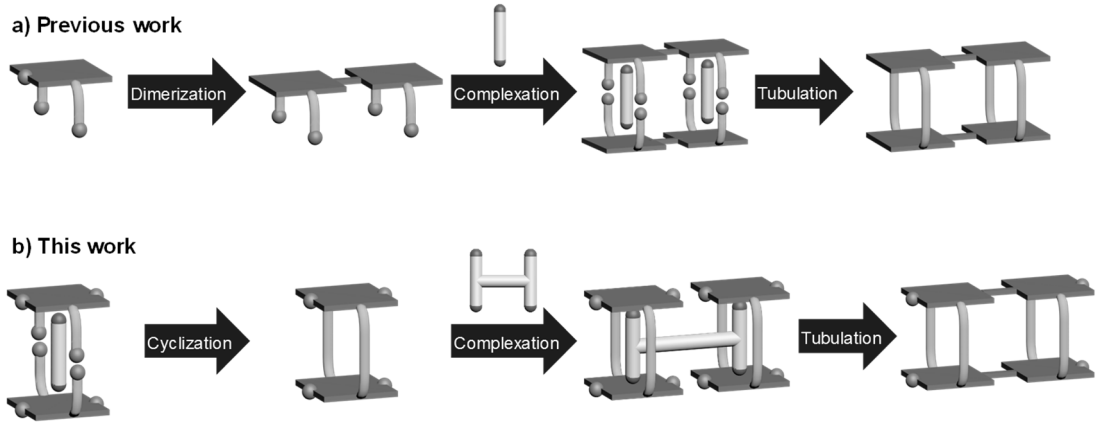

Figure 3-1. Synthetic method for porphyrin tubes.

(Figure. 3-1a). However, basic units with defined molecular length needed to be prepared in order to achieve length-controlled porphyrin tubes in the method.

To prepare structure-controlled porphyrin tubes, a two-step amine template method, that is cyclization and tubulation, is developed (Figure 3-1b). The template method can control not only cavity size but also molecular length, especially controlling dimerization and suppressing the formation of branch polymer in the method (Figure 3-2). In this Chapter, the detailed synthetic method for the porphyrin tube via selective dimerization of porphyrin rings and the structural effects of the template molecules are reported.

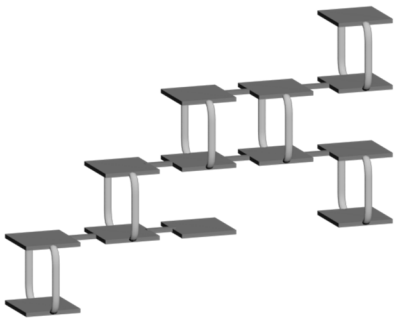

Figure 3-2. Branch polymer.

3-2. Results and Discussions

3-2-1. Template Synthesis of the Cavity Size-Controlled Porphyrin Ring

Porphyrin ring **ZnCP** was adopted as a basic unit of the porphyrin tube (Scheme 3-1). **ZnCP** consists of rigid π-systems, porphyrins and fluorenes, to prevent intramolecular Glaser reactions between two opposite porphyrins in the tubulation. Ethynyl groups were introduced as reaction points. In case of Glaser reactions, two copper acetylides horizontally align at the transition states,[9a] which is expected to be the suitable reaction mechanism for synthesis of

Scheme 3-1. Synthesis of a porphyrin ring **ZnCP**

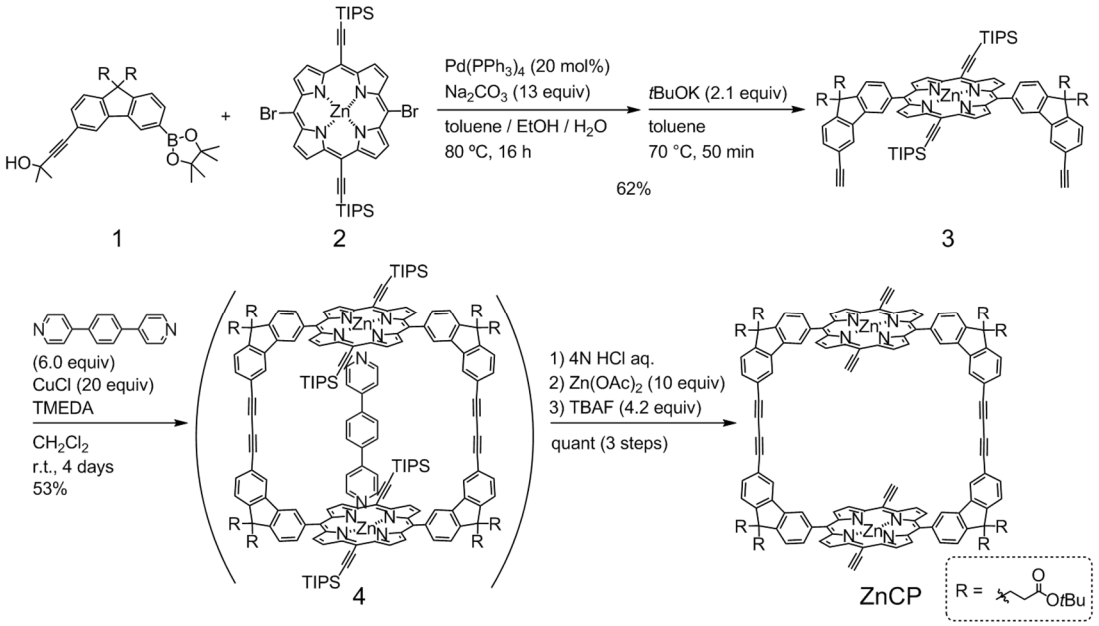

rigid and linear porphyrin tubes. In fact, Glaser reactions with copper catalysts was known to be more effective for molecules with high linearity than that with palladium catalysts.[9b]

The two-step template method contains two Glaser reactions; cyclization of precursor **3** and tubulation of **ZnCP**. Two different ethynyl groups were introduced to fluorene **1** and porphyrin **2** units to distinguish them in deprotection reactions (Scheme 3-1). Porphyrin ring **ZnCP** was prepared as follow (Scheme 3-1). Precursor **3** was synthesized from Suzuki–Miyaura coupling reaction between fluorenes **1** and porphyrin **2** followed by selective deprotection of alcohol groups by ^{t}BuOK. **ZnCP** was successfully synthesized in a good yield by the template cyclization of **3** with 1,4-di(pyridin-4-yl)benzene $\mathbf{T_1}$ as a template molecule based on an amine template method reported by Sanders[8a] before deprotection of triisopropylsilyl (TIPS) groups by tetrabutylammonium fluoride (TBAF).

3-2-2. Synthesis of the Template Molecules

In Chapter 1, it was revealed that 1,4-di(pyridin-4-yl)benzene had appropriate size for the cavity of the porphyrin rings.[10] That unit was adopted as a basic unit of the template molecule for the molecular length-controlled tubulation. Thus, template molecules $\mathbf{T_2}$ **(n=4, 6, 8, 12)** with different numbers of methylene groups were designed to evaluate the effect of linker length on the tubulation (Scheme 3-2). Flexible alkyl chains were introduced as linkers between two 1,4-di(pyridin-4-yl)benzenes to form favorable transition states of Glaser reactions. $\mathbf{T_2'}$ **(n=6)** was also designed as a reference to investigate a relation between the affinity for porphyrin rings and the reaction rate. Template molecules $\mathbf{T_2}$ **(n=4, 6, 8, 12)** were synthesized by Williamson ether synthesis between dibromoalkane and 1,4-diiodophenol **5**

Scheme 3-2. Synthesis of the template molecule $\mathbf{T_2}$ **(n=4, 6, 8, 12)** and $\mathbf{T_2'}$ **(n=6)**

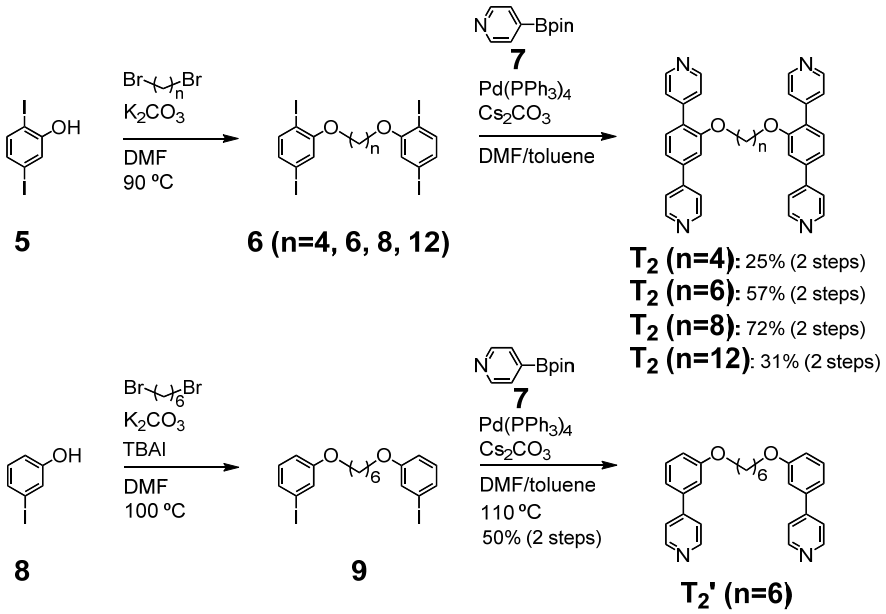

followed by Suzuki–Miyaura coupling with pyridine boronic acid ester **7** (Scheme 3-2). **T_2' (n=6)** was prepared from 3-iodophenol **8** through the same method as the above.

3-2-3. Complexation Study Between ZnCP and T_2 (n=4, 6, 8, 12)

Formation of 2 : 1 complex between porphyrin ring **ZnCP'**[13] and template molecule **T_2 (n=6)** was confirmed by NMR titration in $CDCl_3$ (Scheme 3-3). Porphyrin ring **ZnCP'** with phenyl groups substituted for alkynes of **ZnCP** was used as the reference molecule. In ^1H NMR spectra (Figure 3-3), proton peaks for H_A, H_B, H_C and H_D which correspond to the free **ZnCP** ' disappeared when mixing **ZnCP'** and **T_2 (n=6)** in a 2 : 1 ratio, which revealed the quantitative formation of 2 : 1 complex. This result suggested that two **ZnCP**'s were closed to

Scheme 3-3. Complexation between **ZnCP'** and **T_2 (n=6)**.

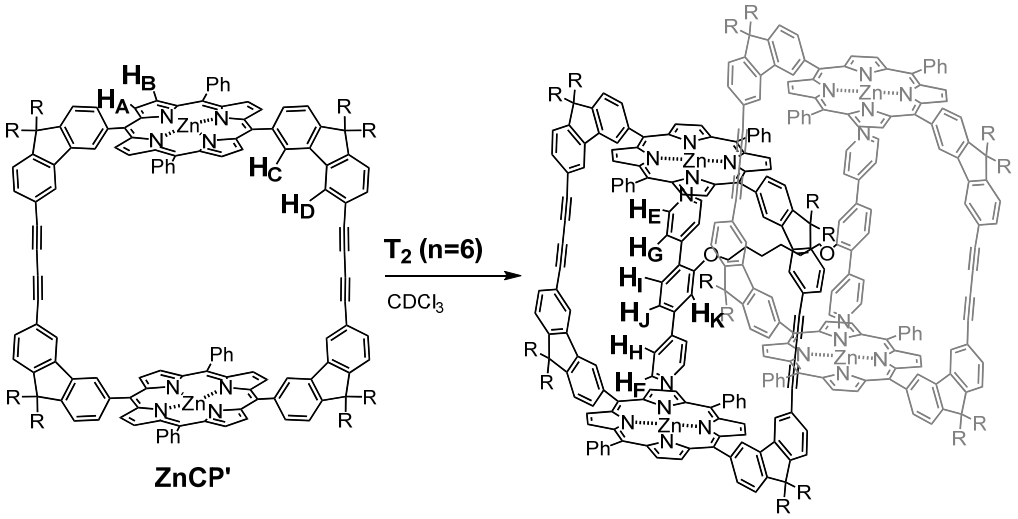

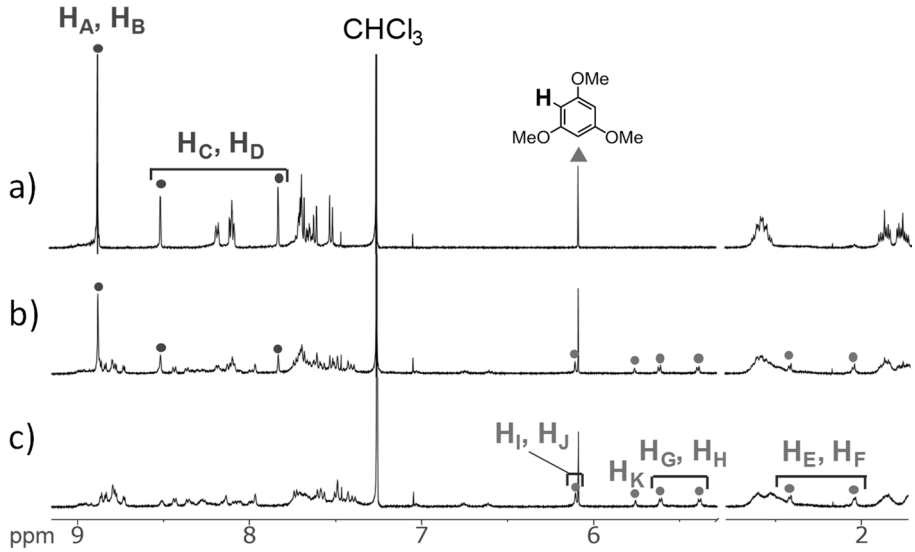

Figure 3-3. NMR ($CDCl_3$, 500 MHz, 298K) titration of **T_2 (n=6)** to **ZnCP**. a) **ZnCP'**, b) **ZnCP'** : **T_2 (n=6)** = 4 : 1, and c) **ZnCP'** : **T_2 (n=6)** = 2 : 1

each other by **T_2 (n=6)**. The complexation between **ZnCP'** and the other template molecules **T_2 (n=4, 8, 12)** was also confirmed by NMR titration experiments as well as **T_2 (n=6)** as shown in Scheme 3-5 and Figure 3-7~3-10 in the Experimental Section.

3-2-4. Template Synthesis of the Length-Controlled Porphyrin Tube

Based on the result of the 2 : 1 complexation between porphyrin rings and template molecules, template-assisted synthesis of **$ZnCP_2$** was investigated (Scheme 3-4). Glaser reaction of **ZnCP** using **T_2 (n=6)** under a high dilution concentration (7.6×10^{-6} M) promoted a dimerization (Figure 3-4b). In sharp contrast, any reaction without **T_2 (n=6)** under the same concentration hardly proceeded (Figure 3-4a). On the other hand, Glaser coupling reaction with higher ratio of TMEDA against copper chloride did not proceed efficiently (Figure 3-4c). Considering the dissociation equilibrium between CuCl and TMEDA, an excess of TMEDA

Scheme 3-4. Template assisted synthesis of the porphyrin tube

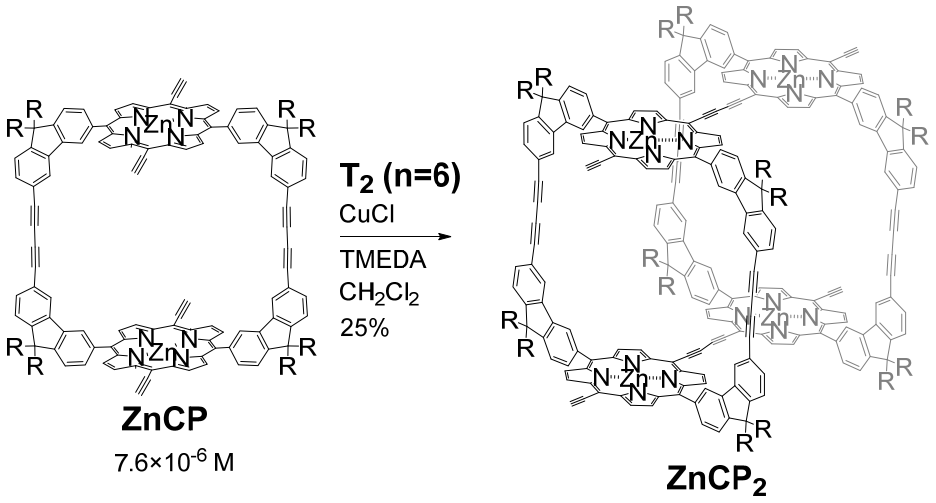

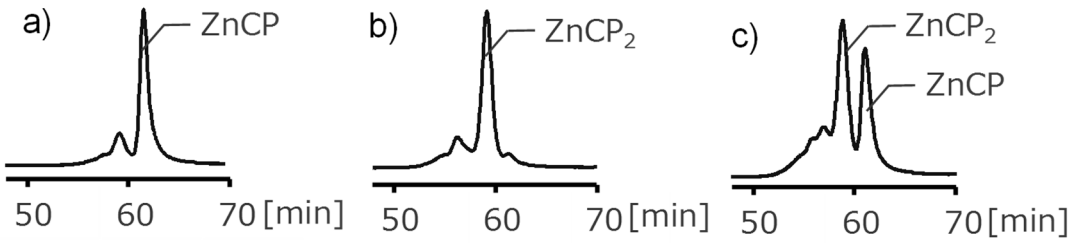

Figure 3-4. GPC chromatograms for Glaser reactions of **ZnCP** with different ratios of CuCl and TMEDA (Eluent : THF, detection : 420 nm). a) CuCl / TMEDA = 4 / 3 without **T_2 (n=6)**, b) CuCl / TMEDA = 1 / 2 with **T_2 (n=6)**, and c) CuCl / TMEDA = 4 / 3 with **T_2 (n=6).**

would prevent the coordination of **T₂ (n=6)** to **ZnCP**. After the tabulation reaction, CuCl and template molecules were removed by a filtration through silica gel (CH_2Cl_2 / EtOAc / pyridine = 10 / 1 / 1) after extraction with water. A preparative recycling gel permeation chromatography (GPC, toluene / pyridine = 100 / 1) of the crude mixture afforded **ZnCP₂** in 25% yield. In ^{1}H NMR spectrum of **ZnCP₂**, four protons at 9.76, 9.56, 8.85, and 8.75 ppm are assigned to β protons of the porphyrins. The β protons and terminal alkynes are measured as a 8 : 1 ratio. Molecular ion peaks of **ZnCP₂** was detected by matrix-assisted laser desorption/ionization time of flight (MALDI-TOF) MS spectrum using *trans*-2-[3-(4-*tert*-butylphenyl)-2-methyl-2-propenylidene]malononitrile (DCTB) as a matrix. As a result, it was clarified that the length-controlled porphyrin tube was selectively synthesized through the template method.

UV-vis spectrum of **ZnCP₂** was shown in Figure 3-5. As the solvent, $CHCl_3$ solution containing 1% pyridine (v / v) was used to avoid aggregation of **ZnCP₂**. Q band of **ZnCP₂** (722 nm) was 90 nm longer than that of **ZnCP** that is the starting material of **ZnCP₂**. Q band around 720 nm was sharp compared to that of a porphyrin dimer **ZnP₂** (Figure 3-5). The dihedral angle of two porphyrins linked by a diyne in **ZnP₂** largely varies because of rotation mode along the axis of diyne, which afforded a broad shape of a UV-vis spectrum (Figure. 3-5). On the other hand, the dihedral angle between two porphyrins of **ZnCP₂** was expected to be fixed due to rigid π-systems, which led to the narrow Q band of **ZnCP₂** (Figure. 3-5).[12]

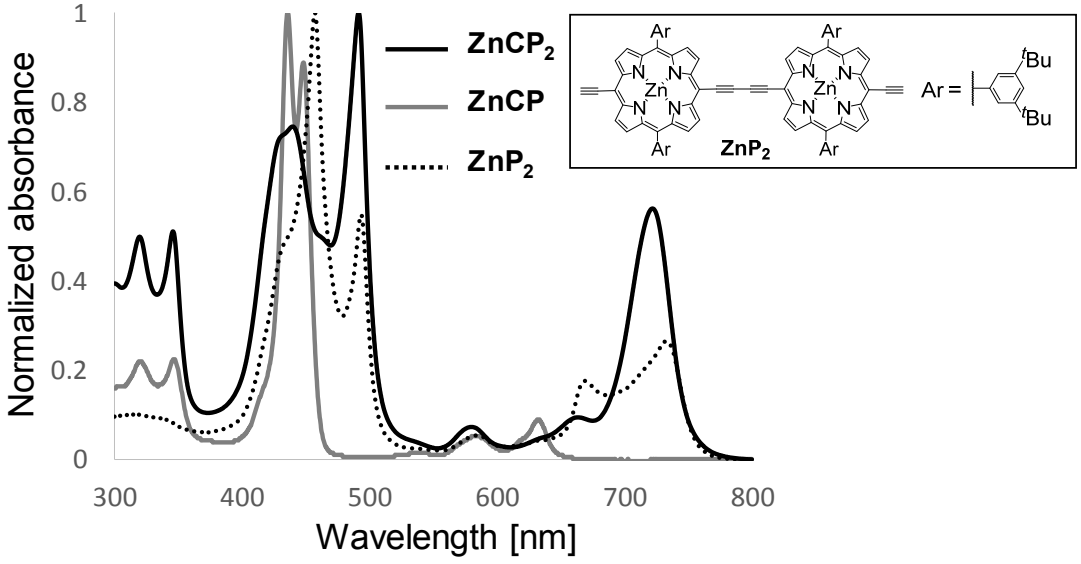

Figure 3-5. Absorption spectrum of **ZnCP₂** and **ZnCP**, **ZnP₂**.
solvent : $CHCl_3$ / pyridine = 100 / 1, temperature : r. t.

3-2-5. Investigation of the Structural Influence on the Template Assisted Tubulation

Next, a relation between the length of the linker and the reaction rate was investigated by UV-vis technique. UV-vis spectra show I_{590} (**ZnCP**) is much larger than I_{730} (**ZnCP**) whereas I_{590} (**$ZnCP_2$**) is much smaller than I_{730} (**$ZnCP_2$**) (Figure 3-5). Therefore, I_{730} / I_{590} could be an indicator of the formation rate of **$ZnCP_2$**. The change of I_{730} / I_{590} over time revealed that **T_2 (n=6)** showed the largest initial rate among **T_2 (n=4, 6, 8, 12)** (Figure 3-6a). The optimized geometry of **$ZnCP_2$** was calculated at the B3LYP level of theory employing the 6-31G(d) for carbons, hydrogens and oxygens and Lanl2DZ for nitrogens and zincs. Stable structures of **T_2 (n=x)** were calculated at the B3LYP level of theory using the 6-31G(d) for carbons, hydrogens and nitrogens. The theoretical calculations showed distance between the two zincs of **$ZnCP_2$** and that between the two nitrogen atoms of **T_2 (n=4, 6, 8, 12)**, that is a distance between 1,4-di(pyridin-4-yl)benzene unit (Figure 3-6b). **T_2 (n=6)** is the most suitable template molecule because of the linker fitting a porphyrin tube **$ZnCP_2$** (Figure 3-6a). Tubulation with **T_2 (n=4)** showed the slowest rate among **T_2 (n=4, 6, 8, 12)**. It is expected that a template molecule with a short alkyl linker made reaction points difficult to get close to each other.

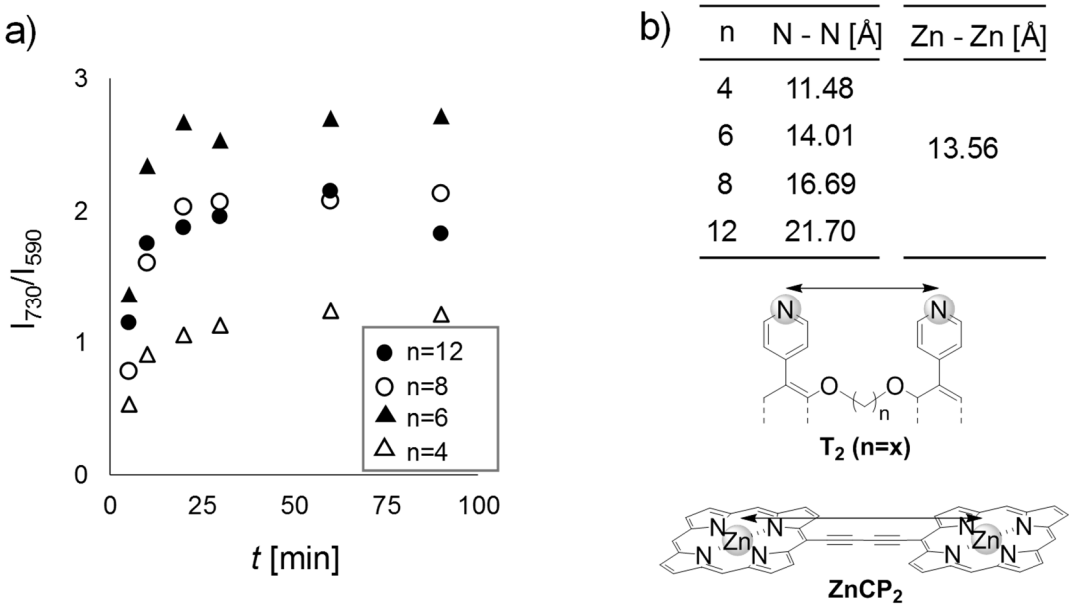

Figure 3-6. Relation between linker length of **T_2 (n=x)** and reaction rate.

a) I_{730} / I_{590} values against reaction time (t).

b) Comparison between distances of N-N of template molecules **T_2 (n=x)** and Zn-Zn of porphyrin tube **$ZnCP_2$**. Arrows indicate interatomic distances, N-N or Zn-Zn.

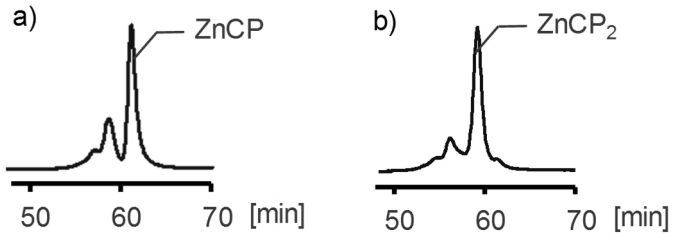

Figure 3-7. SEC chromatograms for the synthesis of **ZnCP$_2$** by template assisted tubulation (Eluent : THF, detection : 420 nm). a) With **T$_2$' (n=6)** and b) with **T$_2$ (n=6)**.

A relation between affinity of template molecules to porphyrin rings and the tubulation was also investigated. In contrast to **T$_2$ (n=6)**, **T$_2$' (n=6)** was not effective for the tubulation (Figure 3-7). A binding constant K_f between **ZnCP'** and **T$_1$** was too high to be determined by direct UV-vis titration. K_f was estimated by analyzing the thermodynamics of template displacement with competing monodentate ligands as follows.[12] First, **ZnCP'·T$_1$** was prepared by adding one equivalent of **T$_1$** to **ZnCP'**. Then, a large excess of imidazole was titrated into solutions of the 1:1 complex to displace **T$_1$** to determine the denaturation constant K_{dn}. A binding constant K_{im} between zinc porphyrin and imidazole as a monodentate ligand can be determinded from the 1 : 1 complexation model using UV-vis titration. In this case, zinc(II) tetraphenylporphyrin instead of **ZnCP'** was used in the titration experiments because a binding constant between zinc(II) tetraphenylporphyrin and imidazole is assumed to be equivalent of one (K_1) between **ZnCP'** and imidazole.[12] Since **ZnCP'** has two binding sites for monodentate ligands, the binding constant K_f can be estimated from a following relationship: $K_f = K_{im}^2 / K_{dn}$. The UV-vis titration of imidazole to **ZnTPP** afforded K_{im} with 2.6×10^4 M^{-1}, whereas K_{dn} obtained from the UV-vis titration of imidazole to **ZnCP'·T$_1$** was K_{dn} = 3.9 M^{-1}. The formula comprised of K_f, K_{im}, and K_{dn} afforded K_f with 1.7×10^8 M^{-1}, which is much higher than the binding constant between 5,10,15,20-tetraphenyl-zinc-porphyrin and pyridine (K_a = 10^3 M^{-1}).[12] **T$_2$ (n=6)** could effectively make two **ZnCP**'s close to each other due to the high affinity to **ZnCP**'s based on the chelate effect, which led to the tubulation via selective dimerization.

3-3. Conclusion

In conclusion, the author developed the template-assisted tubulation method for a synthesis of the porphyrin tubes via selective dimerization. The template-assisted tubulation could accelerate only the target reaction because of the proximity effect. Length of alkyl linkers of the template molecules affected to the proximity effect, in other word reaction rate. Numbers of the –CH_2– units between 1,4-di(pyridin-4-yl)benzene units are important to efficiently synthesize the dimer. These knowledge will be useful to design template molecules for the tubulation.

3-4. Experimental Section

3-4-1. General Remarks

Materials: Reagents were purchased from commercial sources and used without further purification. Solvents were purified as follows: reaction solvents were degassed through freeze-pump-thaw (three times), before use. Dry toluene, THF, and DMF was purchased from Kanto Chemical and further purified by passage through activated alumina under positive argon pressure as described by Grubbs *et al.*[13] A fluorene derivative **10**,[14] porphyrin derivative **2**,[15] 5,15-dibromo-10,20-bis-(3,5-di-*tert*-butylphenyl)porphyrinato]zinc (II),[16] and **T1**[17] were prepared by the previously reported procedures. **ZnP2** was synthesized from 5,15-dibromo-10,20-bis-(3,5-di-*tert*-butylphenyl)porphyrinato]zinc (II) according to previous methods.[18]

NMR Spectroscopy: ^{1}H NMR spectra were measured on a Bruker AVANCE-500 spectrometer. The ^{1}H NMR chemical shifts are reported relative to tetramethylsilane (TMS, 0.00 ppm) or residual protonated solvent (7.26 ppm) in $CDCl_3$ or (5.32 ppm) in CD_2Cl_2. The ^{13}C NMR chemical shifts are reported relative to tetramethylsilane (TMS, 0.00 ppm) or solvent (77.16 ppm) in $CDCl_3$, or (53.84 ppm) in CD_2Cl_2.

Preparative recycling gel permeation chromatography (GPC): Preparative recycling GPC was performed with a JAI LC9104 System equipped with JAIGEL-1H and 2H columns, a JAI UV DETECTOR 310, and a JAI RI DETRCTOR RI-5, a JAI LC9130NEXT System equipped with JAIGEL-2H and 2.5H columns, a JAI UV DETECTOR 370NEXT, and a JAI RI DETRCTOR RI 700NEXT, a JAI LC9140 System equipped with JAIGEL-2.5H and -3H columns, a JAI UV DETECTOR 310, and a JAI RI DETRCTOR RI-5.

Mass spectroscopy (MS): Matrix assisted laser desorption/ionization time-of-flight (MALDI-TOF) mass spectra were obtained with α-cyano-4-hydroxycinnamic acid (CHCA) or trans-2-[3-(4-t-butyl-phenyl)-2-methyl-2-propenylidene]malononitrile (DCTB) as a matrix on a Thermo Fisher Scientific LTQ orbitrapXL or a SHIMADZU Axima Performance. ESI mass spectra were obtained on a Thermo Fisher Scientific EXACTIVE.

Absorption spectroscopy: Absorption spectra were measured with a SHIMADZU UV-2600 spectrophotometer.

3-4-2. Synthetic Procedures

Scheme 3-5. Synthesis of fluorene 1 from 10

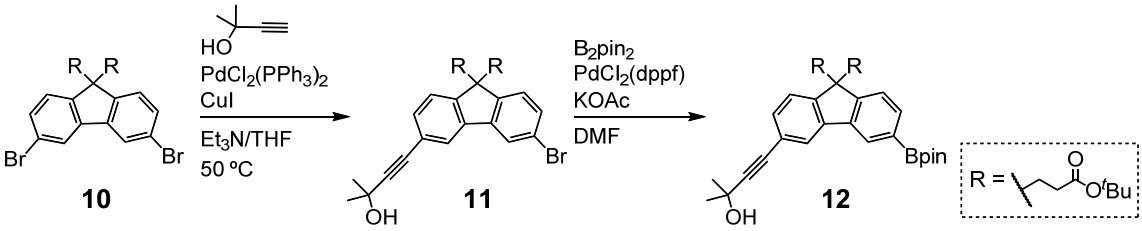

.

Synthesis of 11

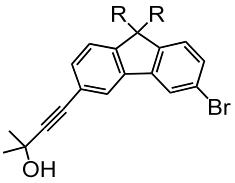

10 (4.69 g, 8.08 mmol), $PdCl_2(PPh_3)_2$ (283 mg, 0.404 mmol), and CuI (38.5 mg, 0.202 mmol) were dissolved in degassed THF / Et_3N (4 / 1, 330 mL) under Ar. 2-Methyl-3-butyn-2-ol (0.706 mL, 7.27 mmol) was added. The solution was stirred at 50 °C overnight, and passed through the Celite pad. The solvent was evaporated, after which the residue was purified by silica gel column chromatography (EtOAc / hexane = 1 / 4) to yield **11** (1.62 g, 34%) as a yellow solid. Unreacted **10** (2.50 g, 4.31 mmol) was recovered as a pure solid during the above purification process.

HR-MS (ESI MS) (m/z) 605.1873 ([**11**+Na^+], $C_{32}H_{39}BrNaO_5$, calcd. 605.1879)

^{1}H NMR (500 MHz, CD_2Cl_2, r. t.): δ 7.84 (d, *J* = 1.5 Hz, 1H, Ar-*H*), 7.74 (s, 1H, Ar-*H*), 7.48 (dd, *J* = 8.0, 1.6 Hz, 1H, Ar-*H*), 7.42 (dd, *J* = 7.8, 1.1 Hz, 1H, Ar-*H*), 7.35 (d, *J* = 7.8 Hz, 1H, Ar-*H*), 7.28 (d, *J* = 8.0 Hz, 1H, Ar-*H*), 2.32 (t, *J* = 8.3 Hz, 4H, -CH_2CH$_2$COO*t*Bu), 1.62 (s, 6H, -C(CH_3)$_2$OH), 1.42 (t, *J* = 8.3 Hz, 4H, -CH$_2$CH_2COO*t*Bu), 1.28 (s, 18H, -COOC(CH_3)$_3$).

^{13}C NMR (126 MHz, CD_2Cl_2, r. t.): δ 172.5, 149.1, 147.6, 143.0, 140.5, 132.0, 131.2, 125.3, 123.76, 123.69, 123.66, 122.8, 121.9, 94.7, 82.0, 80.3, 65.8, 54.12, 34.7, 31.8, 30.3, 28.1.

Synthesis of 12

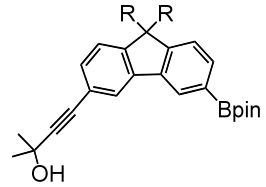

11 (1.34 g, 2.31 mmol), bis(pinacolato)diboron (0.706 g, 2.78 mmol), $PdCl_2$(dppf) (188 mg, 0.231 mmol), and KOAc (302 mg, 3.08 mmol) were dissolved in dehydrated DMF (54.0 mL) under Ar. The solution was stirred at 80 °C overnight, after which the solvent was removed under vacuum. The residue was purified by silica gel column chromatography (EtOAc / hexane = 1 / 4) and GPC with $CHCl_3$ as an eluent to yield **12** (1.01 g, 69%) as a white solid.

HR-MS (ESI-MS) (m/z) 653.3621 ([**12**+Na^+], $C_{38}H_{51}BNaO_7$, calcd. 653.3626)

^{1}H NMR (500 MHz, CD_2Cl_2, r. t.): δ 8.14 (s, 1H, Ar-*H*), 7.84 (s, 1H, Ar-*H*), 7.78 (d, *J* = 7.5 Hz, 1H, Ar-*H*), 7.42-7.38 (m, 2H, Ar-*H*), 7.35 (s, 1H, Ar-*H*), 2.33 (t, *J* = 8.3 Hz, 5H, -

C*H*$_2$CH$_2$COO^{t}Bu), 1.62 (s, 6H, -C(C*H*$_3$)$_2$OH), 1.40 (several peaks, 4H+12H, -CH$_2$C*H*$_2$COO^{t}Bu and B(pin)-*H),* 1.28 (s, 18H, -COOC(C*H*$_3$)$_3$)

^{13}C NMR (126 MHz, CD$_2$Cl$_2$, r. t.): δ 172.7, 152.0, 148.7, 141.8, 140.3, 135.0, 131.2, 126.8, 123.67, 123.49, 123.0, 122.5, 94.4, 84.3, 82.3, 80.2, 65.8, 54.34, 34.9, 31.8, 30.4, 28.1, 25.1.

Synthesis of 3

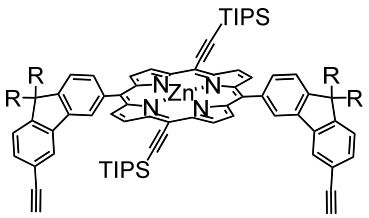

1 (960 mg, 1.52 mmol), **2** (454 mg, 0.509 mmol), Pd(PPh$_3$)$_4$ (119 mg, 0.103 mmol), and Na$_2$CO$_3$ (699 mg, 6.59 mmol) were dissolved in degassed toluene / EtOH / H$_2$O (5 / 1 / 1, 35.0 mL) and dehydrated pyridine (2.5 mL) under Ar. The solution was stirred at 80 ºC for 2 days. The organic layer was extracted with EtOAc, after which the residue was purified by silica gel column chromatography (EtOAc / hexane = 1 / 1) and GPC with CHCl$_3$ as an eluent. The product was dissolved in degassed toluene (34 mL) before ^{t}BuOK (285 μL, 1 M in THF, 5.68 mmol) was added. The solution was stirred at 70 ºC for 30 min. The crude product was purified by silica gel column chromatography (CH$_2$Cl$_2$ / EtOAc = 4 / 1) to yield **3** (345 mg, 42%) as a purple solid.

HR-MS (APCI-MS) (m/z) 1621.770 ([**3**+H$^+$], C$_{100}$H$_{117}$N$_4$O$_8$Si$_2$Zn, calcd. 1620.770)

^{1}H NMR (400 MHz, CDCl$_3$, r. t.): δ 9.80 (d, *J* = 4.6 Hz, 4H, β-*H*), 8.98 (d, *J* = 4.6 Hz, 4H, β-*H*), 8.51 (s, 2H, Ar-*H*), 8.19 (d, *J* = 7.6 Hz, 2H, Ar-*H*), 7.89 (s, 2H, Ar-*H*), 7.75 (d, *J* = 7.5 Hz, 2H, Ar-*H*), 7.57 (d, *J* = 8.1 Hz, 2H, Ar-*H*), 7.49 (d, *J* = 8.0 Hz, 2H, Ar-*H*), 3.03 (s, 2H, -CC*H*), 2.63-2.51 (m, 8H, -C*H*$_2$CH$_2$COO^{t}Bu), 1.90-1.73 (m, 8H, -CH$_2$C*H*$_2$COO*t*Bu), 1.51-1.43 (m, 36H+42H, -COOC(C*H*$_3$)$_3$, -Si(C*H*(C*H*$_3$)$_2$)$_3$).

^{13}C NMR (126 MHz, CDCl$_3$, r. t.): δ 172.7, 152.5, 150.2, 149.6, 147.5, 141.9, 141.2, 138.8, 134.6, 132.9, 132.0, 131.5, 126.2, 124.0, 123.3, 122.3, 121.6, 121.3, 109.2, 102.0, 98.9, 83.7, 80.5, 54.0, 34.8, 30.5, 28.1, 19.1.

Synthesis of ZnCP

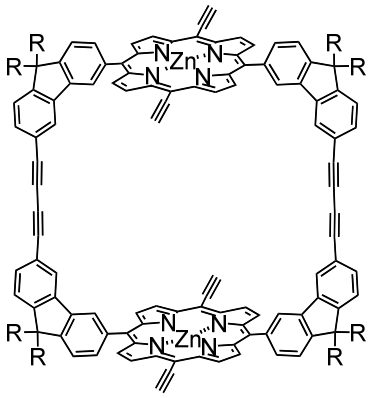

3 (325 mg, 0.200 mmol) and **T1** (281 mg, 1.21 mmol) were dissolved in dehydrated CH_2Cl_2 (509 mL), and CuCl (2.46 g, 24.8 mmol) was added to the solution under Ar before dried TMEDA (1.8 mL) was added slowly. Ar was substituted to dry air, after which the solution was stirred at r. t. for 15 h. The solution was passed through the Celite pad before extracted with EtOAc. The residue was purified by silica gel column chromatography (EtOAc / hexane / pyridine = 1 / 1 / 0.01) and GPC using $CHCl_3$ as an eluent. Pyridine was added as an eluent to remove **T1** from **ZnCP**. The product was dissolved in THF (83 mL) before addition of TBAF (0.400 mL, 0.400 mmol, 1M in THF). The solution was stirred at r. t. for 30 min. the crude mixture was purified by GPC using $CHCl_3$ as an eluentt o afford **ZnCP** (169 mg, 65%) as a purple solid.

HR-MS (MALDI-TOF MS) (m/z) 2613.965 ([**ZnCP**+H^+], $C_{164}H_{149}N_8O_{16}Zn_2$, calcd. 2613.967)

^{1}H NMR (500 MHz, $CDCl_3$, r. t.): δ 9.57 (d, *J* = 3.5 Hz, 8H, β-*H*), 8.79 (d, *J* = 3.9 Hz, 8H, β-*H*), 8.42 (s, 4H, Ar-*H*), 7.98 (d, *J* = 6.7 Hz, 4H, Ar-*H*), 7.81 (s, 4H, Ar-*H*), 7.62 (d, *J* = 6.8 Hz, 4H, Ar-*H*), 7.54 (d, *J* = 7.9 Hz, 4H, Ar-*H*), 7.37 (d, *J* = 6.9 Hz, 4H, Ar-*H*), 3.99 (s, 4H, -CC*H*), 2.44-2.35 (m, 16H, -C*H*$_2$CH$_2$COO*t*Bu), 1.70-1.60 (m, 16H, -C*H*$_2$CH$_2$COO*t*Bu), 1.32 (s, 72H, -CH$_2$CH$_2$COOC(C*H*$_3$)$_3$).

^{13}C NMR (126 MHz, $CDCl_3$, r. t.): δ 172.7, 152.4, 150.33, 150.24, 147.6, 141.9, 141.4, 138.7, 135.0, 132.86, 131.4, 125.9, 124.0, 123.6, 122.1, 121.43, 121.32, 100.23, 100.12, 85.9, 84.2, 81.7, 80.6, 74.1, 54.1, 34.7, 30.5, 28.1.

Synthesis of 2,5-diiodophenol 5

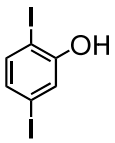

3-Iodophenol **8** (8.46 g, 38.5 mmol), KI (4.48 g, 27.0 mmol), and KIO_3 (2.48 g, 11.6 mmol) were dissolved in 3.8% H_2SO_4 aq. (w / w, 246 mL). The solution was stirred at r. t. for 14 h, after which I_2 was quenched by $Na_2S_2O_3$. The residue was extracted by EtOAc three times and the organic layers were washed with brine. The organic layer was dried over Na_2SO_4 and evaporated to afford a brown oil. The oil was purified by silica gel column chromatography (CH_2Cl_2 / hexane = 19 / 1) to afford **5** (7.81 g, 70%) as a white solid.

HR-MS (EI MS) (m/z) 345.8348 ([**5**]$^+$, $C_6H_4I_2O$, calcd. 345.8352)

^{1}H NMR (500 MHz, $CDCl_3$, r. t.): δ 7.34 (d, *J* = 2.0 Hz, 1H, Ar-*H*), 7.34 (d, *J* = 8.3 Hz, 1H, Ar-*H*), 7.00 (dd, *J* = 8.3, 2.0 Hz, 1H, Ar-*H*), 5.29 (s, 1H, -O*H*).

^{13}C NMR (126 MHz, $CDCl_3$, r. t.): δ 155.6, 139.4, 131.7, 124.4, 94.6, 85.4.

Synthesis of T_2 (n=4)

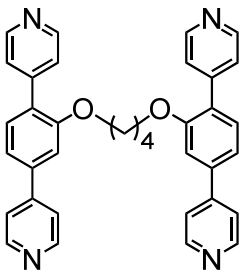

5 (300 mg, 1.00 mmol), K_2CO_3 (222 mg, 1.61 mmol), and 1,4-dibromobutane (57.8 μL, 0.485 mmol) were dissolved in dehydrated DMF (15 mL) under Ar. The solution was stirred at 90 °C overnight, after which the residue was washed by water twice and brine once. The organic layer was dried by Na_2SO_4 and evaporated. The residue was purified by silica gel column chromatography (CH_2Cl_2 / hexane = 1 / 9) to afford **6 (n=4)** (202 mg, 0.271 mmol) as a white solid. Half amount of **6 (n=4)** (101 mg, 0.136 mmol), **7** (333 mg, 1.63 mmol), Cs_2CO_3 (530 mg, 1.63 mmol), and $Pd(PPh_3)_4$ (94.0 mg, 81.3 μmol) were dissolved in DMF / toluene (1 / 1, 6.6 mL) under Ar. The solution was stirred at 125 °C overnight. The solvents were removed under vacuum, after which the residue was passed through a Celite pad. The crude mixture was purified by silica gel column chromatography (CH_2Cl_2 / MeOH = 100 / 1 to 10 / 1) to afford **T_2 (n=4)** (34.0 mg, 25% for 2 steps) as a yellow solid.

HR-MS (APCI MS) (m/z) 551.2429 ([**T_2 (n=4)**+H^+], $C_{36}H_{31}N_4O_2$, calcd. 551.2427);
^{1}H NMR (500 MHz, $CDCl_3$, r. t.): δ 8.69 (dd, *J* = 4.5, 1.5 Hz, 4H, Ar-*H*), 8.59 (dd, *J* = 4.5, 1.5 Hz, 4H, Ar-*H*), 7.52 (dd, *J* = 4.5, 1.6 Hz, 4H, Ar-*H*), 7.47-7.45 (m, 6H, Ar-*H*), 7.33 (dd, *J* = 7.9, 1.6 Hz, 2H, Ar-*H*), 7.17 (d, *J* = 1.6 Hz, 2H, Ar-*H*), 4.09 (t, *J* = 4.5 Hz, 4H, -OC*H*$_2$CH$_2$CH$_2$-), 1.90 (m, 4H, -OCH$_2$C*H*$_2$CH$_2$-).
^{13}C NMR (126 MHz, $CDCl_3$, r. t.): δ 156.5, 150.5, 149.6, 147.8, 145.8, 140.4, 131.3, 128.7, 124.3, 121.7, 120.0, 111.1, 68.3, 26.2.

Synthesis of T_2 (n=6)

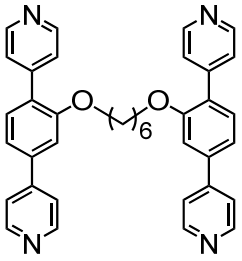

5 (200 mg, 0.669 mmol), K_2CO_3 (105 mg, 0.760 mmol), and 1,6-dibromohexane (46.1 μL, 0.304 mmol) were dissolved in dehydrated DMF (10 mL). The solution was stirred at 90 °C overnight under Ar, after which the solution was extracted by EtOAc and washed by water four times and brine once. The residue was purified by silica gel column chromatography (CH_2Cl_2 / hexane = 1 / 10) to afford **6 (n=6)** as a white solid (153 mg, 0.198 mmol). **6 (n=6)** (153 mg, 0.198 mmol), **7** (406 mg, 1.98 mmol), Cs_2CO_3 (538 mg, 1.98 mmol) and $Pd(PPh_3)_4$ (68.6 mg, 59.4 μmol) were dissolved in DMF / toluene (1 / 1, 9.6 mL) under Ar. The solution was stirred at 110 °C overnight. The solvents were removed under vacuum, after which the residue was passed through a Celite pad. The crude

mixture was purified by silica gel column chromatography (CH_2Cl_2 : MeOH = 100 : 1 to 20 : 1) to afford **T_2 (n=6)** (101 mg, 57% for 2 steps) as a yellow solid.

HR-MS (APCI MS) (m/z) 579.2739 ([**T_2 (n=6)**+H^+], $C_{40}H_{38}N_4O_2$, calcd. 579.2760)
^{1}H NMR (500 MHz, $CDCl_3$, r. t.): δ 8.69 (dd, *J* = 4.5, 1.3 Hz, 4H, Ar-*H*), 8.61 (dd, *J* = 4.3, 1.3 Hz, 4H, Ar-*H*), 7.54 (dd, *J* = 4.6, 1.3 Hz, 4H, Ar-*H*), 7.48 (dd, *J* = 4.5, 1.3 Hz, 4H, Ar-*H*), 7.46 (d, *J* = 7.9 Hz, 2H, Ar-*H*), 7.32 (dd, *J* = 7.8, 1.1 Hz, 2H, Ar-*H*), 7.21 (d, *J* = 1.1 Hz, 2H, Ar-*H*), 4.05 (t, *J* = 6.2 Hz, 4H, -OC*H*$_2$CH$_2$CH$_2$-), 1.79-1.74 (m, 4H, -OCH$_2$C*H*$_2$CH$_2$-), 1.45-1.42 (m, 4H, -OCH$_2$CH$_2$C*H*$_2$-).
^{13}C NMR (126 MHz, $CDCl_3$, r. t.): δ 156.7, 150.5, 149.6, 147.9, 145.8, 140.3, 131.2, 128.7, 124.3, 121.8, 119.9, 111.2, 68.7, 29.1, 25.9.

Synthesis of T_2 (n=8)

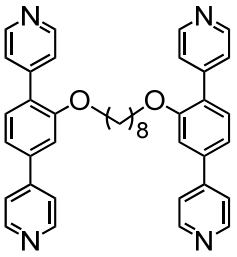

5 (400 mg, 1.16 mmol), K_2CO_3 (216 mg, 1.56 mmol), and 1,8-dibromooctane (72.0 μL, 0.387 mmol) were dissolved in dehydrated DMF (20 mL) under Ar. The solution was stirred at 100 °C for 36 h, after which DMF was removed under vacuum. The residue was purified by silica gel column chromatography (CH_2Cl_2 / hexane = 1 / 4 to 1 / 2) to afford **6 (n=8)** (305 mg, 0.380 mmol) as a white solid. **6 (n=8)** (305 mg, 0.380 mmol), **7** (624 mg, 3.04 mmol), Cs_2CO_3 (990 mg, 3.04 mmol) and $Pd(PPh_3)_4$ (87.8 mg, 76.0 μmol) were dissolved in DMF / toluene (1 / 1, 26.0 mL). The solution was stirred at 125 °C overnight. The solvents were removed under vacuum, after which the residue was passed through a Celite pad. The crude mixture was purified silica gel column chromatography (CH_2Cl_2 / MeOH = 100 / 1 to 20 / 1) to afford **T_2 (n=8)** (168 mg, 72% for 2 steps) as a yellow solid.

HR-MS (APCI MS) (m/z) 607.3062 ([**T_2 (n=8)**+H^+], $C_{40}H_{39}N_4O_2$, calcd. 607.3073)
^{1}H NMR (500 MHz, $CDCl_3$, r. t.): δ 8.69 (dd, *J* = 4.7, 1.3 Hz, 4H, Ar-*H*), 8.63 (d, *J* = 5.9 Hz, 4H, Ar-*H*), 7.54 (dd, *J* = 4.6, 1.4 Hz, 4H, Ar-*H*), 7.51 (dd, *J* = 4.7, 1.3 Hz, 4H, Ar-*H*), 7.46 (d, *J* = 7.8 Hz, 2H), 7.32 (dd, *J* = 7.9, 1.3 Hz, 2H, Ar-*H*), 7.23 (d, *J* = 1.2 Hz, 2H, Ar-*H*), 4.07 (t, *J* = 6.3 Hz, 4H, -OC*H*$_2$CH$_2$-), 1.78-1.73 (m, 4H, -OCH$_2$C*H*$_2$CH$_2$CH$_2$-), 1.40-1.37 (m, 4H, -OCH$_2$CH$_2$C*H*$_2$CH$_2$-), 1.31 (d, *J* = 6.3 Hz, 4H, -OCH$_2$CH$_2$CH$_2$C*H*$_2$-).
^{13}C NMR (126 MHz, $CDCl_3$, r. t.): δ 156.8, 150.5, 149.6, 148.0, 145.8, 140.3, 131.2, 128.6, 124.4, 121.8, 119.8, 111.2, 68.9, 29.21, 26.1, 25.0.

Synthesis of T_2 (n=12)

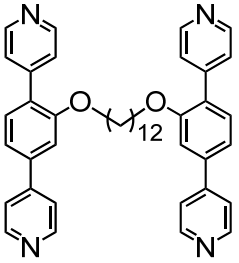

5 (500 mg, 1.52 mmol), K_2CO_3 (210 mg, 1.52 mmol), and 1,12-dibromododecane (176 mg, 0.508 mmol) were dissolved in dehydrated DMF (23.0 mL) under N_2. The solution was stirred at 100 ºC overnight, after which the solution was filtered through the Celite pad. The residue was purified by silica gel column chromatography (EtOAc / hexane = 1 / 40) to afford **6 (n=12)** (192 mg, 0.224 mmol) as a white solid. **6 (n=12)** (172 mg, 0.200 mmol), **7** (328 mg, 1.60 mmol), Cs_2CO_3 (521 mg, 1.60 mmol) and $Pd(PPh_3)_4$ (46.2 mg, 40.0 μmol) were dissolved in DMF / toluene (1 / 1, 13.6 mL) under N_2. The solution was stirred at 130 ºC overnight. The solvents were removed under vacuum, after which the residue was passed through a Celite pad. The crude mixture was purified by silica gel column chromatography (CH_2Cl_2 / MeOH = 100 / 1 to 10 / 1) to afford **T_2 (n=12)** (92 mg, 31% for 2 steps) as a pale yellow solid.

HR-MS (APCI MS) (m/z) 663.3675 ([**T_2 (n=12)**+H^+], $C_{44}H_{47}N_4O_2$, calcd. 663.3699)

^{1}H NMR (500 MHz, CDCl$_3$, r. t.): δ 8.69 (dd, *J* = 4.6, 1.3 Hz, 4H, Ar-*H*), 8.64 (dd, *J* = 4.7, 1.2 Hz, 4H, Ar-*H*), 7.54-7.51 (two double doublet peaks overlapped, 8H, Ar-*H*), 7.46 (d, *J* = 7.8 Hz, 2H, Ar-*H*), 7.31 (dd, *J* = 7.9, 1.0 Hz, 2H, Ar-*H*), 7.22 (d, *J* = 1.1 Hz, 2H, Ar-*H*), 4.07 (t, *J* = 6.4 Hz, 4H, -OC*H*$_2$CH$_2$CH$_2$CH$_2$CH$_2$CH$_2$-), 1.77 (dt, *J* = 14.3, 6.9 Hz, 4H, -OCH$_2$C*H*$_2$CH$_2$CH$_2$CH$_2$CH$_2$-), 1.41 (dt, *J* = 14.5, 7.1 Hz, 4H, -OCH$_2$CH$_2$C*H*$_2$CH$_2$CH$_2$CH$_2$-), 1.33-1.26 (several peaks overlapped, 4H+4H+4H, -OCH$_2$CH$_2$CH$_2$C*H*$_2$C*H*$_2$C*H*$_2$-).

^{13}C NMR (126 MHz, CDCl$_3$, r. t.): δ 156.9, 150.5, 149.6, 148.0, 145.8, 140.3, 131.2, 128.7, 124.4, 121.8, 119.7, 111.2, 68.9, 29.7 (two methylene carbons were overlapped), 29.40, 29.25, 26.2.

Synthesis of T_2' (n=6)

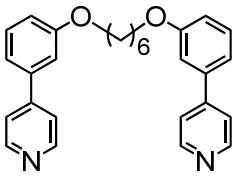

8 (400 mg, 1.82 mmol), K_2CO_3 (315 mg, 2.28 mmol), 1,6-dibromohexane (138 μL, 0.910 mmol), and tetrabutylammonium iodide (16.8 mg, 45.5 μmol) were dissolved in dehydrated DMF (20.0 mL) under N_2. The solution was stirred at 100 ºC overnight, after which the solution was filtered through the Celite pad. The residue was purified by silica gel column chromatography (CH_2Cl_2 / hexane = 1 / 8) to afford **9** as a white solid (393 mg, 0.753 mmol). The half amount of **9** (197 mg, 0.377 mmol), **7** (385 mg, 1.88 mmol), Cs_2CO_3 (612 mg, 1.88 mmol) and $Pd(PPh_3)_4$ (65.1 mg, 56.3 μmol) were dissolved in DMF / toluene (1 / 1, 10.6 mL) under N_2. The solution was stirred at 110 ºC overnight. The solvents were removed under vacuum, after which the residue was passed through a Celite pad. The crude mixture was purified by silica gel column chromatography (CH_2Cl_2 / EtOAc = 1 / 2) to afford **T_2' (n=6)** (96.4 mg, 50% for 2 steps) as a pale yellow solid.

HR-MS (MALDI-TOF MS) (m/z) 425.2218 ([**T_2' (n=6)**+H^+], $C_{28}H_{28}N_2O_2$, calcd. 425.2229)
^{1}H NMR (500 MHz, $CDCl_3$, r. t.): δ 8.63 (dd, *J* = 4.5, 1.6 Hz, 4H, Ar-*H*), 7.47 (dd, *J* = 4.5, 1.7 Hz, 4H, Ar-*H*), 7.37 (t, *J* = 7.9 Hz, 2H, Ar-*H*), 7.20-7.18 (m, 2H, Ar-*H*), 7.15 (t, *J* = 2.1 Hz, 2*H*, Ar-*H*), 6.96 (ddd, *J* = 8.2, 2.5, 0.7 Hz, 2H, Ar-*H*), 4.04 (t, *J* = 6.4 Hz, 4H, Ar-OC*H*$_2$CH$_2$CH$_2$-), 1.89-1.84 (m, Ar-OCH$_2$C*H*$_2$CH$_2$), 1.59 (m, 4H, Ar-OCH$_2$CH$_2$C*H*$_2$-).
^{13}C NMR (126 MHz, $CDCl_3$, r. t.): δ 159.7, 150.3, 148.3, 139.6, 130.2, 121.7, 119.3, 114.9, 113.5, 68.0, 29.3, 25.9.

Synthesis of $ZnCP_2$

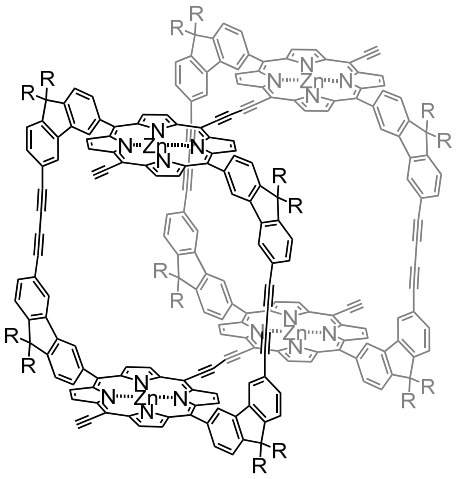

ZnCP (2.17 mg, 0.83 μmol) and **T_2 (n=6)** (0.248 mg, 0.428 μmol) were dissolved in CH_2Cl_2 (217 mL) followed by slow additions of CuCl (171 mg, 1.73 mmol) and TMEDA (190 μL, 1.30 mmol) under air the solution was stirred at r. t. for 18 h under air. The same reaction as the above was conducted in the another batch. The combined reaction mixture was carefully washed with NH_4Cl aq. with TMEDA once and NH_4Cl aq. once, water once and brine once to remove copper residue from the solution. The organic layer was dried over Na_2SO_4, then the solvent was removed in vacuo. The residue was filtered through silica gel (CH_2Cl_2 / EtOAc / pyridine = 100 / 10 / 1) to eliminate **T_2 (n=6)** from **$ZnCP_2$**. The crude product was purified by GPC (toluene / pyridine = 100 / 1) to afford $ZnCP_2$ (1.1 mg, 25%).

HR-MS (MALDI-TOF MS) (m/z) 5221.91 ([**$ZnCP_2$**]$^+$, $C_{328}H_{292}N_{16}O_{32}Zn_4$, calcd. 5221.8879)
^{1}H NMR (500 MHz, $CDCl_3$, r. t.) δ: 9.76 (d, *J* = 4.3 Hz, 8H, β-*H*), 9.56 (d, *J* = 4.4 Hz, 8H, β-*H*), 8.85 (d, *J* = 4.4 Hz, 8H, β-*H*), 8.75 (d, *J* = 4.4 Hz, 8H, β-*H*), 8.51 (s, 8H, Ar-*H*), 7.97 (d, *J* = 6.9 Hz, 8H, Ar-H), 7.67 (s, 8H, Ar-*H*), 7.62 (d, *J* = 7.9 Hz, 8H, Ar-*H*), 7.55 (d, *J* = 8.5 Hz, 8H, Ar-*H*), 4.09 (s, 4H), 2.62-2.57 (m, 32H), 1.89-1.68 (m, 32H), 1.45 (s, -CH$_2$CH$_2$COOC(C*H*$_3$)$_3$),1.42 (s, -CH$_2$CH$_2$COOC(C*H*$_3$)$_3$).

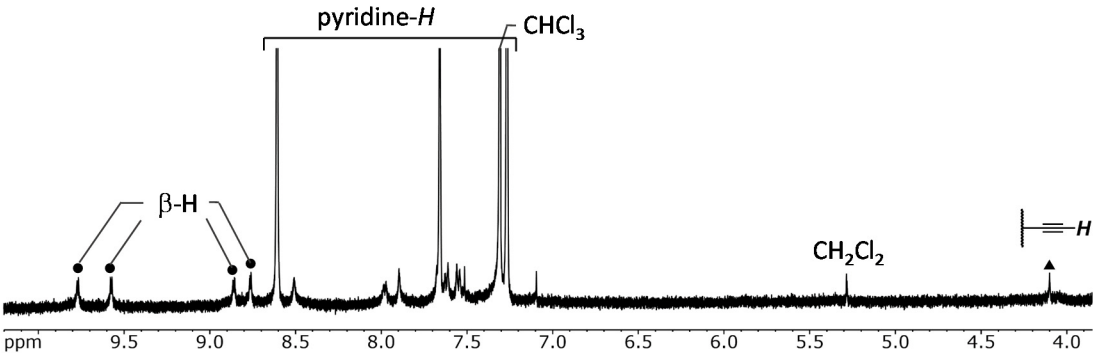

Figure 3-7. ^{1}H NMR (500 MHz, $CDCl_3$ / pyridine-d_5, 298K) of **$ZnCP_2$**

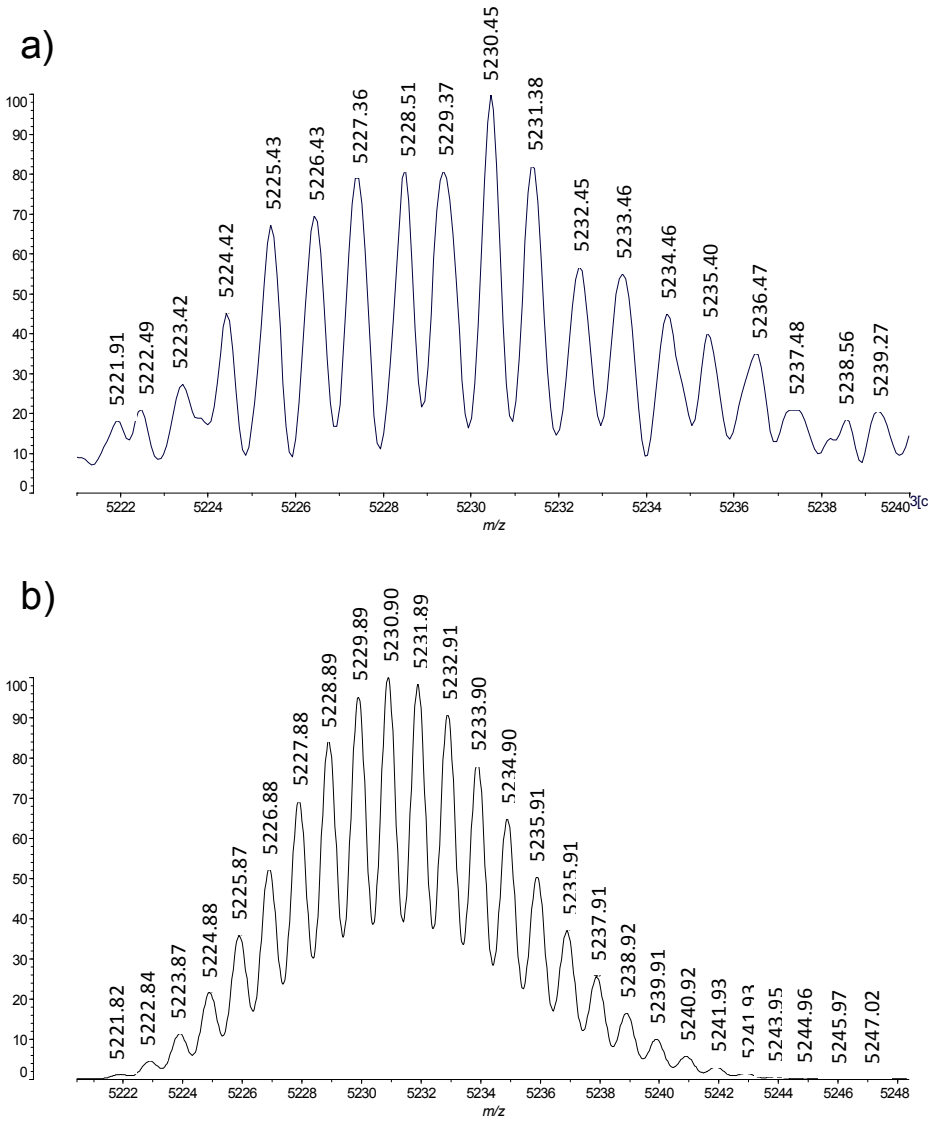

Figure 3-8. Measured (a) and theoretical (b) masses of MALDI TOF-TOF production ions of [**$ZnCP_2^+$**] using DCTB as a matrix

3-4-3. Complexation Study

Scheme 3-5. Complexation between **ZnCP'** and **T_2 (n=x)**

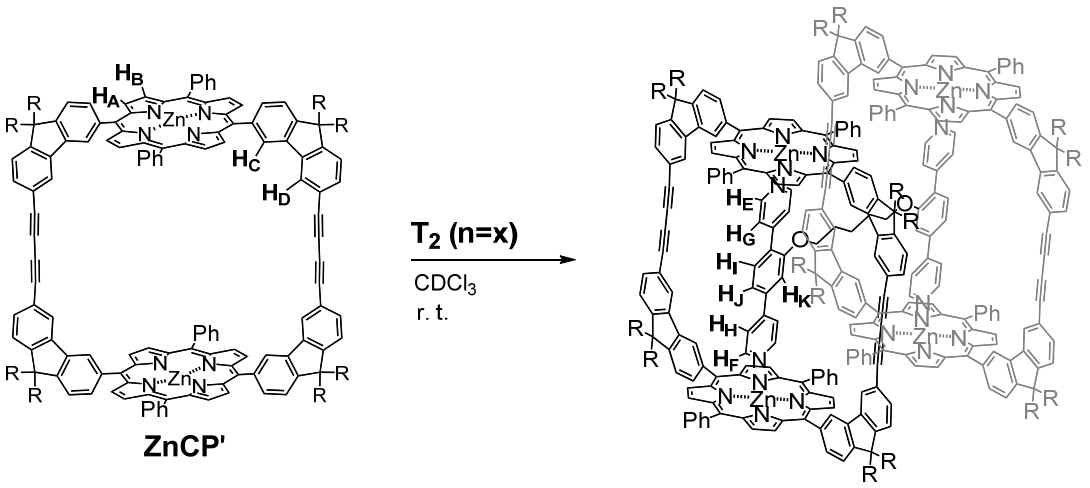

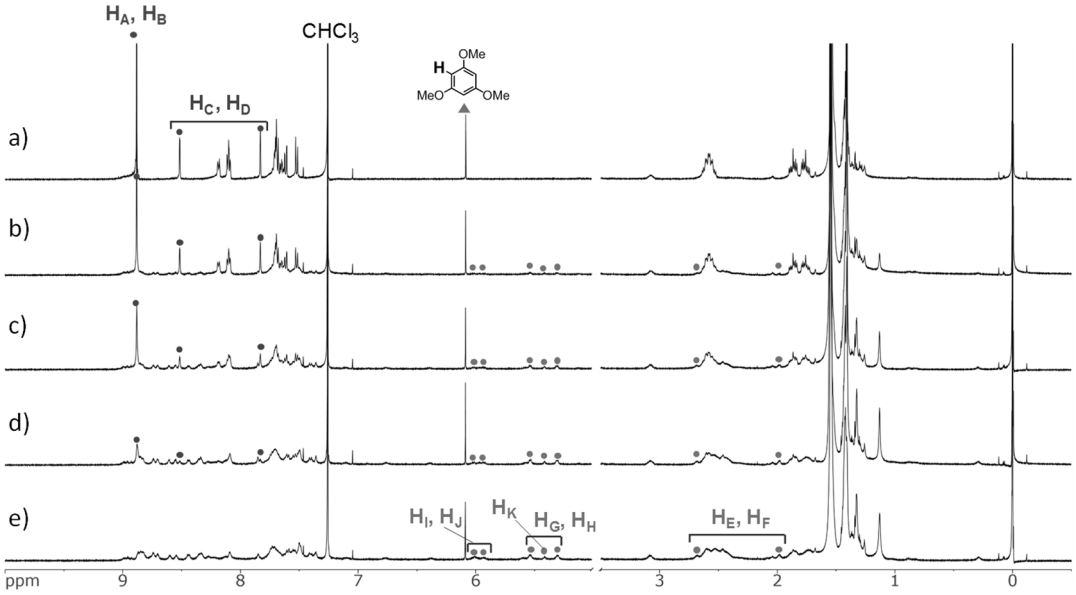

Figure 3-9. ^{1}H NMR (500 MHz, 298K) titration of **T_2 (n=4)** to **ZnCP'** in $CDCl_3$. a) 0 equiv., b) 0.125 equiv., c) 0.250 equiv., d) 0.375 equiv., and e) 0.500 equiv. 1,3,5-Trimethoxybenzene (triangle) was added as an internal standard.

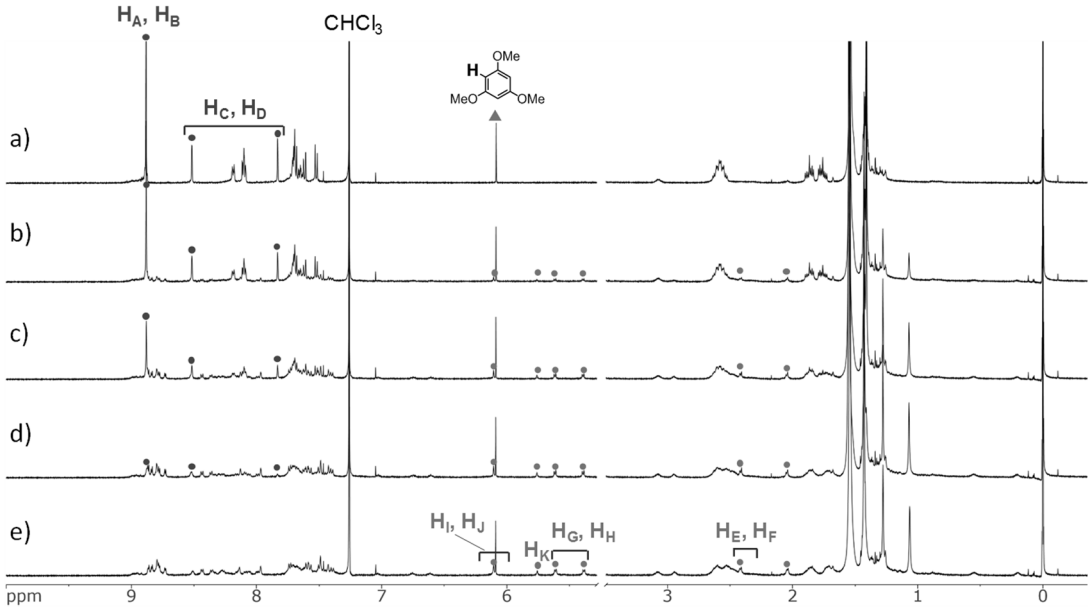

Figure 3-10. ^{1}H NMR (500 MHz, 298K) titration of **T_2 (n=6)** to **ZnCP'** in $CDCl_3$. a) 0 equiv., b) 0.125 equiv., c) 0.250 equiv., d) 0.375 equiv., and e) 0.500 equiv. 1,3,5-Trimethoxybenzene (triganle) was added as an internal standard.

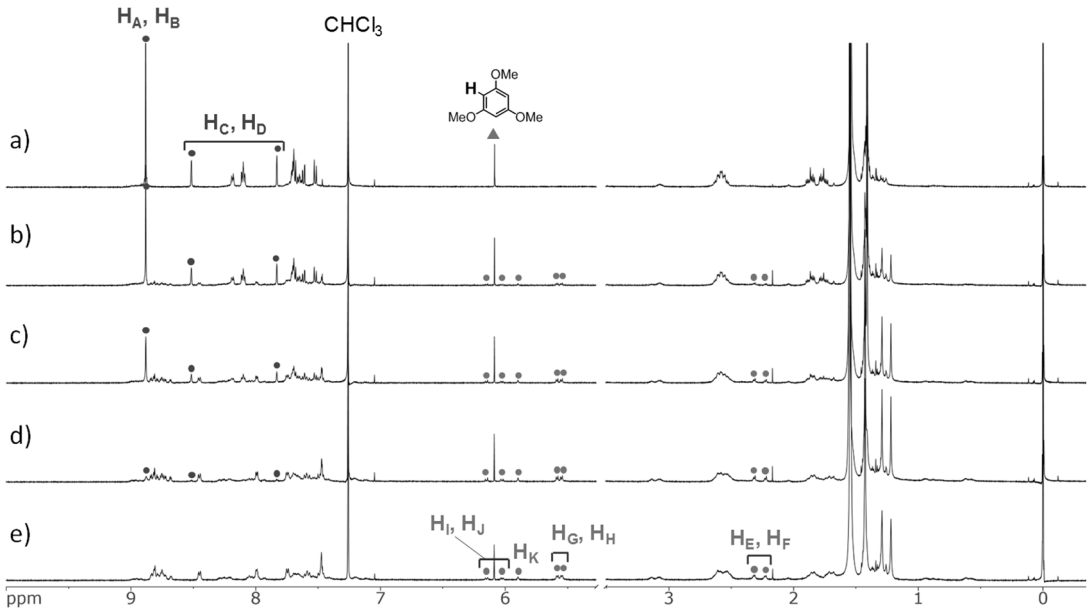

Figure 3-11. ^{1}H NMR (500 MHz, 298K) titration of **T_2 (n=8)** to **ZnCP'** in $CDCl_3$. a) 0 equiv., b) 0.125 equiv., c) 0.250 equiv., d) 0.375 equiv., and e) 0.500 equiv. 1,3,5-Trimethoxybenzene (triganle) was added as an internal standard.

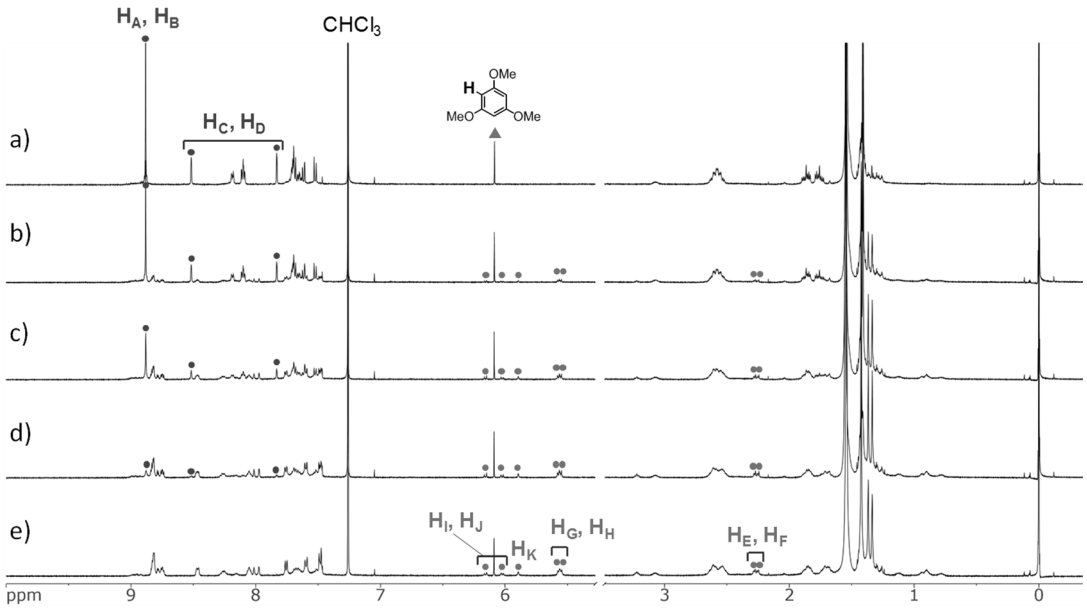

Figure 3-12. ^{1}H NMR (500 MHz, 298K) titration of **T_2 (n=12)** to **ZnCP'** in $CDCl_3$. a) 0 equiv., b) 0.125 equiv., c) 0.250 equiv., d) 0.375 equiv., and e) 0.500 equiv. 1,3,5-Trimethoxybenzene (triangle) was added as an internal standard.

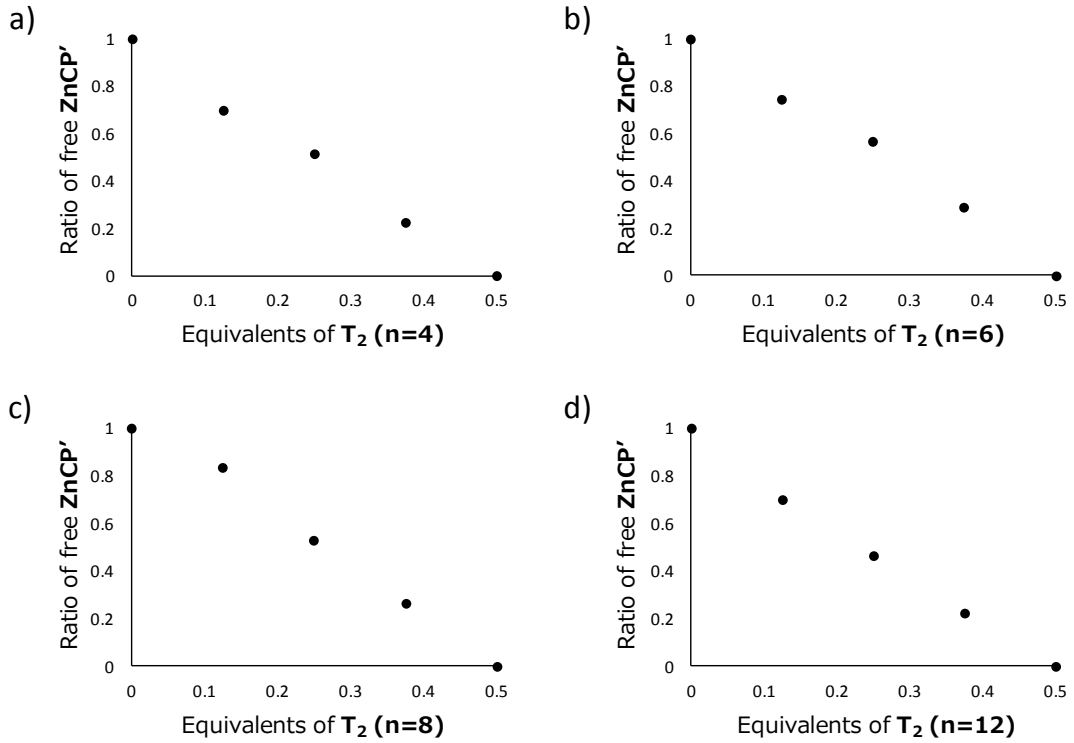

Figure 3-13. Conversion ratio of free **ZnCP'** in ^{1}H NMR titration of **T_2 (n=x)** to **ZnCP'** in $CDCl_3$. a) **T_2 (n=4)**, b) **T_2 (n=6)**, c) **T_2 (n=8)**, and d) **T_2 (n=12)**.

3-4-4. Binding Study

The simple two-state 2-site model was applied to indirectly determine the binding constant K_f for **ZnCP'(T1)**. The titration of **ZnCP'(T1)** with imidazole **Im** was analyzed assuming that each pyridyl unit of **T1** binds independently, so that the equilibrium can be treated as the displacement of a 2-site ligand **T1** from a 2-site receptor **ZnCP'**.

$$\mathbf{ZnCP'(T_1)} + 2\mathbf{Im} \underset{}{\overset{K_d}{\rightleftharpoons}} \mathbf{ZnCP'(Im)_2} + \mathbf{T_1}$$

$$K_d = \frac{[\mathbf{ZnCP'(Im)_2}][\mathbf{T_1}]}{[\mathbf{ZnCP'(T_1)}][\mathbf{Im}]^2} \quad \text{(S1)}$$

The denaturation equilibrium constant, K_d, defined by equation (S1) was determined by fitting the binding isotherm to equation (S2).[19]

$$\Delta A = \frac{L(-K_{dn}[\mathbf{Im}]^2 + \sqrt{K_{dn}^2[\mathbf{Im}]^2 + 4K_{dn}[\mathbf{Im}]^2[\mathbf{ZnCP'(T_1)}]_0})}{2[\mathbf{ZnCP'(T_1)}]_0} \quad \text{(S2)}$$

where ΔA is the change of absorption at any point in the titration, L is ΔA at 100 % complexation, [**Im**] is the total concentration of imidazole at each point in the titration and $[\mathbf{ZnCP'(T_1)}]_0$ is the initial concentration of **ZnCP'(T1)**. To determine the 1 : 1 formation constant for **ZnCP'(T1)**, the following thermodynamic cycle was used:

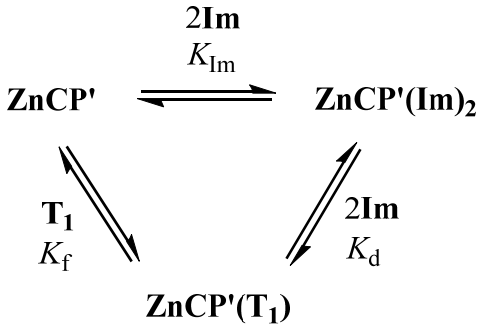

The addition of excess imidazole, **Im** to **ZnCP'(T1)** results in the displacement of the ligand **T1** from **ZnCP'**, to generate **ZnCP'(Im)2**. K_f can be calculated using equation (S3),

$$K_f = \frac{K_{Im}^2}{K_d}$$

(S3)

The binding constant, K_{Im} was determined by fitting the binding isotherm to equation (S4).[10s]

$$\Delta A = \frac{L(1+K_{Im}[\mathbf{Im}] + K_{Im}[\mathbf{ZnCP'(T_1)}]_0 - \sqrt{L^2(K_{Im}[\mathbf{Im}]+K_{Im}[\mathbf{ZnCP'(T_1)}]_0)^2 - 4K_{Im}^2[\mathbf{Im}][\mathbf{ZnCP'(T_1)}]_0 L^2})}{2K_{Im}[\mathbf{Im}]} \quad \text{(S4)}$$

where ΔA is the change of absorption at any point in the titration, L is ΔA at 100 % complexation, [**Im**] is the total concentration of imidazole at each point in the titration and [**ZnCP'(T$_1$)**]$_0$ is the initial concentration of **ZnCP'(T$_1$)**. The value of K_{Im} obtained from fitting the binding isotherms (S4) at 423 nm to a 1 : 1 binding model for **ZnTPP** and **Im** (Scheme 3-6, Figure 3-14) instead of **ZnCP'** and **Im** is $K_{Im} = 2.6\times10^4$ M^{-1}.

Scheme 3-6. Complexation of **ZnTPP** with imidazole (**Im**) in $CHCl_3$

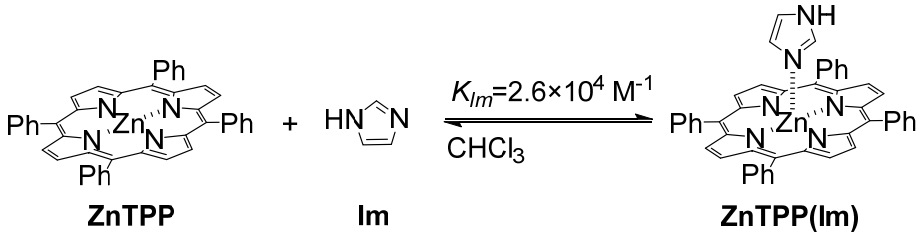

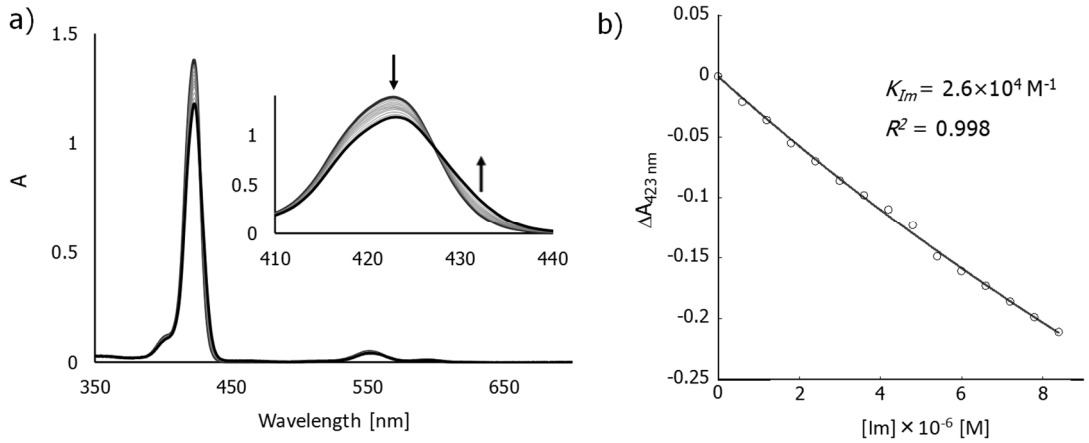

Figure 3-14. a) UV titration of imidazole, **Im** with 5,10,15,20-tetraphenyl-zink-porphyrin, **ZnTPP** (6.0×10^{-6} M, r. t., $CHCl_3$). Arrows indicate areas of increasing and decreasing absorption during the titration. b) The data at 423 nm were fitted to a 1 : 1 binding isotherm to give a binding constant of $K_{Im} = 2.6\times10^4$ M^{-1}.

In the case of denaturation equilibrium constant K_d obtained from fitting the binding isotherms (S2) at 426 nm is $K_d = 3.9$ M^{-1} (Scheme 3-7, Figure 3-15). The value of K_f obtained from S3 was 1.7×10^8 M^{-1}.

Scheme 3-7. Displacement of the ligand $\mathbf{T_1}$ from **ZnCP'** by imidazole in $CHCl_3$

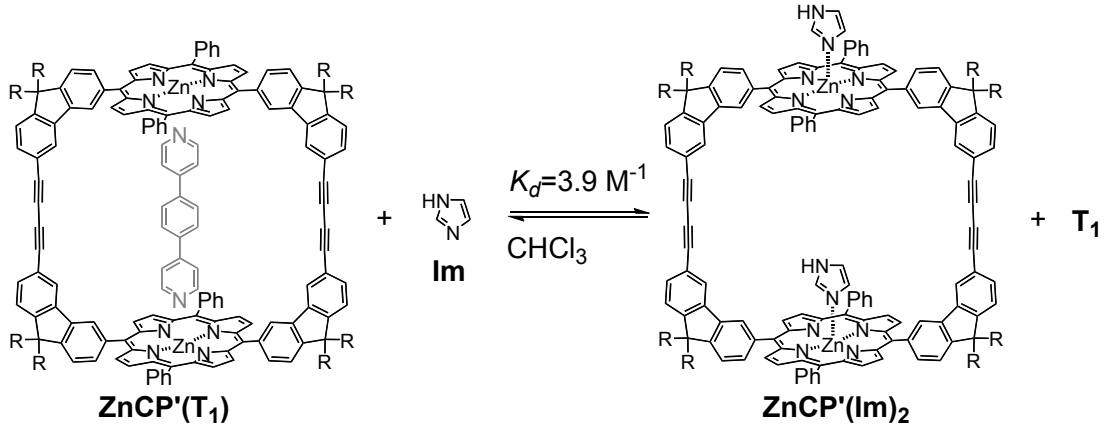

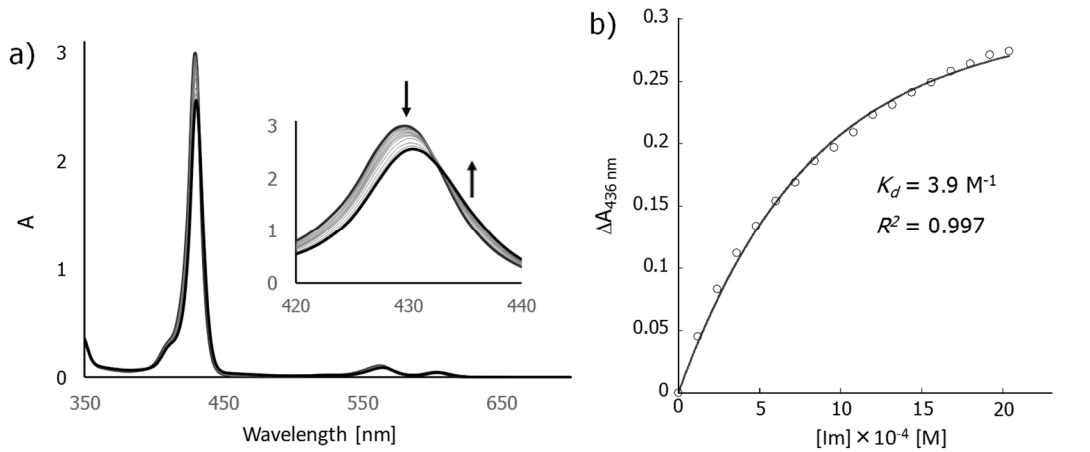

Figure 3-15. a) UV titration of imidazole, **Im** with **ZnCP'** (3.0×10^{-6} M, r. t., $CHCl_3$). Arrows indicate areas of increasing and decreasing absorption during the titration. b) The data at 436 nm were fitted to a 1 : 1 binding isotherm (S2) to give a binding constant of K_d = 3.9 M^{-1}.

3-4-5. Computational Study

Method

The optimized geometry of **$ZnCP_2$** was calculated at the B3LYP level of theory employing the 6-31G(d) for carbons, hydrogens and oxygens and Lanl2DZ for nitrogens and zincs, neglecting ester groups of **$ZnCP_2$** in the calculation. Stable structures of **T_2 (n=x)** were calculated at the B3LYP level of theory using the 6-31G(d) for carbons, hydrogens and nitrogens. All DFT calculations were carried out using Gaussian 09.[20]

DFT Optimized Structure

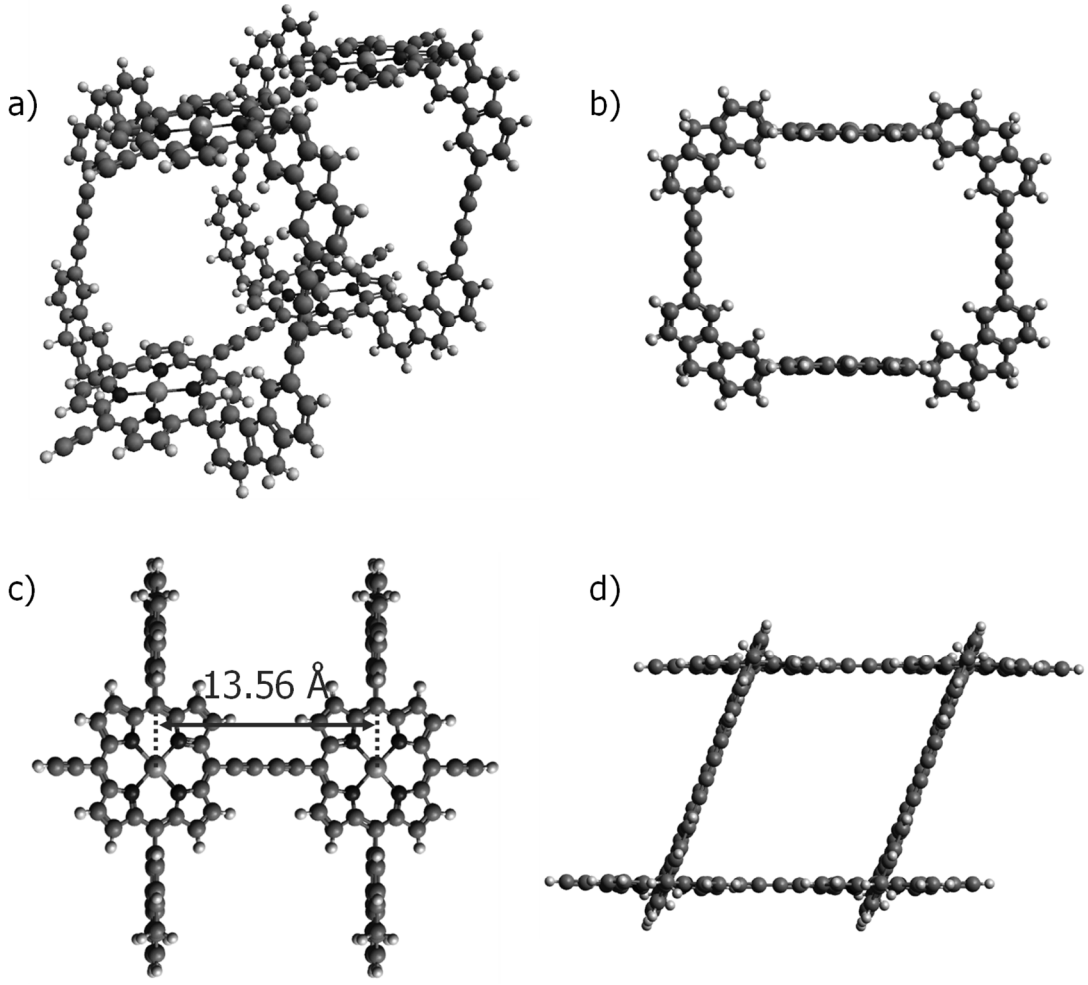

Figure 3-16. The optimized structure of **$ZnCP_2$**. a) Slanting view, b) front view, c) top view, and d) side view

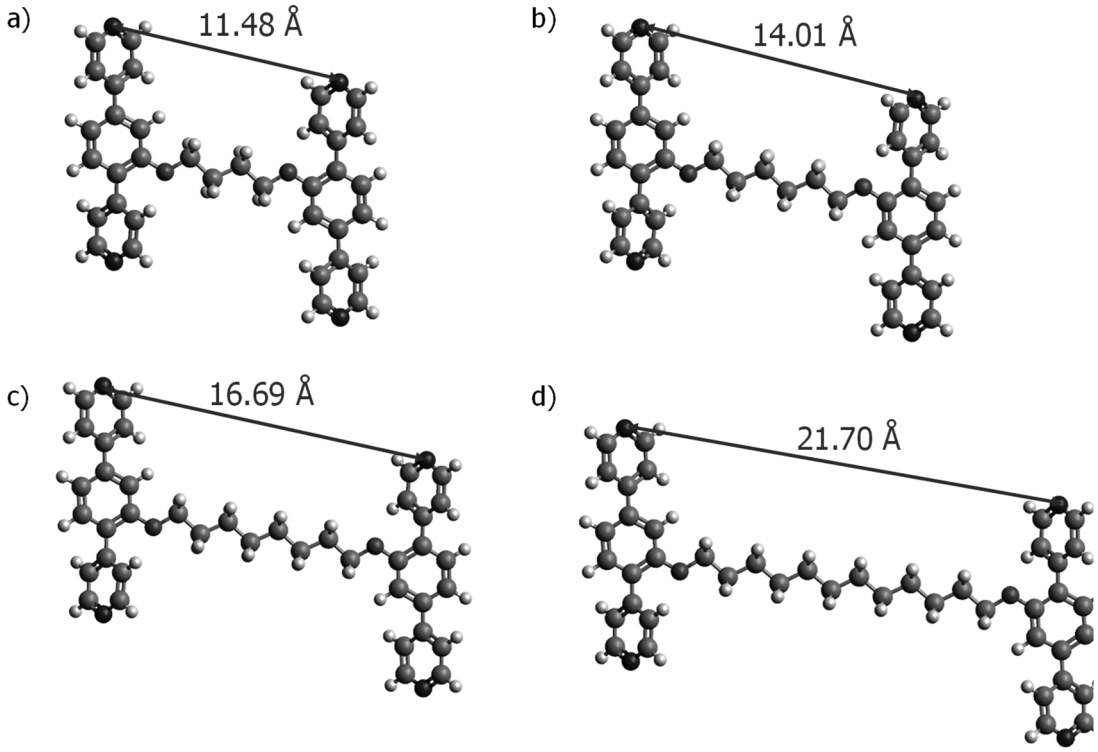

Figure 3-17. The optimized structures of **T_2 (n=x)**. a) **T_2 (n=4)**, b) **T_2 (n=6)**, c) **T_2 (n=8)**, and d) **T_2 (n=12).** Double headed arrows indicate interatom distance of nitrogens.

References and Notes

1. a) Shimizu, T. *Bull. Chem. Soc. Jpn.* **2008**, *81*, 1554. b) Shimizu, T. *J. Polym. Sci., Part A: Polym. Chem.* **2006**, *44*, 5137. c) Kameta, N.; Minamikawa, H.; Masuda, M. *Soft Matter*. **2011**, *7*, 4539. d) Bakbo Block, M. A.; Kaiser, C.; Khan, A.; Hecht, S. *Top Curr. Chem.* **2005**, *245*, 89.
2. a) Kamimura, T.; Ohkubo, K.; Kawashima, Y.; Ozako, S.; Sakaguchi, K.; Fukuzumi, S.; Tani, F. *J. Phys. Chem.C* **2015**, *119*, 25634. b) Nobukuni, H.; Shimazaki, Y.; Uno, H.; Naruta, Y.; Ohkubo, K.; Kojima, T.; Fukuzumi, S.; Seki, S.; Sakai, H.; Hasobe, T.; Tani, F. *Chem. Eur. J.* **2010**, *16*, 11611. c) Sakaguchi, K.; Kamimura, T.; Uno, H.; Mori, S.; Ozako, S.; Nobukuni, H.; Ishida, M.; Tani, F. *J. Org. Chem.* **2014**, *79*, 2980. d) Nobukuni, H.; Shimazaki, Y.; Tani, F.; Naruta, Y. *Angew. Chem., Int. Ed.* **2007**, *46*, 8975. e) Yamaguchi, T.; Ishii, N.; Tashiro, K.; Aida, T. *J. Am. Chem. Soc.* **2003**, *125*, 13934.
3. Fukuzumi, S. *Phys. Chem. Chem. Phys.* **2008**, *10*, 2283.
4. Sariciftci, N. S.; Smilowitz, L.; Heeger, A. J.; Wudl, F. *Science* **1992**, *258*, 1474.
5. Tsuda, A.; Hu, H.; Tanaka, R.; Aida, A. *Angew. Chem., Int. Ed.* **2005**, *44*, 4884.
6. a) Tashiro, K.; Aida, T.; Zheng, J.-Y.; Kinbara, K.; Saigo, K.; Sakamoto, S.; Yamaguchi, K. *J. Am. Chem. Soc.* **1999**, *121*, 9477. b) Zheng, J.-Y.; Tashiro, K.; Hirabayashi, Y.; Kinbara, K.; Saigo, K.; Aida, T.; Sakamoto, S.; Yamaguchi, K. *Angew. Chem., Int. Ed.* **2001**, *40*, 1857. c) Shoji, Y.; Tashiro, K.; Aida, T. *J. Am. Chem. Soc.* **2004**, *126*, 6570. d) Kieran, A. L.; Pascu, S.; Jarrosson, T.; Sanders, J. K. M. *Chem. Commun.* **2005**, 1276. e) Tashiro, K.; Aida, T. *Chem. Soc. Rev.* **2007**, *36*, 189. f) Yanagisawa, M.; Tashiro, K.; Yamasaki, M.; Aida, T. *J. Am. Chem. Soc.*, **2007**, *129*, 11912. g) Nobukuni, H.; Shimazaki, Y.; Tani, F.; Naruta, Y. *Angew. Chem., Int. Ed.*, **2007**, *46*, 8975. h) Song, J.; Aratani, N.; Shinokubo, H.; Osuka, A. *J. Am. Chem. Soc.* **2010**, *132*, 16356. i) Zhang, C.; Wang, Q.; Long, H.; Zhang, W. *J. Am. Chem. Soc.* **2011**, *133*, 20995. j) Hernandez-Eguia, L. P.; Escudero-Adan, E. C.; Pintre, I. C.; Ventura, B.; Flamigni, L.; Ballester, P. *Chem. Eur. J.* **2011**, *17*, 14564. k) HernandezEguía, L. P.; Escudero-Adan, E. C.; Pinzon, J. R.; Echegoyen, L.; Ballester, P. *J. Org. Chem.* **2011**, *76*, 3258. l) Zhang, C.; Long, H.; Zhang, W. *Chem. Commun.* **2012**, *48*, 6172. m) Kang, B.; Totten, R. K.; Weston, M. H.; Hupp, J. T.; Nguyen, S. T. *Dalton Trans.* **2012**, *41*, 12156. n) Chenxi, C.; Long, H.; Zhang, W. *Chem. Commun.* **2012**, *48*, 6172. o) Durot, A.; Taesch, J.; Heitz, V. *Chem. Rev.* **2014**, *114*, 8542. p) Yu, C.; Jin, Y.; Zhang, W. *Chem. Rec.* **2015**, 15, 97.
7. Glaser reaction: a) Anderson, H. L.; Sanders, J. K. M. *Angew. Chem., Int. Ed. Engl.* **1990**, *29*, 1400. b) Hoffmann, M.; Wilson, C. J.; Odell, B.; Anderson, H. L. *Angew. Chem., Int. Ed.* **2007**, *46*, 3122. c) Hoffmann, M.; Karnbratt, J.; Chang, M.-H.; Herz, L. M.; Albinsson, B.; Anderson, H. L. *Angew. Chem., Int. Ed.* **2008**, *47*, 4993. d) O'Sullivan, M. C.; Sprafke,

J. K.; Kondratuk, D. V.; Rinfray, C.; Claridge, T. D. W.; Saywell, A.; Blunt, M. O.; O'Shea, J. N.; Beton, P. H.; Malfois, M.; Anderson, H. L. *Nature* **2011**, *469*, 72. e) Kondratuk, D. V.; Perdigao, L. M. A.; O'Sullivan, M. C.; Svatek, S.; Smith, G.; O'Shea, J. N.; Beton, P. H.; Anderson, H. L. *Angew. Chem., Int. Ed.* **2012**, *51*, 6696. f) Kondratuk, D. V.; Sprafke, J. K.; O'Sullivan, M. C.; Perdigao, L. M. A.; Saywell, A.; Malfois, M.; O'Shea, J. N.; Beton, P. H.; Thompson, A. L.; Anderson, H. L.; *Chem. Eur. J.* **2014**, *20*, 12826. g) Neuhaus, L. P.; Kondratuk, D. V.; Balaban, T. S.; Anderson, H. L. *Angew. Chem., Int. Ed.* **2014**, *53*, 7770. h) Kondratuk, D. V.; Perdigão, L. M. A.; Esmail, A. M. S.; O'Shea, J. N.; Beton, P. H.; Anderson, H. L. *Nat. Chem.* **2015**, *7*, 317. i) Liu, S.; Kondratuk, D. V.; Rousseaux, S. A. L.; Gil-Ramírez, G.; O'Sullivan, M. C.; Cremers, J.; Claridge, T. D. W.; Anderson, H. L. *Angew. Chem., Int. Ed.* **2015**, *54*, 5355. j) Liu, P.; Hisamune, Y.; Peeks, M. D.; Odell, B.; Gong, J. Q.; Herz, L. M.; Anderson, H. L.; *Angew. Chem., Int. Ed.* **2016**, *55*, 8358. k) Rickhaus, M.; Jentzsch, A. V.; Tejerina, L.; Grübner, I.; Jirasek, M.; Claridge, T. D. W.; Anderson, H. L. *J. Am. Chem. Soc.* **2017**, *139*, 16502. metathesis reaction: l) Mulholland, A. R.; Woodward, C. P.; Langford, S. J. *Chem. Commun.* **2011**, *47*, 1494. m) Zhu, B.; Chen, H.; Lin, W.; Ye, Y.; Wu, J.; Li, S. *J. Am. Chem. Soc.* **2014**, *136*, 15126.

8. a) Ishida, T.; Morisaki, Y.; Chujo, Y. *Tetrahedron Lett.* **2006**, *47*, 5265. b) Youm, K.-T.; Nguyen, S. T.; Hupp, J. T. *Chem. Commun.* **2008**, 3375. c) Neuhaus, P.; Cnossen, A.; Gong, J. Q. Herz, L. M.; Anderson, H. L. *Angew. Chem., Int. Ed.* **2015**, *54*, 7344.
9. a) Sindhu, K. S.; Anilkumar, G. *RSC Adv.* **2014**, *4*, 27867. b) Hisaki, I.; Hiroto, S.; Kim, K. S.; Noh, S. B.; Kim, D.; Shinokubo, H.; Osuka, A. *Angew. Chem., Int. Ed.* **2007**, *46*, 5125. c) Tokuji, S.; Yorimitsu, H.; Osuka, A. *Angew. Chem., Int. Ed.* **2012**, *51*, 12357.
10. Terao, J.; Chiba, Y.; Fujihara, T.; Tsuji, Y. *Chem. Lett.* **2014**, *43*, 1374.
11. Peeks, M. D.; Neuhaus, P.; Anderson, H. L. *Phys. Chem. Chem. Phys.* **2016**, *18*, 5264.
12. Favereau, L.; Cnossen, A.; Kelber, J. B.; Gong, J. Q.; Oetterli, R. M.; Cremers, J.; Herz, L. M.; Anderson, H. L. *J. Am. Chem. Soc.* **2015**, *137*, 14256.
13. Pangborn, A. B.; Giardello, M. A.; Grubbs, R. H.; Rosen, R. K.; Timmers, F. J. *Organometallics* **1996**, *15*, 1518.
14. Kobin, B.; Grubert, L.; Blumstengel, S.; Henneberger, F.; Hecht, S. *J. Mater. Chem.* **2012**, *22*, 383.
15. Screen, T. E. O.; Lawton, K. B.; Wilson, G. S.; Dolney, N.; Ispasoiu, R.; Goodson III, T.; Martin, S. J.; Bradley, D. D. C.; Anderson, H. L. *J. Mater. Chem.* **2001**, *11*, 312.
16. Plater, M. J.; Aiken, S.; Bourfill, G. *Tetrahedron* **2002**, *58*, 2405.
17. Barnes, J. C.; Juriček, M.; Strutt, N. L.; Frasconi, M.; Sampath, S.; Giesener, M. A.; McGrier, P. L.; Bruns, C. J.; Stern, C. L.; Sarjeant, A. A.; Stoddart, J. F. *J. Am. Chem. Soc.* **2013**, *135*, 183.

18. Taylor, P. N.; Anderson, H. L. *J. Am. Chem. Soc.* **1999**, *121*, 11538.
19. Rousseaux, S. A. L.; Gong, J. Q.; H, Renée; Odell, B.; Claridge, T. D. W.; Herz, L. M.; Anderson, H. L. *J. Am. Chem. Soc.* **2015**, *137*, 12713.
20. Frisch, M. J.; Trucks, G. W.; Schlegel, H. B.; Scuseria, G. E.; Robb, M. A.; Cheeseman, J. R.; Scalmani, G.; Barone, V.; Mennucci, B.; Petersson, G. A.; Nakatsuji, H.; Caricato, M.; Li, X.; Hratchian, H. P.; Izmaylov, A. F.; Bloino, J.; Zheng, G.; Sonnenberg, J. L.; Hada, M.; Ehara, M.; Toyota, K.; Fukuda, R.; Hasegawa, J.; Ishida, M.; Nakajima, T.; Honda, Y.; Kitao, O.; Nakai, H.; Vreven, T.; Montgomery, Jr., J. A. ; Peralta, J. E.; Ogliaro, F.; Bearpark, M.; Heyd, J. J.; Brothers, E.; Kudin, K. N.; Staroverov, V. N.; Keith, T.; Kobayashi, R.; Normand, J.; Raghavachari, K.; Rendell, A.; Burant, J. C.; Iyengar, S. S.; Tomasi, J.; Cossi, M.; Rega, N.; Millam, J. M.; Klene, M.; Knox, J. E.; Cross, J. B.; Bakken, V.; Adamo, C.; Jaramillo, J.; Gomperts, R.; Stratmann, R. E.; Yazyev, O.; Austin, A. J.; Cammi, R.; Pomelli, C.; Ochterski, J. W.; Martin, R. L.; Morokuma, K.; Zakrzewski, V. G.; Voth, G. A.; Salvador, P.; Dannenberg, J. J.; Dapprich, S.; Daniels, A. D.; Farkas, O.; Foresman, J. B.; Ortiz, J. V.; Cioslowski, J.; and Fox, D. J.; Gaussian09; Revision C.01; Gaussian, Inc.; Wallingford CT; **2010**.

Chapter 4

Investigation of the Host–Guest Complexation Between a Porphyrin Tube and a Porphyrin Dimer

A triple stranded porphyrin dimer was constructed by cooperative effect with coordination bonding and host–guest complexation among the porphyrin tube, a butadiyne-linked porphyrin dimer and bidentate ligands. The porphyrin dimer as a guest was thought to be fixed to planer structure in the cavity of the porphyrin tube because multiple interactions prohibited the porphyrin dimer from rotating around the diyne. The fixation of π-conjugated molecules in porphyrin tubes is expected to be a promising method to realize effective elongation of conjugation length.

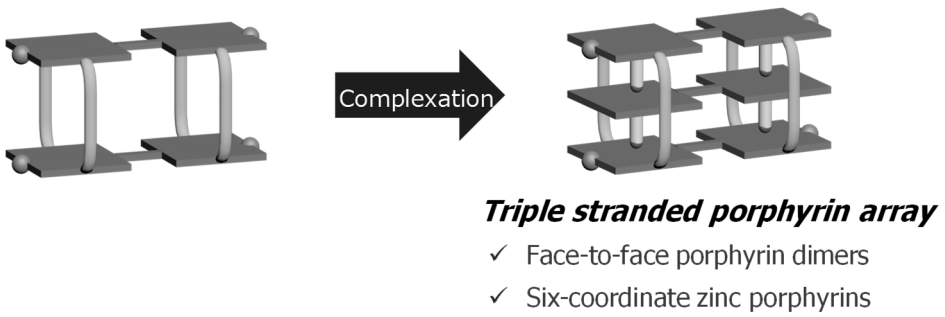

4-1. Introduction

Chemists have mimiced natural host–guest interactions to develop molecular sensors, purification, catalysts and so on.[1] Proteins are known to have molecular recognition abilities to transform and transport molecules, in which flexible proteins as hosts and small molecules as guests change their structures to fit each other based on induced fit[2] or mutual induced fit model.[3] In case of rigid hosts, structural changes of guest molecules induce host–guest complexation. A bowl-shaped corannulene derivative, which exhibits bowl-to-bowl inversion through a planar transition state, was encapsulated by an artificial host molecule to easily form a planar structure.[4] Rigid host molecules can determine structures of flexible guest molecules.

π-Conjugated polymers are promising materials in organic electronics (organic solar cells[5] and organic light-emitting diodes[6]). However, rotation of π-unit around axes of covalent bonds causes inefficient elongation of π-conjugation length and deactivation of excitons.[7] Control of the molecular dynamics has improved optical properties such as charge transport, π-conjugation, and exciton diffusion length.[8,9d] Until now three methods have been developed to fix π-conjugated molecules in planar structures; covalent linkages (Figure 4-1 (a) and (b)),[9,10] intramolecular non-covalent interactions (Figure 4-1 (c)),[11,12] and intermolecular non-covalent interactions (Figure 4-1 (d)).[13] The third one can integrate π-conjugated polymers under control of intermolecular distance. However, the low stability of non-covalent bonds will induce degradation of the property due to thermodynamic dissociation. It is necessary to develop methods for enhancing stability of integrated π-conjugated molecules.

Hence, the author proposes a novel method to fix π-conjugate molecules in stable planar structures using cooperative host–guest complexation of porphyrin tubes (Figure 4-1 (e)). Because porphyrin arrays are regarded as artificial photosynthesis motif,[14] a butadiyne-linked zinc porphyrin dimer was selected as a flexible guest molecule. In Chapter 2, it was

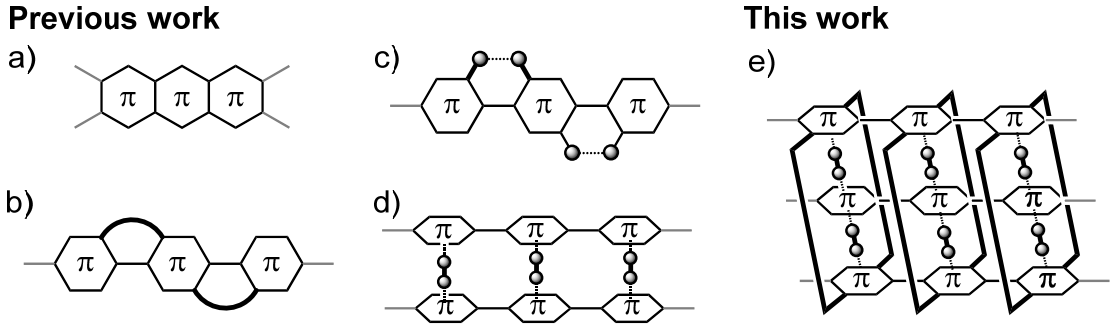

Figure 4-1. Methods to fix π-conjugated molecules in planar structures.
a) Construction of fused π-system. b) Covalent linkage between π-units. c) Non-covalent linkage between π-units. d) Non-covalent bonds between π-units. e) Cooperative

revealed that coordination bonds were kinetically stabilized by cooperative effect of host–guest complexation.[15] The porphyrin tube is expected to stabilize planar structures of the porphyrin dimer. The host–guest complexation between the porphyrin tube and porphyrin dimer are described in this chapter.

4-2. Results and Discussions

4-2-1. Synthesis of Porphyrin Dimer ZnP_2

Porphyrin dimer **ZnP_2** having aryl rings with three dodecyloxy groups as soluble units was synthesized via 4 steps from **ZnP** (Scheme 4-1). Selective mono-deprotection of bis-silyl-protected alkynes of **ZnP**, followed by Sonogashira coupling reaction with 1-iodo-3,4,5-(tridodecyloxy)benzene **2** afforded **3**. Deprotection of the other silyl group of **3** before homo coupling via Glaser reaction yielded porphyrin dimer **ZnP_2**. **ZnP_2** was soluble in various organic solvents, for example $CHCl_3$, ethyl acetate, toluene, even non-polar solvent; hexane and CCl_4. The high solubility of **ZnP_2** is advantageous to prepare highly concentrated solution of **ZnP_2** for NMR titration experiments.

Scheme 4-1. Synthesis of porphyrin dimer **ZnP_2**

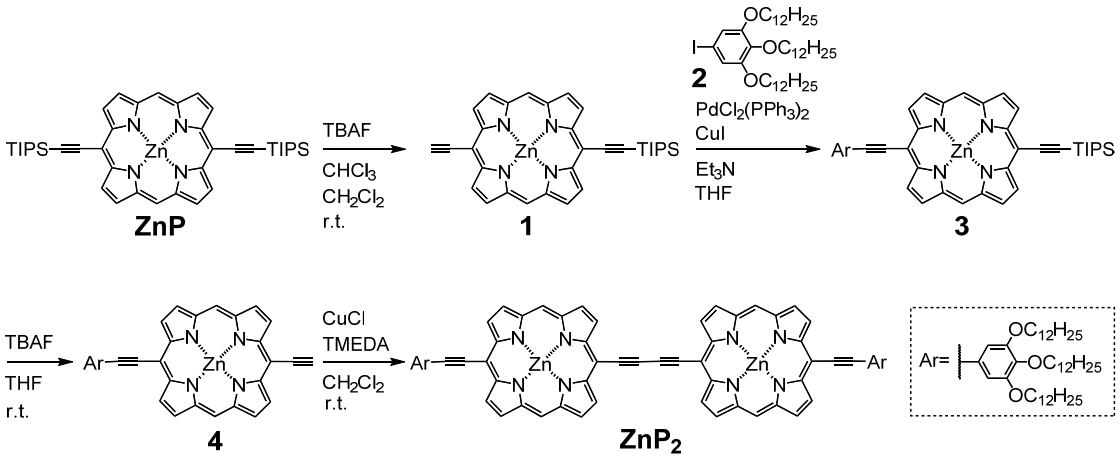

4-2-2. Complexation Study Between ZnCP and ZnP

At first complexation dynamics among **ZnCP, ZnP** and DABCO was studied by NMR titration experiments (Scheme 4-2). In case of a mixture of **ZnP** and DABCO or that of **ZnCP** and DABCO in $CDCl_3$, only one broad peak around –2 ppm was observed. The broad peak was caused by fast association/dissociation between DABCO and zinc porphyrin on the NMR timescale. This observation suggested weak coordination bonds between zinc porphyrins and DABCO. On the other hand, upon adding **ZnP** to a solution of **ZnCP** : DABCO (1 : 2 molar ratio) using 1,3,5-trimethoxybenzene as an internal standard in $CDCl_3$, two peaks were observed at –5.2 and –5.6 ppm, respectively (Figure 4-1.i). These were assigned to methylene

protons of DABCO binded between two porphyrins.[16] The integration of peaks at –5.6 ppm gave the maximum at 1 equivalent of **ZnP** (Figure 4-1.ii), which suggested that a mixture of **ZnCP**, DABCO and **ZnP** formed a 1 : 2 : 1 complex. Comparing the integral of the NMR peak for the complex with that of the internal standard, 45% of **ZnCP** formed a face-to-face complex. Until now only one example for six-coordinate zinc porphyrin in solution has been reported because association constant between an amine and five-coordinated zinc porphyrin was very small ($K < 1$).[17] In the cyclic molecule, kinetic stabilization described in Chapter 2 probably helped formation of the six-coordinated zinc porphyrin.

Scheme 4-2. Synthesis of face-to-face zinc porphyrin complexes

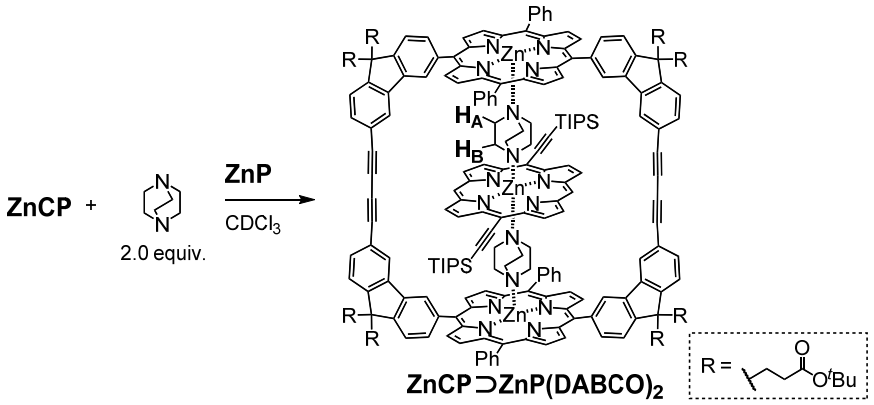

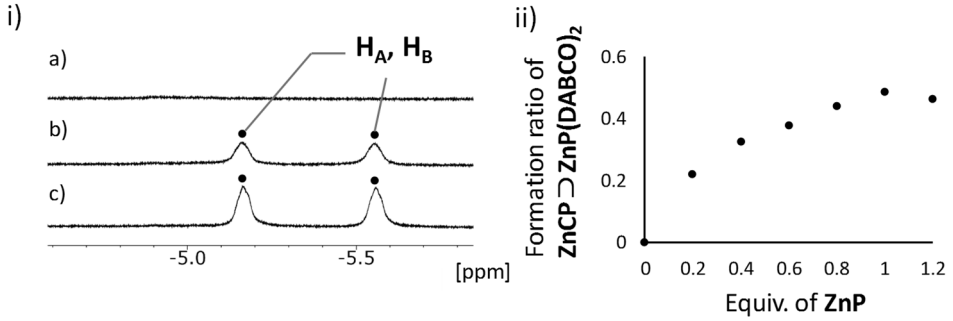

Figure 4-1. i) ^{1}H NMR (500 MHz) titration study for face-to-face zinc porphyrin complexes among **ZnCP**, **ZnP**, and DABCO in $CDCl_3$. a) 0 equiv. of **ZnP**, b) 0.35 equiv. of **ZnP**, and c) 1.0 equiv. of **ZnP**. Circles indicate protons that were assigned to the methylene protons for **ZnCP⊃ZnP(DABCO)$_2$**. ii) Changes of formation ratio of **ZnCP⊃ZnP(DABCO)$_2$**.

4-2-3. Complexation Study Between $ZnCP_2$ and ZnP_2

Porphyrin tube **$ZnCP_2$** is promissing for encapsulation of porphyrin dimer **ZnP_2** as a guest molecules. In the case, the guest is expected to be fixed to the planar structure due to multiple interaction points in the cavity. The complexation among **$ZnCP_2$**, **ZnP_2** and DABCO was also

studied by NMR titration experiments using 1,3,5-trimethoxybenzene as an internal standard (Scheme 4-3). In a mixture of **ZnP_2** : DABCO (1 : 1, molar ratio) in $CDCl_3$, only one broad peak corresponding to the methylene protons of DABCO in double stranded porphyrins **$(ZnP_2)_2(DABCO)_2$** appeared at –4.8 ppm (Figure 4-2 (i)-d). On the other hand, upon adding **ZnP_2** to a solution of **$ZnCP_2$** : DABCO (1 : 4, molar ratio) in $CDCl_3$, two peaks were observed at –5.0 and –5.4 ppm, respectively (Figure 4-2 (i)-b and c). Moreover, the peaks stemmed from one molecule because a COSY cross peaks was observed between the two peaks. The integration of the peak at –5.4 ppm gave the maximum at around 1 equivalent of **ZnP_2**, which suggested that the mixture of **$ZnCP_2$**, **DABCO** and **ZnP_2** formed a 1 : 4 : 1 complex (Figure 4-2.ii). This result suggested that **$ZnCP_2 \supset ZnP_2(DABCO)_4$** was more thermodynamically stable than **$(ZnP_2)_2(DABCO)_2$** due to multiple interactions.

Scheme 4-3. Synthesis of face-to-face zinc porphyrin complexes, some parts of fluorene units being removed from the structure formula for clarity

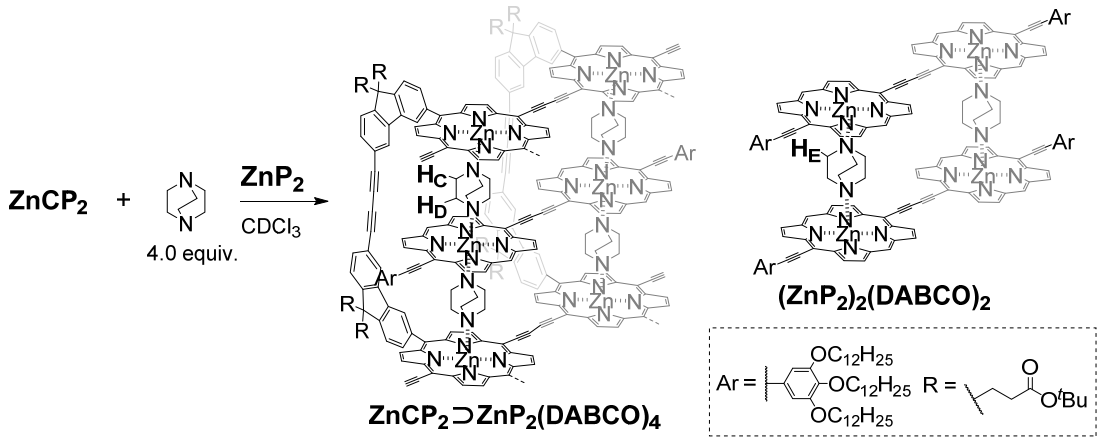

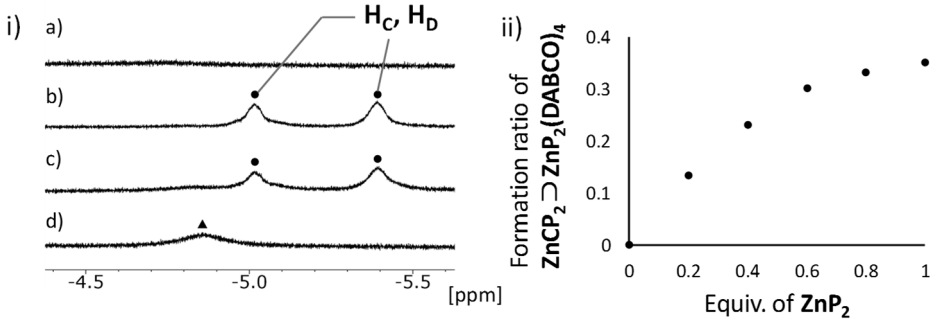

Figure 4-2. i) ^1H NMR (500 MHz) titration study for face-to-face zinc porphyrin complexes in $CDCl_3$. a) 0 equiv. of **ZnP_2**, b) 0.40 equiv. of **ZnP_2**, c) 1.0 equiv of **ZnP_2**, and d) **ZnP_2** : DABCO = 1 : 1 without **$ZnCP_2$**. Circles and triangle show protons corresponding to the methylene protons for **$ZnCP_2 \supset ZnP_2(DABCO)_4$** and **$(ZnP_2)_2(DABCO)_2$**, respectively. ii) Changes of formation ratio of **$ZnCP_2 \supset ZnP_2(DABCO)_4$**.

4-3. Conclusion

In conclusion, the novel method to fix π-conjugated molecules in planar conformation has been developed. In the cavity of the porphyrin tube, a porphyrin dimer favored a planar structure based on cooperative effect with host–guest complexation and coordination bonds. Because the porphyrin tube consists of two porphyrin dimers, the host–guest complexation induced a face-to-face triple stranded porphyrin dimers. The porphyrin tube induced six-coordinate complex with amines due to multiple interactions, although it generally formed five-coordinate complex. The method will shed light on the integration method of π-conjugated molecules to improve optical properties.

4-4. Experimental Section

4-4-1. General Remarks

Materials: Reagents were purchased from commercial sources and used without further purification. Solvents were purified as follows: reaction solvents were degassed through freeze-pump-thaw (three times), before use. Dry toluene was purchased from Kanto Chemical and further purified by passage through activated alumina under positive argon pressure as described by Grubbs *et al.*[18] 5,15-Bis[(triisopropylsilyl)ethynyl]porphyrin[19] and 1-bromo-3,4,5-tridodecyloxybenzene[20] were prepared according to previous literatures.

NMR Spectroscopy: ^{1}H NMR spectra were measured on a JEOL ECX-400 spectrometer and a Bruker AVANCE-500 spectrometer. The ^{1}H NMR chemical shifts are reported relative to tetramethylsilane (TMS, 0.00 ppm) or residual protonated solvent (7.26 ppm) in $CDCl_3$. The ^{13}C NMR chemical shifts are reported relative to tetramethylsilane (TMS, 0.00 ppm) or solvent (77.16 ppm) in $CDCl_3$.

Preparative recycling gel permeation chromatography (GPC): Preparative recycling GPC was performed with a JAI LC9104 System equipped with JAIGEL-1H and 2H columns, a JAI UV DETECTOR 310, and a JAI RI DETRCTOR RI-5, a JAI LC9130NEXT System equipped with JAIGEL-2H and 2.5H columns, a JAI UV DETECTOR 370NEXT, and a JAI RI DETRCTOR RI 700NEXT, a JAI LC9140 System equipped with JAIGEL-2.5H and -3H columns, a JAI UV DETECTOR 310, and a JAI RI DETRCTOR RI-5.

Mass Spectroscopy (MS): Matrix assisted laser desorption/ionization time-of-flight (MALDI-TOF) mass spectra were obtained with α-cyano-4-hydroxycinnamic acid (CHCA) as a matrix and NaTFA as a cationization reagent on a Thermo Fisher Scientific LTQ orbitrapXL. ESI and atmospheric pressure chemical ionization (APCI) mass spectra were obtained on a

Thermo Fisher Scientific EXACTIVE.

4-4-2. Synthetic Procedures

Synthesis of ZnP

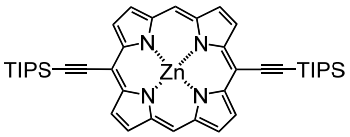

5,15-Bis[(triisopropylsilyl)ethynyl]porphyrin (302 mg, 0.450 mmol) and $Zn(OAc)_2$ (823 mg, 4.47 mmol) was dissolved in $CHCl_3$ (160 mL). The solution was refluxed overnight followed by washed with water three times and brine once. The organic layer was dried by Na_2SO_4 and removed under vacuum. The residue was purified by silica gel chromatography (CH_2Cl_2 / pyridine = 20 / 1) to afford **ZnP** (quant, 408 mg) as a green solid.

HR-MS (APCI-MS): (m/z) 733.3081 ([**1**+H^+], $C_{42}H_{53}N_4Si_2Zn$, calcd. 733.3100)
^{1}H NMR (500 MHz, $CDCl_3$, r. t.): δ 10.08 (s, 2H, *meso-H*), 9.82 (d, *J* = 4.3 Hz, 4H, β-*H*), 9.33 (d, *J* = 4.3 Hz, 4H, β-*H*), 1.52-1.50 (m, 42H, ^{i}Pr-*H*).
^{13}C NMR (126 MHz, $CDCl_3$, r. t.): δ 152.5, 149.5 (pyridine), 143.82, 135.8 (pyridine), 132.33, 132.27, 122.4 (pyridine), 110.1, 107.6, 100.2, 97.5, 19.3, 12.2.

Synthesis of 2

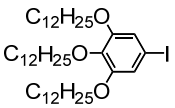

1-Bromo-3,4,5-tridodecyloxybenzene (569 mg, 0.801 mmol), NaI (240 mg, 1.60 mmol), and CuI (16.7 mg, 0.0877 mmol) were dissolved in dry dioxane (4.0 mL). *trans-N,N'*-Dimethylcyclohexane-1,2-diamine was added to the solution before stirring at r. t. for 210 min. The solution was diluted with CH_2Cl_2 and extrated by NH_3 aq. and water followed. The residue after evaporation was purified by silica gel chromatography (EtOAc / hexane = 1 / 100 to 1 / 10) to afforded a white solid (575 mg). NMR analysis showed that the products contained **2** and 1-bromo-3,4,5-tridodecyloxybenzene (9 / 1, molar ratio). The mixture was used without further purification.

Synthesis of 3

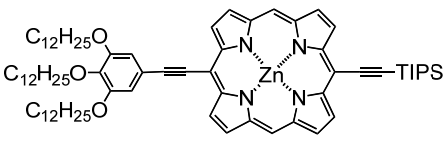

ZnP (296 mg, 0.364 mmol) was dissolved in CH_2Cl_2 / $CHCl_3$ (21 mL / 5.6 mL). To the solution tetrabutylammonium fluoride (546 μL, 1M in THF, 0.546 mmol) was slowly added. The progress of the reaction was monitored by TLC (CH_2Cl_2 / EtOAc / hexane / pyridine = 1 / 0.4 / 4 / several percent). Further tetrabutylammonium fluoride (330 μL, 1M in THF, 0.330 mmol) was added to the solution four times followed by filtration through silica gel (CH_2Cl_2 / pyridine = 20 / 1). The residue was purified by GPC using $CHCl_3$ as an eluent to afford **1** (107 mg) as a green solid. Next, **1**, **2** (284 mg, 0.375 mmol), and $Pd(PPh_3)_4$ (23.4 mg, 0.0202 mmol) were dissolved in a mixture

of THF (1.5 mL), degassed Et_3N (1.5 mL) and pyridine (0.15 mL). The solution was stirred at r. t. overnight after addition of CuI (1.6 mg, 0.0084 mmol). The mixture was purified by silica gel chromatography (EtOAc / hexane = 1 / 20) and GPC using $CHCl_3$ as an eluent to afford **3** (99.4 mg, 23% in 2 steps) as a green solid.

HR-MS (APCI-MS): (m/z) 1205.754 ([**3**+H^+], $C_{75}H_{109}N_4O_3SiZn$, calcd. 1205.756)
^{1}H NMR (500 MHz, $CDCl_3$ / pyidine-d_5, r. t.): δ 9.32 (d, *J* = 4.1 Hz, 2H, β-*H*), 9.27 (d, *J* = 4.1 Hz, 2H, β-*H*), 9.24 (s, 2H, meso-*H*), 8.78 (d, *J* = 4.1 Hz, 2H, β-*H*), 8.74 (d, *J* = 4.1 Hz, 2H, β-*H*), 7.28 (s, 2H, Ar-*H*), 6.05-6.03 (m, pyridine-*H*), 5.22-5.19 (m, pyridine-*H*), 4.27 (t, *J* = 6.4 Hz, 4H, -OC*H*$_2$CH$_2$-), 4.14 (t, *J* = 6.5 Hz, 2H, -OCH$_2$C*H*$_2$-), 2.07 (br, pyridine-*H*), 2.06-1.94 (m, 4H, methylene protons), 1.92-1.83 (m, 2H, methylene protons), 1.70-1.58 (m, 6H, methylene protons), 1.53-1.21 (m, 69H, methylene protons and ^{i}Pr-*H*), 0.93-0.86 (m, 9H, methyl protons).
^{13}C NMR (126 MHz, $CDCl_3$, / pyridine-d_5, r. t.): δ 153.6, 151.4, 150.6 (pyridine), 148.3, 148.1, 142.9, 139.6, 135.6 (pyridine), 131.5, 131.3, 130.6, 130.4, 122.0 (pyridine), 119.2, 110.5, 109.8, 106.8, 99.6, 99.2, 97.3, 96.4, 91.6, 73.9, 69.7, 32.16, 32.13, 30.7, 30.03-29.90 (several peaks overlapped), 29.80, 29.76, 29.62, 29.58, 26.48, 26.43, 22.91, 22.88, 19.5, 14.31, 14.29, 12.3.

Synthesis of ZnP_2

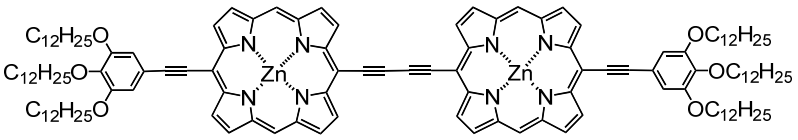

3 (50.0 mg, 0.0414 mmol) was dissolved in THF (4.1 mL). To the solution tetrabutylammonium fluoride (45.4 μL, 1M in THF, 0.0454 mmol) was slowly added. The solution was stirred at r. t. for 1 h followed by filtration through silica gel (EtOAc / hexane = 1 / 1) to afford **4**. The product was used for the next reaction without purification. **4** was dissolved in CH_2Cl_2 before addition of CuCl (16.0 mg, 0.162 mmol) and TMEDA (30 μL, 0.20 mmol). The solution was stirred at r. t. overnight. Purification of the mixture by GPC using $CHCl_3$ as an eluent afforded **ZnP_2** (33.2 mg, 66% in 2 steps) as a green solid.

HR-MS (APCI-MS): (m/z) 2096.223 ([**ZnP_2**+H^+], $C_{132}H_{175}N_8O_6Zn_2$, calcd. 2096.222)
^{1}H NMR (500 MHz, $CDCl_3$, / pyridine-d_5, r. t.): δ 9.99 (d, *J* = 4.3 Hz, 4H, β-*H*), 9.97 (s, 4H, meso-*H*), 9.81 (d, *J* = 4.3 Hz, 4H, β-*H*), 9.33 (d, *J* = 4.4 Hz, 4H, β-*H*), 9.26 (d, *J* = 4.3 Hz, 4H, β-*H*), 7.30 (s, 4H, Ar-*H*), 4.21 (t, *J* = 6.5 Hz, 8H, -OC*H*$_2$CH$_2$-), 4.12 (t, *J* = 6.5 Hz, 4H, -OCH$_2$C*H*$_2$-), 1.97-1.91 (m, 8H, methylene protons), 1.89-1.83 (m, 4H, methylene protons), 1.62-1.55 (m, 12H, methylene protons), 1.46-1.25 (m, 96H, methylene protons), 0.92-0.87 (m, 18H, methyl protons).
^{13}C NMR (126 MHz, $CDCl_3$/ pyridine-d_5, r. t.): δ 153.5, 153.1, 151.8, 149.4, 149.3, 149.2, 149.1, 148.9, 139.6, 135.6, 135.4, 135.2, 132.6, 132.1, 131.3, 131.2, 123.3, 123.1, 122.9, 118.9, 110.4,

108.1, 101.0, 98.2, 96.8, 91.9, 88.3, 82.2, 73.8, 69.5, 32.02, 32.00, 30.5, 29.85, 29.80-29.75 (several peaks overlapped), 29.60, 29.57, 29.48, 29.44, 26.3, 22.8, 14.2.

References and Notes

1. a) Cooper, G. M. *The Cell, A Molecular Approach,* 2nd ed., Sinauer Associates Inc, Sunderland, **2000**. b) Zheng, J.; Trudeau, M. C. *Handbook of Ion Channels*, CRC Press, New York, **2016**.
2. a) Koshland, D. E., Jr. *Proc. Natl. Acad. Sci. U.S.A.* **1958**, *44*, 98. b) Koshland, D. E., Jr. *Angew. Chem., Int. Ed. Engl.* **1994**, *33*, 2375.
3. a) Pingoud, A.; Jeltsch, A. *Eur. J. Biochem.* **1997**, *246*, 1. b) Mao, H.; White, S. A.; Williamson, J. R. *Nat. Struct. Biol.* **1999**, *6*, 1139. c) Frankel, A. D. *Nat. Struct. Biol.* **1999**, *6*, 1081.
4. Juríček, M.; Strutt, N. L.; Barnes, J. C.; Butterfield, A. C.; Dale, E. J.; Baldridge, K. K.; Stoddart, J. F.; Siegel, J. S. *Nat. Chem.* **2014**, *6*, 222.
5. a) Ajayaghosh, A. *Chem. Soc. Rev.* **2003**, *32*, 181. b) Facchetti, A. *Chem. Mater.* **2011**, *23*, 733. c) Heeger, A. J. *Adv. Mater.* **2014**, *26*, 10.
6. a) Borchardt, J. K. *Mater. Today* **2004**, *7*, 42. b) Perepichka, I. F.; Perepichka, D. F.; Meng, H.; Wudl, F. *Adv. Mater.* **2005**, *17*, 2281. c) AlSalhi, M. S.; Alam, J.; Dass, L. A.; Raja, M. *Int. J. Mol. Sci.* **2011**, *12*, 2036. d) Ying, L.; Ho, C. L.; Wu, H.; Cao, Y.; Wong, W. -Y. *Adv. Mater.* **2014**, *26*, 2459.
7. a) Scholes, G. D.; Rumbles, G. *Nat. Mater.* **2006**, *5*, 683. b) De Leener, C.; Hennebicq, E.; Sancho-Garcia, J. -C.; Beljonne, D. *J. Phys. Chem. B* **2009**, *113*, 1311. c) Barford, W.; Trembath, D. *Phys. Rev. B* **2009**, *80*, 165418. d) Barford, W.; Lidzey, D. G.; Makhov, D. V.; Meijer, A. J. H. *J. Chem. Phys.* **2010**, *133*, 044504.
8. a) Scherf, U. *J. Mater. Chem.* **1999**, *9*, 1853. b) Prins, P.; Grozema, F. C.; Schins, J. M.; Patil, S.; Scherf, U.; Siebbeles, L. D. A. *Phys. Rev. Lett.* **2006**, *96*, 146601. c) Grimsdale, A. C.; Chan, K. L.; Martin, R. E.; Jokisz, P. G.; Holmes, A. B. *Chem. Rev.* **2009**, *109*, 897.
9. a) Van Deusen, R. L. *J. Polym. Sci., Part B: Polym. Lett.* **1966**, *4*, 211. b) Scherf, U.; Müllen, K. *Makromol. Chem., Rapid Commun.* **1991**, *12*, 489. c) Crisp, G. T.; Bubner, T. P. *Tetrahedron* **1997**, *53*, 11899. d) Tour, J. M.; Lamba, J. J. S. *J. Am. Chem. Soc.* **1993**, *115*, 4935. d) Tsuda, A.; Osuka, A. *Science* **2001**, *293*, 79. e) Tsuda, A.; Nakamura, Y.; Osuka, A. *Chem. Commun.* **2003**, 1096. f) Crossley, M. J.; Burn, P. L. *J. Chem. Soc., Chem. Commun.* **1991**, 1569.
10. Lee, J.; Kalin, A. J.; Yuan, T.; Al-Hashimi, M.; Fang, L. *Chem. Sci.* **2017**, *8*, 2503.
11. Zhu, C.; Fang, L. *Macromol. Rapid Commun.* **2017**, 1700241.
12. a) Qiao, Y.; Guo, Y.; Yu, C.; Zhang, F.; Xu, W.; Liu, Y.; Zhu, D. *J. Am. Chem. Soc.* **2012**,

134, 4084. b) Delnoye, D. A. P.; Sijbesma, R. P.; Vekemans, J. A. J. M.; Meijer, E. W. *J. Am. Chem. Soc.* **1996**, *118*, 8717. c) Wakamiya, A.; Taniguchi, T.; Yamaguchi, S. *Angew. Chem., Int. Ed.* **2006,** *45*, 3170. d) Henson, Z. B.; Welch, G. C.; van der Poll, T.; Bazan, G. C. *J. Am. Chem. Soc.* **2012**, *134*, 3766. e) Kim, H. G.; Kang, B.; Ko, H.; Lee, J.; Shin, J.; Cho, K. *Chem. Mater.* **2015**, *27*, 829. f) Kim, B. -G.; Jeong, E. J.; Chung, J. W.; Seo, S.; Koo, B.; Kim, J. *Nat. Mater.* **2013**, *12*, 659. g) Huang, H.; Chen, Z.; Ortiz, R. P.; Newman, C.; Usta, H.; Lou, S.; Youn, J.; Noh, Y. -Y.; Baeg, K. -J.; Chen, L. X.; Facchetti, A.; Marks, T. *J. Am. Chem. Soc.* **2012**, *134*, 10966. h) Xu, Y. X.; Zhan, T. G.; Zhao, X.; Fang, Q. A.; Jiang, X. K.; Li, Z. T. *Chem. Commun.* **2011**, *47*, 1524.

13. a) Anderson, H. L. *Inorg. Chem.* **1994**, *33*, 972. b) Taylor, P. N.; Anderson, H. L. *J. Am. Chem. Soc.* **1999**, *121*, 11538. c) Wilson, G. S.; Anderson, H. L. *Chem. Commun.* **1999**, 1539. d) Lee, S. J.; Mulfort, K. L.; O'Donnell, J. L.; Zuo, X.; Goshe, A. J.; Wesson, P. J.; Nguyen, S. T.; Hupp, J. T.; Tiede, D. M. *Chem. Commun.* **2006**, 4581. e) Morisue, M.; Hoshino, Y.; Shimizu, K.; Shimiu, M.; Kuroda, Y. *Chem. Sci.* **2015**, *6*, 6199.
14. Fukuzumi, S.; Kojima, T. *J. Mater. Chem.* **2008**, *18*, 1427. b) Drain, C. M.; Varotto, A.; Radivojevic, I. *Chem. Rev.* **2009**, *109*, 1630. c) Medforth, C. J.; Wang, Z.; Martin, K. E.; Song, Y.; Jacobsen, J. L.; Shelnutt, J. A. *Chem. Commun.* **2009**, 7261.
15. Chiba, Y. ; Liu, M.; Tachibana, Y.; Fujihara, T.; Tsuji, Y.; Terao, J. *Chem. Asian. J.* **2017**, *12*, 1900.
16. Mak, C. C.; Bampos, N.; Sanders, J. K. M. *Chem. Commun.* **1999**, 1085.
17. Favereau, L.; Cnossen, A.; Kelber, J. B.; Gong, J. Q.; Oetterli, R. M.; Cremers, J.; Herz, L. M.; Anderson, H. L. *J. Am. Chem. Soc.* **2015**, *137*, 14256.
18. Pangborn, A. B.; Giardello, M. A.; Grubbs, R. H.; Rosen, R. K.; Timmers, F. J. *Organometallics* **1996**, *15*, 1518.
19. Screen, T. E. O.; Lawton, K. B.; Wilson, G. S.; Dolney, N.; Ispasoiu, R.; Goodson III, T.; Martin, S. J.; Bradley, D. D. C.; Anderson, H. L. *J. Mater. Chem.* **2001**, *11*, 312.
20. Yasuda, T.; Shimizu, T.; Liu, F.; Ungar, G.; Kato, T. *J. Am. Chem. Soc.* **2011**, *133*, 13437.

Chapter 5

Template Synthesis of a Length-Controlled Porphyrin Tube via Selective Trimerization of Porphyrin Rings and Its Mechanism

A template method for the length-controlled porphyrin tube via selective trimerization of porphyrin rings has been developed. The cyclic molecules quantitatively formed 3 : 1 complexes with the template molecules so that the connecting units come close together. It was revealed that the complexation quickly proceeded at r. t. including penetration of the cyclic molecules to the template molecules. The high association constant between the cyclic molecules and the template molecules led to effective tubulation. As a result, the two-step template method for the porphyrin tube is expected to be applied to longer porphyrin tubes.

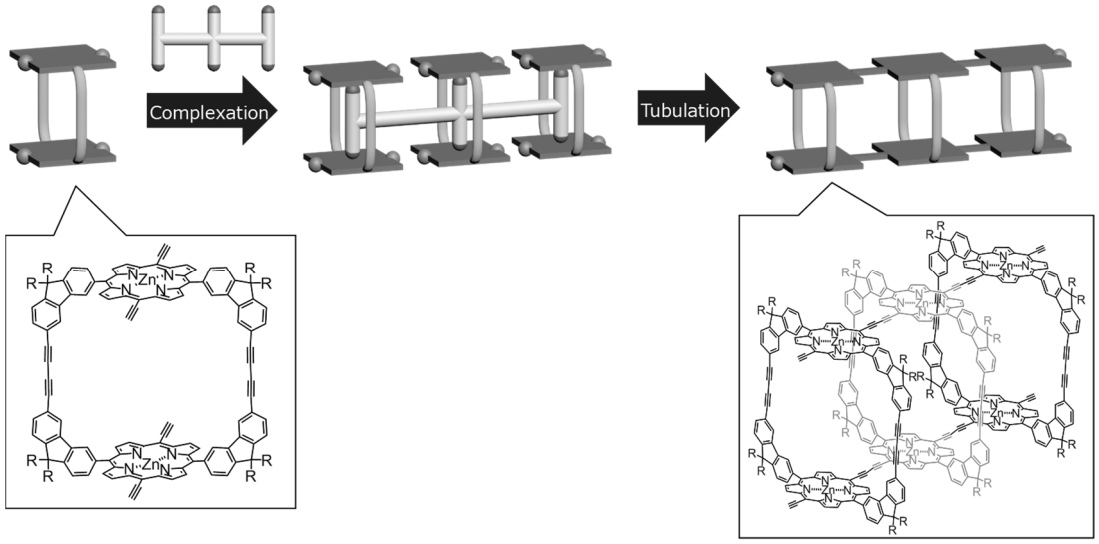

5-1. Introduction

Functionalization of molecular tubes via host–guest complexation will provide novel methods to design materials.[1] Porphyrin tubes are promising host molecules for solar cells,[2] artificial photosynthesis,[3] two photon absorption materials,[4] and conductive materials.[5] The properties of molecular tubes, for example inclusion abilities and optical properties, depend on the structural factors; cavity size, molecular length, and electronic states. Until now, template methods for porphyrin tubes have been reported by Chujo *et al.*, Hupp *et al.* and Anderson *et al.*[6] However, molecular length of the porphyrin tubes was limited to two units of porphyrins. It is necessary to develop a synthetic method for longer porphyrin tubes.

One of the synthetic methods for long molecular tubes was the rotaxane method reported by Harada *et al.*[7] They adopted cyclodextrins, which were capable of encapsulating various organic molecules in water,[8] as the basic unit of the molecular tube. The method realized cyclodextrin tube with high degree of polymerization through the formation of the rotaxane with cyclodextrins and polyethylene glycols. The method consists of four steps; 1) formation of the pseud rotaxane, 2) fixation of the rotaxane structure by introducing stopper moiety to prevent dethreading of cyclodextrins, 3) tubulation of cyclodextrins, and 4) removals of the stopper moiety. The rotaxane method is effective to synthesize length-controlled molecular tubes because the molecular length of the cyclodextrin tubes depended on the polyethylene glycols.

In the case of synthesizing molecular tubes with a large cavity via the rotaxane method, stopper molecules should be large enough to fix cyclic molecules on the template molecules, which has difficulty in terms of synthesis. In Chapter 3, the template method for the dimeric porphyrin tube was reported. The method consists of two steps; 1) formation of pseud rotaxanes and 2) tubulation. In contrast to the previous rotaxane method, stopper molecules were not necessary because of the high association constant between the cyclic molecules and the template molecules. In this chapter, a template method for the porphyrin tube via selective trimerization of porphyrin rings is described (Figure 5-1).

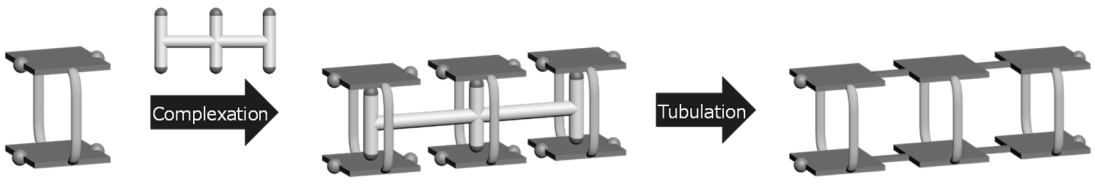

Figure 5-1. Template synthesis of a porphyrin tube via selective trimerization of porphyrin rings.

5-2. Results and Discussions

5-2-1. Synthesis of the Template Molecule

The structures of the template molecule **T3a** (n = 6) and **T3b** (n = 8) were shown in Scheme 5-1. As described in Chapter 3, 1,4-di(pyridin-4-yl)benzene was adopted as a basic unit of the template molecule. **T3a** was prepared as follows. The reaction of **1** with 1,6-dibromohexane afforded **2a.** Then, treatment of **2a** with **3** gave intermeidate **4a**. Finally, **T3a** was obtained via Suzuki–Miyaura coupling reaction of **4a** with excess amount of **5**. **T3b** which has longer alkyl linkers as compared to **T3a** was also synthesized with a similar method using 1,8-dibromooctane in place of 1,6-dibromohexane. **T3a** and **T3b** were characterarised by NMR and MS spectra.

Scheme 5-1. Synthesis of the template molecules **T3a** (n=6) and **T3b** (n=8)

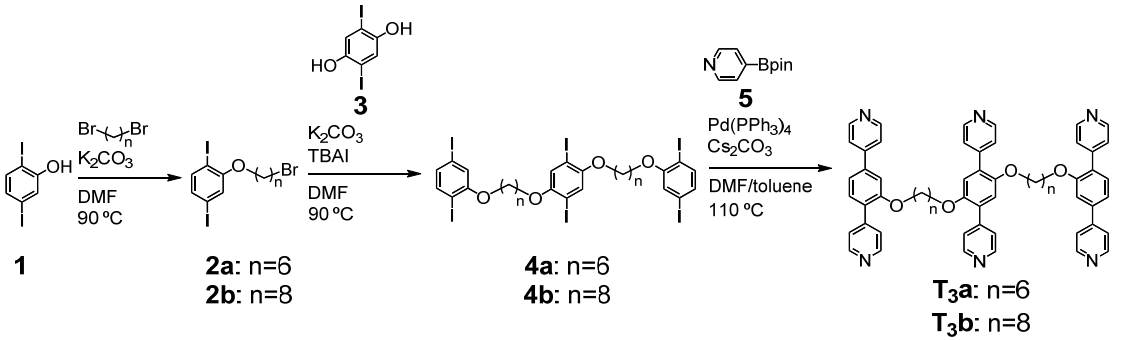

5-2-2. Complexation Study between ZnCP' and T3b

When **T3a** and **T3b** work as template molecules in the tubulation, porphyrin rings need to penetrate the template molecules. To confirm complexation ability of **T3a** and **T3b** with porphyrin rings, the reaction of cyclic porphyrin **ZnCP'** with **T3a** and **T3b** was carried out as a model reaction (Scheme 5-2). Although **T3a** with proper alkyl linkers would be suitable for

Scheme 5-2. Complexation between **ZnCP'** and **T3b**, Some parts of fluorene units being removed for clarity

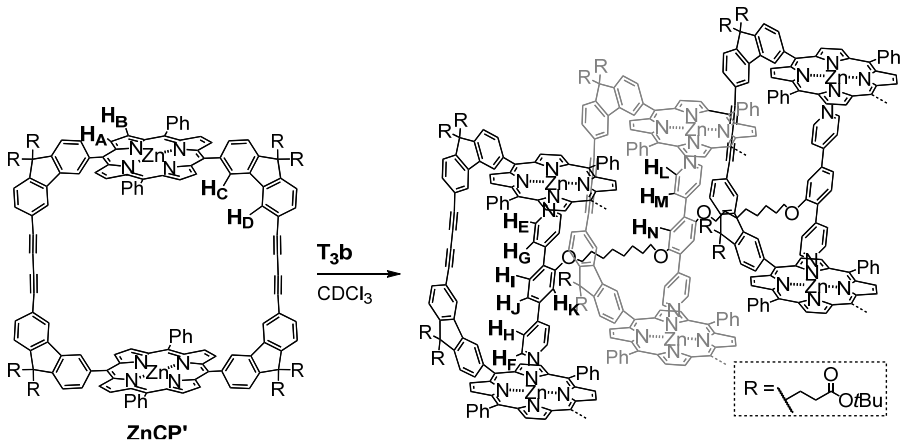

the tubulation (as described in Chapter 3), the compound had low solubility in toluene, $CHCl_3$, and CH_2Cl_2 which were proper solvents for a Glaser reaction. Therefore, **T3b** was used as a template molecule in complexation study. Similary to the result of titration experiments in Chapter 3, all ^1H signals assigned to free **T3b** were shifted to the upfield region due to ring-current effect of the porphyrins.The extent of the shift depends on the distance between porphyrins and protons of **T3b**. Chemical shifts corresponding ortho protons H_E, H_F, and H_L of complexed pyridine units was observed around 2.25–2.32 ppm because the protons are closes to the porphyrin among the protons of **T3b**. Addition of **T3b** to **ZnCP'** split H_A and H_B in more than six peaks from 8.70 ppm to 8.85 ppm, which suggested that there were rotamers around axes of alkyl linkers of **T3b.** When **ZnCP'** and **T3b** were mixed in $CDCl_3$ in a ratio of 3 : 1, proton peaks of free **ZnCP'** (H_A, H_B, H_C, and H_D) disappeared within 10 min (Figure 5-

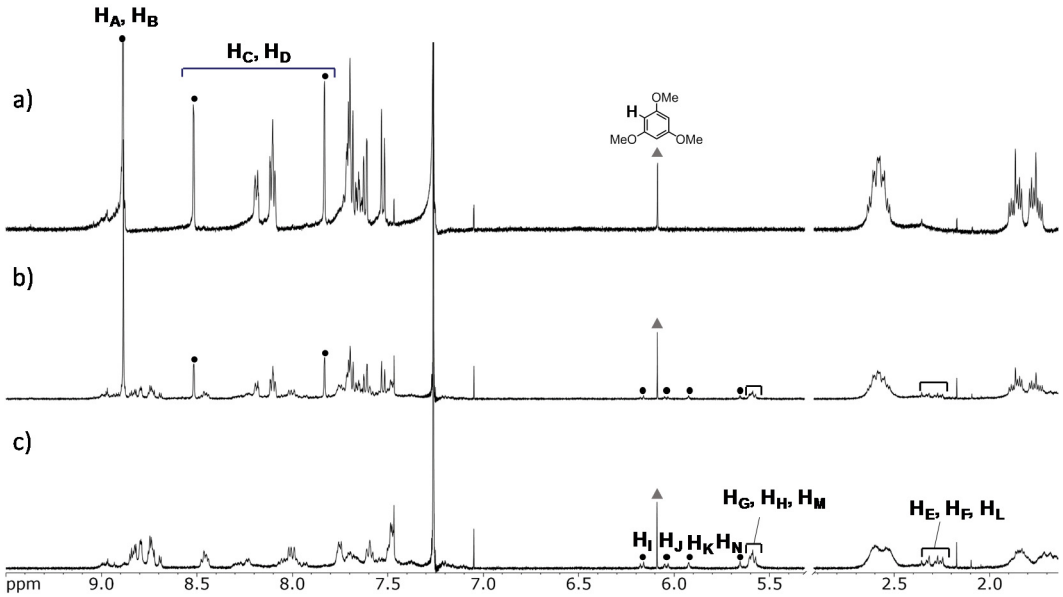

Figure 5-2. ^1H NMR (500 MHz, 298K) titration of **T3b (n=8)** to **ZnCP'** in $CDCl_3$. a) **ZnCP'**, b) **ZnCP'** : **T3b** = 3 : 0.4, and c) **ZnCP'** : **T3b** = 3 : 1.

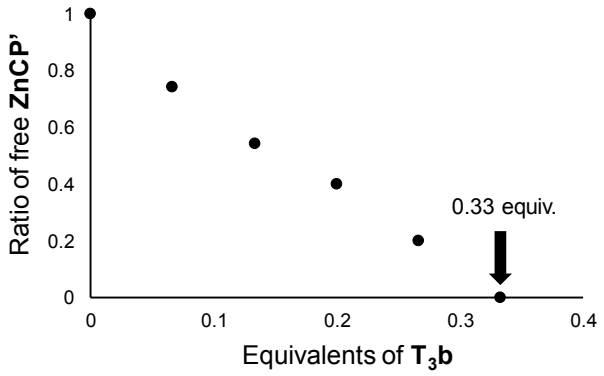

Figure 5-3. Conversion ratio of free **ZnCP'** in ^1H NMR titration of **T3b** to **ZnCP'** in $CDCl_3$.

2, 5-3). These observation strongly suggests the formation of 3 : 1 complex between **ZnCP'** and **T3b** and that **T3b** could effectively make cyclic porphyrin dimers close to each other.

5-2-3. Template Synthesis of the Length-Controlled Porphyrin Tube

Next, template-assisted synthesis of **ZnCP3** was tried by tubulation of **ZnCP** having unprotected acetylene moieties based on the complex study (Scheme 5-3). **ZnCP** and **T3b** in a ratio of 3 : 1 was dissolved in a large amount of CH_2Cl_2 to prevent undesired polymerization (concentration of **ZnCP** was 7.6×10^{-6} M). After addition of CuCl and TMEDA to the solution, the solution was stirred at r. t. overnight under air. Similar to the results for dimeric compound described in Chapter 3, the formation of **ZnCP3** was observed as a main product in an analytical SEC chromatogram (Figure 5-4b), whereas any reaction without **T3b** under the same concentration hardly proceeded (Figure 5-4a). As a result, it was revealed that **T3b** could accelerate trimerization of **ZnCP**s. Considering the result in Chapter 3, the length of

Scheme 5-3. Template assisted synthesis of porphyrin tube **ZnCP3**

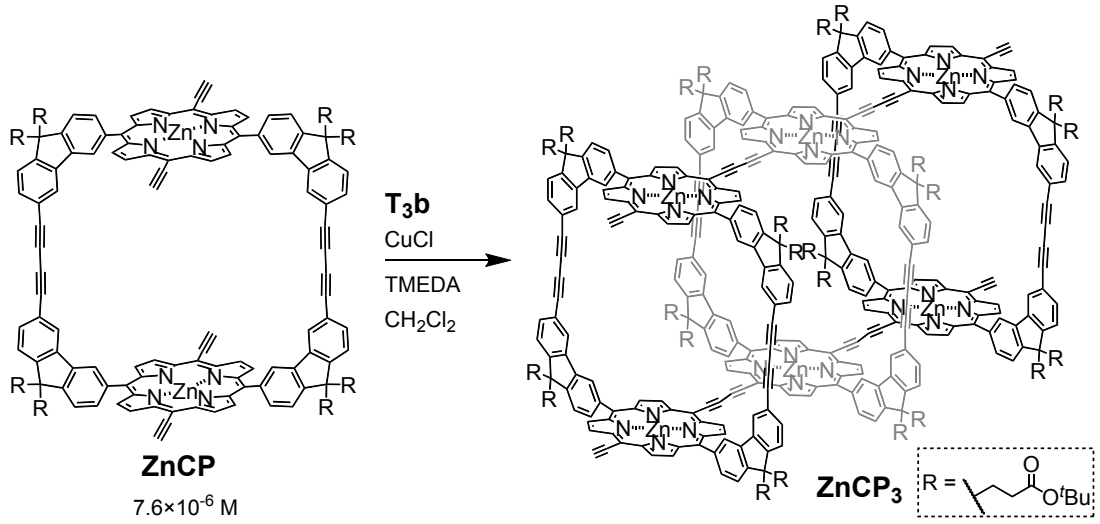

porphyrin tubes can be perfectly controlled by the number of 1,4-di(pyridin-4-yl)benzene units in the template molecule.

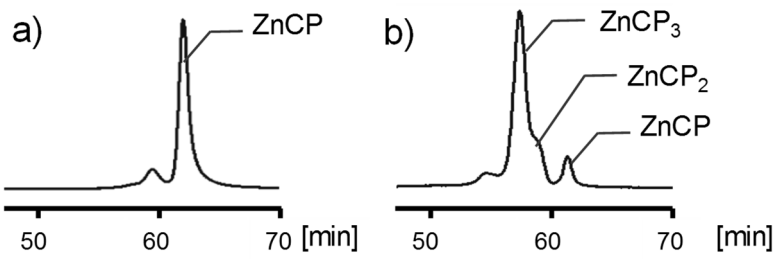

Figure 5-4. SEC chromatograms for a synthesis of **ZnCP3** by template assisted tubulation (Eluent : THF, detection : 420 nm). a) without **T3b** and b) with **T3b**.

5-3. Conclusion

In conclusion, it was revealed that the two-step template method can be applied to the synthesis of a porphyrin tube via selective trimerization of porphyrin rings. Efficient complexation between the cyclic molecules and the template molecule induced the selectivity. In contrast to the previous rotaxane method, stopper molecules to prevent dethreading of cyclic molecules were not necessary due to the high association constant between cyclic molecules and template molecules. Longer porphyrin tubes are expected to be selectively prepared by the rotaxane type template method in near future.

5-4. Experimental Section

5-4-1. General Remarks

Materials: Reagents were purchased from commercial sources and used without further purification. Solvents were purified as follows: reaction solvents were degassed through freeze-pump-thaw (three times), before use. Dry toluene was purchased from Kanto Chemical and further purified by passage through activated alumina under positive argon pressure as described by Grubbs *et al.*[9]

NMR Spectroscopy: ^{1}H NMR spectra were measured on a Bruker AVANCE-500 spectrometer. The ^{1}H NMR chemical shifts are reported relative to tetramethylsilane (TMS, 0.00 ppm) or residual protonated solvent (7.26 ppm) in $CDCl_3$. The ^{13}C NMR chemical shifts are reported relative to tetramethylsilane (TMS, 0.00 ppm) or solvent (77.16 ppm) in $CDCl_3$.

Preparative recycling gel permeation chromatography (GPC): Preparative recycling GPC was performed with a JAI LC9104 System equipped with JAIGEL-1H and 2H columns, a JAI UV DETECTOR 310, and a JAI RI DETRCTOR RI-5, a JAI LC9130NEXT System equipped with JAIGEL-2H and 2.5H columns, a JAI UV DETECTOR 370NEXT, and a JAI RI DETRCTOR RI 700NEXT, a JAI LC9140 System equipped with JAIGEL-2.5H and -3H columns, a JAI UV DETECTOR 310, and a JAI RI DETRCTOR RI-5.

Mass spectroscopy (MS): Matrix assisted laser desorption/ionization time-of-flight (MALDI-TOF) mass spectra were obtained with α-cyano-4-hydroxycinnamic acid (CHCA) as a matrix and NaTFA as a cationization reagent on a Thermo Fisher Scientific LTQ orbitrapXL. ESI and atmospheric pressure chemical ionization (APCI) mass spectra were obtained on a Thermo Fisher Scientific EXACTIVE.

5-4-2. Synthetic Procedures

Synthesis of 2a

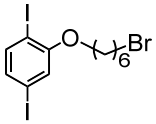

1 (1.00 g, 2.89 mmol), K_2CO_3 (900 mg, 2.0 mmol), 1,6-dibromohexane (1.76 mL, 11.6 mmol), and tetrabutylammonium iodide (53.4 mg, 145 μmol) were dissolved in dehydrated DMF (100 mL). The solution was stirred at 100 ºC overnight, after which DMF was removed under vacuum. The residue was filtered through the Celite pad and purified by silica gel column chromatography (CH_2Cl_2 / hexane = 1 / 40 to 1 / 20) to afford **2a** (821 mg, 56%) as a white solid.

HR-MS (APCI-TOF MS): (m/z) 507.8388 ([**2a**]$^+$, $C_{12}H_{15}BrI_2O$, calcd. 507.8396)
^{1}H NMR (500 MHz, $CDCl_3$, r. t.): δ 7.45 (d, *J* = 8.2 Hz, 1H, Ar-*H*), 7.06 (d, *J* = 1.9 Hz, 1H, Ar-*H*), 7.02 (dd, *J* = 8.2, 1.9 Hz, 1H, Ar-*H*), 3.99 (t, *J* = 6.2 Hz, 2H, -O-*CH*$_2$-*C*H$_2$-), 3.44 (t, *J* = 6.8 Hz, 2H, -CH$_2$-*CH*$_2$-Br), 1.89-1.95 (m, 2H, -O-CH$_2$-*CH*$_2$-), 1.86-1.82 (m, 2H, -*CH*$_2$-CH$_2$-Br), 1.57-1.53 (m, 4H, methylene protons).
^{13}C NMR (126 MHz, $CDCl_3$, r. t.): δ 158.3, 140.6, 131.7, 121.4, 93.9, 86.4, 69.4, 33.9, 32.8, 28.9, 27.9, 25.4.

Synthesis of 2b

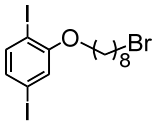

1 (1.00 g, 2.89 mmol), K_2CO_3 (912 mg, 6.60 mmol), 1,8-dibromooctane (2.20 mL, 11.9 mmol), and tetrabutylammonium iodide (54.5 mg, 147 μmol) were dissolved in dehydrated DMF (100 mL). The solution was stirred at 100 ºC overnight, after which DMF was removed under vacuum. The residue was filtered through the Celite pad and purified by silica gel column chromatography (CH_2Cl_2 / hexane = 1 / 4) to afford **2b** (638 mg, 41%) as a white solid.

HR-MS (APCI-TOF MS): (m/z) 535.8697 ([**2b**]$^+$, $C_{14}H_{19}BrI_2O$, calcd. 535.8709)
^{1}H NMR (500 MHz, $CDCl_3$, r. t.): δ 7.41 (dd, *J* = 8.1, 1.1 Hz, 1H, Ar-*H*), 7.04 (s, 1H, Ar-*H*), 6.98 (dt, *J* = 8.1, 1.5 Hz, 1H, Ar-*H*), 3.94 (t, *J* = 6.24 Hz, 2H, Ar-OC*H*$_2$CH$_2$CH$_2$-), 3.39 (t, *J* = 6.94 Hz, 2H, -C*H*$_2$-Br), 1.86-1.76 (m, 4H, methylene protons), 1.52-1.34 (m, 8H, methylene protons).
^{13}C NMR (126 MHz, $CDCl_3$, r. t.): δ 158.1, 140.3, 131.3, 121.1, 94.0, 86.4, 69.34, 34.10, 32.74, 29.01, 28.87, 28.62, 28.05, 25.89.

Synthesis of 3a

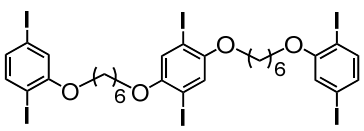

2a (703 mg, 1.38 mmol), K_2CO_3 (244 mg, 1.77 mmol), 2,5-diiodohydroquinone (202 mg, 0.557 mmol), and tetrabutylammonium iodide (20.0 mg, 5.53 μmol) were dissolved in dehydrated DMF (5.2 mL). The solution was stirred at 100 ºC overnight, after

which DMF was removed under vacuum. The residue was filtered through the Celite pad and purified by silica gel column chromatography (CH_2Cl_2 / hexane = 1 / 1) to afford **3a** (78.0 mg, 11%) as a white solid.

HR-MS (APCI-TOF MS): (m/z) 1217.655 ([**3a**]$^+$, $C_{30}H_{32}I_6O_4$, calcd. 1217.657)
^{1}H NMR (500 MHz, $CDCl_3$, r. t.): δ 7.43 (d, *J* = 8.1 Hz, 2H, Ar-*H*), 7.16 (s, 2H, Ar-*H*), 7.06 (d, *J* = 1.8 Hz, 2H, Ar-*H*), 7.00 (dd, *J* = 8.1, 1.8 Hz, 2H, Ar-*H*), 4.01 (t, *J* = 6.2 Hz, 4H, -O-*CH_2*-CH_2-), 3.96 (t, *J* = 6.3 Hz, 4H, -O-*CH_2*-CH_2-), 1.91-1.83 (m, 8H, methylene protons), 1.64-1.60 (m, 8H, methylene protons).
^{13}C NMR (126 MHz, $CDCl_3$, r. t.): δ 158.6, 153.1, 140.8, 131.8, 123.1, 121.6, 94.16, 86.72, 86.68, 70.28, 69.52, 29.28, 29.12, 25.82.

Synthesis of 3b

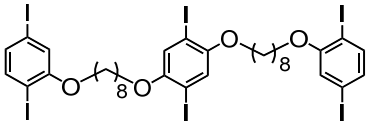

2b (337 mg, 0.628 mmol), K_2CO_3 (107 mg, 0.775 mmol), 2,5-diiodohydroquinone (90.9 mg, 0.251 mmol), and tetrabutylammonium iodide (4.64 mg, 12.6 μmol) were dissolved in dehydrated DMF (2.2 mL). The solution was stired at 100 ºC overnight, after which DMF was removed under vacuum. The residue was filtered through the Celite pad and purified by silica gel column chromatography (CH_2Cl_2 / hexane = 1 / 1) to afford **3b** (295 mg, 92%) as a white solid.

HR-MS (ESI-TOF MS): (m/z) 1273.718 ([**3b**]$^+$, $C_{34}H_{41}I_6O_4$, calcd. 1274.720)
^{1}H NMR (500 MHz, $CDCl_3$, r. t.): δ 7.44 (d, *J* = 8.2 Hz, 2H), 7.17 (s, 2H), 7.06 (d, *J* = 1.8 Hz, 2H), 7.01 (dd, *J* = 8.2, 1.8 Hz, 2H), 3.98 (t, *J* = 6.4, 4H, -O-*CH_2*-CH_2-), 3.93 (t, *J* = 6.4 Hz, 4H, -O-*CH_2*-CH_2-), 1.87-1.78 (m, 8H, methylene protons), 1.57-1.50 (m, 8H, methylene protons), 1.42 (m, 8H, methylene protons).
^{13}C NMR (126 MHz, $CDCl_3$, r. t.): δ 158.62, 153.19, 140.78, 131.75, 123.14, 121.57, 94.15, 86.71 (two peaks overlapped), 70.65, 69.82, 29.50, 29.49, 29.46, 29.27, 26.33, 26.31.

Synthesis of T_3a

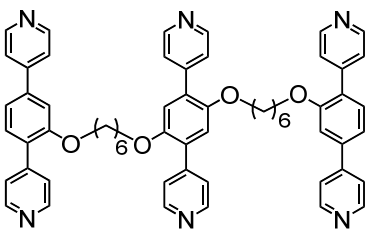

3a (60.0 mg, 49.0 μmol), **5** (291 mg, 1.42 mmol), Cs_2CO_3 (319 mg, 0.98 mmol), and $Pd(PPh_3)_4$ (11.3 mg, 9.80 μmol) were dissolved in DMF / toluene (1 / 1, 3.8 mL). The solution was stirred at 110 ºC overnight. The solvent was removed under vacuum, after which the residue was passed through a Celite pad. The crude mixture was purified by silica gel column

chromatography (EtOAc / CH_2Cl_2 = 10 / 3) to afford **T_3a** (14.9 mg, 33%) as a white solid. **T_3a** showed low solubility in $CHCl_3$, CH_2Cl_2, toluene and EtOAc.

HR-MS (ESI-TOF MS): (m/z) 925.4423 ([**T_3a**+H^+], $C_{60}H_{57}N_6O_4$, calcd. 925.4441)
^{1}H NMR (500 MHz, $CDCl_3$, r. t.): δ 8.69 (dd, *J* = 4.5, 1.6 Hz, 4H, Ar-*H*), 8.62-8.60 (br, 8H, Ar-*H*), 7.54 (dd, *J* = 4.5, 1.6 z, 4H, Ar-*H*), 7.48 (br, 8H, Ar-*H*), 7.46 (d, *J* = 7.9 Hz, 2H, Ar-*H*), 7.33-7.31 (dd, *J* = 7.9, 1.5 Hz, 2H, Ar-*H*), 7.20 (d, *J* = 1.5 Hz, 2H, Ar-*H*), 6.97 (s, 2H, Ar-*H*), 4.03 (t, *J* = 6.3 Hz, 4H, -O-*CH_2*-CH_2-), 3.92 (t, *J* = 6.3 Hz, 4H, -O-*CH_2*-CH_2-), 1.77-1.72 (m, 4H, methylene protons), 1.72-1.66 (m, 4H, methylene protons), 1.40-1.36 (m, 8H, methylene protons).

Synthesis of T_3b

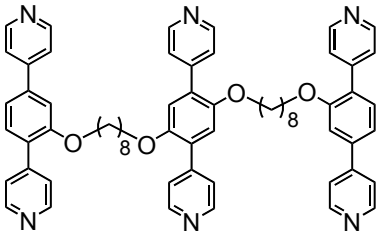

3b (40.9 mg, 32.1 μmol), **5** (186.8 mg, 0.910 mmol), Cs_2CO_3 (206 mg, 0.628 mmol), and $Pd(PPh_3)_4$ (7.7 mg, 6.7 μmol) were dissolved in DMF / toluene (1 / 1, 2.4 mL). The solution was stirred at 110 °C overnight. The solvent was removed under vacuum, after which the residue was passed through a Celite pad and membrane filter. The crude mixture was purified by silica gel column chromatography (EtOAc / CH_2Cl_2 = 10 / 3 to EtOAc / MeOH / Et_3N = 30 / 9 / 1) to afford **T_3b** (26.6 mg, 86%) as a white solid.

HR-MS (ESI-TOF MS): (m/z) 981.5045 ([**T_3b**]$^+$, $C_{64}H_{65}N_6O_4$, calcd. 981.5067)
^{1}H NMR (500 MHz, $CDCl_3$, r. t.): δ 8.70-8.67 (broad, 4H, Ar-H), 8.65-8.62 (broad, 8H, Ar-H), 7.56-7.53 (broad, 4H, Ar-H), 7.53-7.50 (broad, 8H, Ar-H), 7.46 (d, J = 7.8, 2H, Ar-H), 7.32 (d, J = 7.8, 2H, Ar-H), 7.23 (s, 2H, Ar-H), 6.99 (s, 2H, Ar-H), 4.07 (t, J = 6.3 Hz, 4H), 3.95 (t, J = 6.2 Hz, 4H), 1.79-1.73 (m, 4H), 1.73-1.67 (m, 4H), 1.38-1.24 (m, 16H).
^{13}C NMR (126 MHz, $CDCl_3$, r. t.): δ 156.8 (two peaks overlapped), 150.53, 150.51, 149.65, 149.61, 147.9, 145.93, 145.78, 140.3, 131.2, 129.2, 128.6, 124.4, 121.8, 119.8, 115.6, 111.2, 69.7, 68.8, 29.35, 29.28 (two peaks overlapped), 29.20, 26.14, 26.12.

Synthesis of $ZnCP_3$

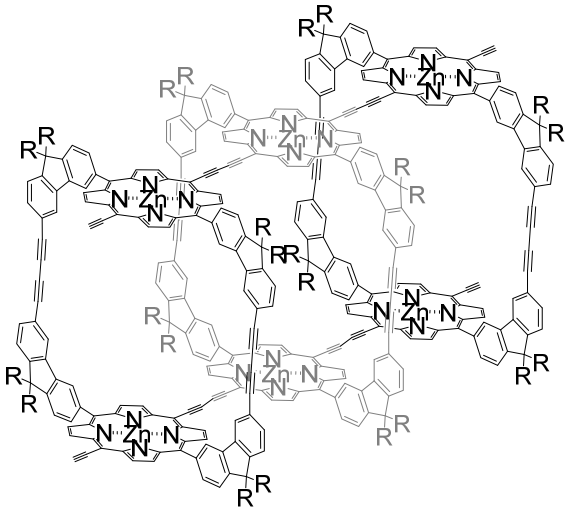

ZnCP (1.00 mg, 0.84 μmol) and **T_3b** (0.27 mg, 0.28 μmol) from a stock solution were added to a round bottom flask after which a solvent was removed under vacuum. These compounds were dissolved in CH_2Cl_2 (100 mL) followed by slow additions of CuCl (5.3 mg, 53.5 μmol) and TMEDA (190 μL, 13.7 μmol) under air. The solution was stirred at r. t. overnight. The progress of the reaction was monitored by GPC using THF as an eluent after 14 h.

References and Notes

1. a) Bakbo Block, M. A.; Kaiser, C.; Khan, A.; Hecht, S. *Top Curr. Chem.* **2005**, *245*, 89. b) Shimizu, T. *J. Polym. Sci., Part A: Polym. Chem.* **2006**, *44*, 5137. c) Shimizu, T. *Bull. Chem. Soc. Jpn.* **2008**, *81*, 1554. d) Kameta, N.; Minamikawa, H.; Masuda, M. *Soft Matter.* **2011**, *7*, 4539.
2. a) Guldi, D. M. *Chem. Soc. Rev.* **2002**, *31*, 22. b) Li, L. -L.; Diau, E. W. -G. *Chem. Soc. Rev.* **2013**, *42*, 291.
3. a) Fukuzumi, S.; Kojima, T. *J. Mater. Chem.* **2008**, *18*, 1427. b) Drain, C. M.; Varotto, A.; Radivojevic, I. *Chem. Rev.* **2009**, *109*, 1630. c) Medforth, C. J.; Wang, Z.; Martin, K. E.; Song, Y.; Jacobsen, J. L.; Shelnutt, J. A. *Chem. Commun.* **2009**, 7261.
4. Pawlicki, M.; Collins, H. A.; Denning, R. G.; Anderson, H. L. *Angew. Chem., Int. Ed.* **2009**, *48*, 3244.
5. a) Grozema, F. C.; Houarner-Rassin, C.; Prins, P.; Siebbeles, L. D. A.; Anderson, H. L. *J. Am. Chem. Soc.* **2007**, *129*, 13370. b) Sedghi, G.; García-Suárez, V. M.; Esdaile, L. J.; Anderson, H. L.; Lambert, C. J.; Martín, S.; Bethell, D.; Higgins, S. J.; Elliott, M.; Bennett, N.; Macdonald, J. E.; Nichols, R. J. *Nat. Nanotech.* **2011**, *6*, 517.
6. a) Ishida, T.; Morisaki, Y.; Chujo, Y. *Tetrahedron Lett.* **2006**, *47*, 5265. b) Youm, K. -T.; Nguyen, S. T.; Hupp, J. T. *Chem. Commun.* **2008**, 3375. c) Neuhaus, P.; Cnossen, A.; Gong, J. Q. Herz, L. M.; Anderson, H. L. *Angew. Chem., Int. Ed.* **2015**, *54*, 7344.
7. Harada, A.; Li, J.; Kamachi, M. *Nature* **1993**, *364*, 516.
8. Atwood, J. L.; Davies, J. E. D.; MacNicol, D. D.; Vögtle, F. *Comprehensive Supramolecular Chemistry, Vol. 3. Cyclodextrins,* Pergamon, Oxford, **1996**.

9. Pangborn, A. B.; Giardello, M. A.; Grubbs, R. H.; Rosen, R. K.; Timmers, F. J. *Organometallics* **1996**, *15*, 1518.

List of Publications

The present thesis is composed of the following papers.

Chapter 1

(1) Template Synthesis of Cavity Size-Controlled Porphyrin Rings and the Inclusion Abilities
Terao, J.; Chiba, Y.; Fujihara, T.; Tsuji, Y. *Chem. Lett.* **2014**, *43*, 1374.

Chapter 2

(2) Kinetically Stabilized Hetero Face-to-Face Porphyrin Array Using a Porphyrin Ring and Its Optical Property
Chiba, Y.; Liu, M.; Tachibana, Y.; Fujihara, T.; Tsuji, Y.; Terao, J. *Chem. Asian. J.* **2017**, *12*, 1900.

Chapter 3

(3) Template Synthesis of a Length-Controlled Porphyrin Tube via Selective Dimerization of Porphyrin Rings and Its Mechanism
Chiba, Y.; Fujihara, T.; Tsuji, Y.; Terao, J.
In preparation.

Chapter 4

(4) Investigation of the Host–Guest Complexation Between a Porphyrin Tube and a Porphyrin Dimer
Chiba, Y.; Fujihara, T.; Tsuji, Y.; Terao, J.
In preparation.

Chapter 5

(5) Template Synthesis of a Length-Controlled Porphyrin Tube via Selective Trimerization of Porphyrin Rings and Its Mechanism
Chiba, Y.; Oka, Y.; Fujihara, T.; Tsuji, Y.; Terao, J.
In preparation.

Acknowledgment

The studies described in this thesis have been carried out under the direction of Professor Yasushi Tsuji from April, 2012 to March, 2018 at the Department of Energy and Hydrocarbon Chemistry, Graduate School of Engineering, Kyoto University.

The author would like to express his sincerest gratitude to Professor Tsuji forgiving opportunities to study in his laboratory at Kyoto University (2012–2018). His enthusiastic guidance and advice always encouraged the author to challenge his study with utmost effort.

The author deeply appreciates to Professor Jun Terao and Professor Tetsuaki Fujihara at Kyoto University for their support during the course of this study. Their guidance, discussions and suggestions stimulated his interest in chemistry to promote his study. He thanks to Mrs. Aya Uehara and Mrs. Kinuyo Toritani for their kind support. It is his great pleasure to collaborate with Dr. Hiroshi Masai, Mr. Yohei Konoshima, Dr. Wakana Matsuda, Mr. Takuro Hosomi, Mr. Masami Ohsawa, Mr. Daiki Inamori, Mr. Shunichi Kaneko and Mr. Yuki Oka for their fruitful researches and discussions. The author greatly wishes to thank all members of Professor Tsuji's group for sharing invaluable moments and enjoying their studies.

The author is grateful to Professor Yasuhiro Tachibana and Dr. Maning Liu for analysis of charge transfer. He wishes to show his appreciation to Professor Koichi Ohe and Professor Yasujiro Murata for their helpful discussions.

Finally, the author wishes to show his sincere appreciation to his family, Mr. Kaoru Chiba, Mrs. Hiromi Chiba, and Mr. Hiroki Chiba for their affectionate assistance and encouragement.

Yusuke Chiba